8.0 RESULTS OF SITE-SPECIFIC STUDIES

The results of the specific studies at each site are discussed separately below.

8.1 St. Francis River Site

8.1.1 Site Geology

The topography at the St. Francis River Site is given in Figure 8.1. The following geologic units, listed from the ground surface downward, characterize local geology at the St. Francis River Bridge:

- Approximately 20 feet of low plasticity silty clay,
- Approximately 0-15 feet of clayey silt
- Approximately 5-10 feet of silty sand,
- Approximately 150 feet of coarse sand, containing numerous thin gravel lenses, and,
- Limestone bedrock, assumed to represent either the Lower Jefferson City or Upper Roubidoux Formations.

An example cross-section from the St. Francis River Site is shown on Figure 8.2. Figure 8.3 shows the soil profile from boring B-1 for the St. Francis River Site.

8.1.2 Selected Base Rock Motion

Herrmann, (2000) recommends ten rock base motions for PE 10% in 50 years and the other ten for PE 2% in 50 years for each site. All of the 40 rock motions have been used for one-dimensional wave propagation analysis using the *SHAKE91* program. Based on wave propagation analysis, peak ground accelerations for each rock motion were obtained. A total of 12 ground motions were selected based on these peak ground acceleration values.

Table 8.1a lists 5-ground motion for PE 10% in 50 years with corresponding maximum peak ground accelerations for M6.2 with epicentral distance of 40 km and 5-more ground motions of M7.2 and epicentral-distance of 100 km. Table 8.1b shows listing of ground motion for PE 2 % in 50 years with different M's and epicentral-distance. In these tables columns 1-4 are basic data from Herrmann (2000).

Twelve synthetic ground motions at the rock base (6 for each PE) are selected as representative of the "worst case scenarios". They are given in Table 8.1. The associated acceleration-time histories are shown in Figures 8.4a-8.4d.

8.1.3 Seismic Response of Soil

The *SHAKE* and *SHAKEDIT* programs were used to propagate the design earthquake base rock motions to the ground surface. This resulted in peak ground motions and time histories of acceleration at the soil surface, the base of bridge abutments and the piers

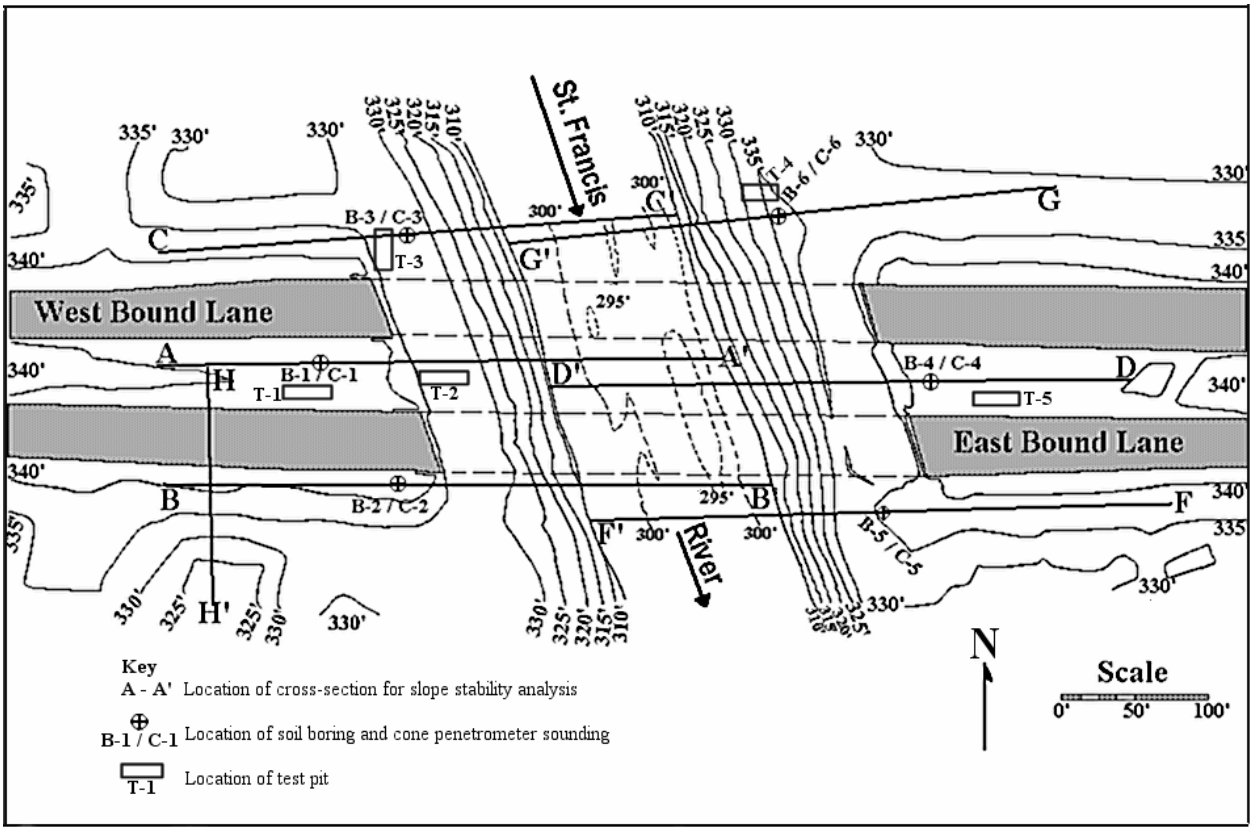

Figure 8.1 St. Francis River Site Topography, Cross-Section and Boring Locations

.

8.1.3.1 Horizontal Seismic Response of Soil

Figure 8.1 shows the location of the St. Francis River Site. A brief description of the soil profile including observed SPT (N_{obs}) and corrected $(N_1)_{60}$ values, is shown in Figure 8.3 for borehole B1. The subsurface soil consists of up to 25 feet of medium to stiff clay underlain by about 30 ft of medium dense sand underlain by a dense to very dense sand to a depth of up to 192.0 ft. The soil profile from bore log B1, as shown in Figure 8.3 has been used in the seismic response analysis since B1 is located close to the bridge abutment and there is complete soil information up to rock base.

The initial shear modulus (G_o) as well as shear wave velocity, which are needed in the wave propagation analysis, are calculated by direct measurement of shear wave velocity up to 35 feet and by correlation with the measured N_{spt} value and depths beyond 35 feet. This calculation is performed in the *SHAKEDIT* program itself. The non-linear soil properties such as modulus degradation with shear strain and material damping with shear strain, have been adopted for each soil type.

.

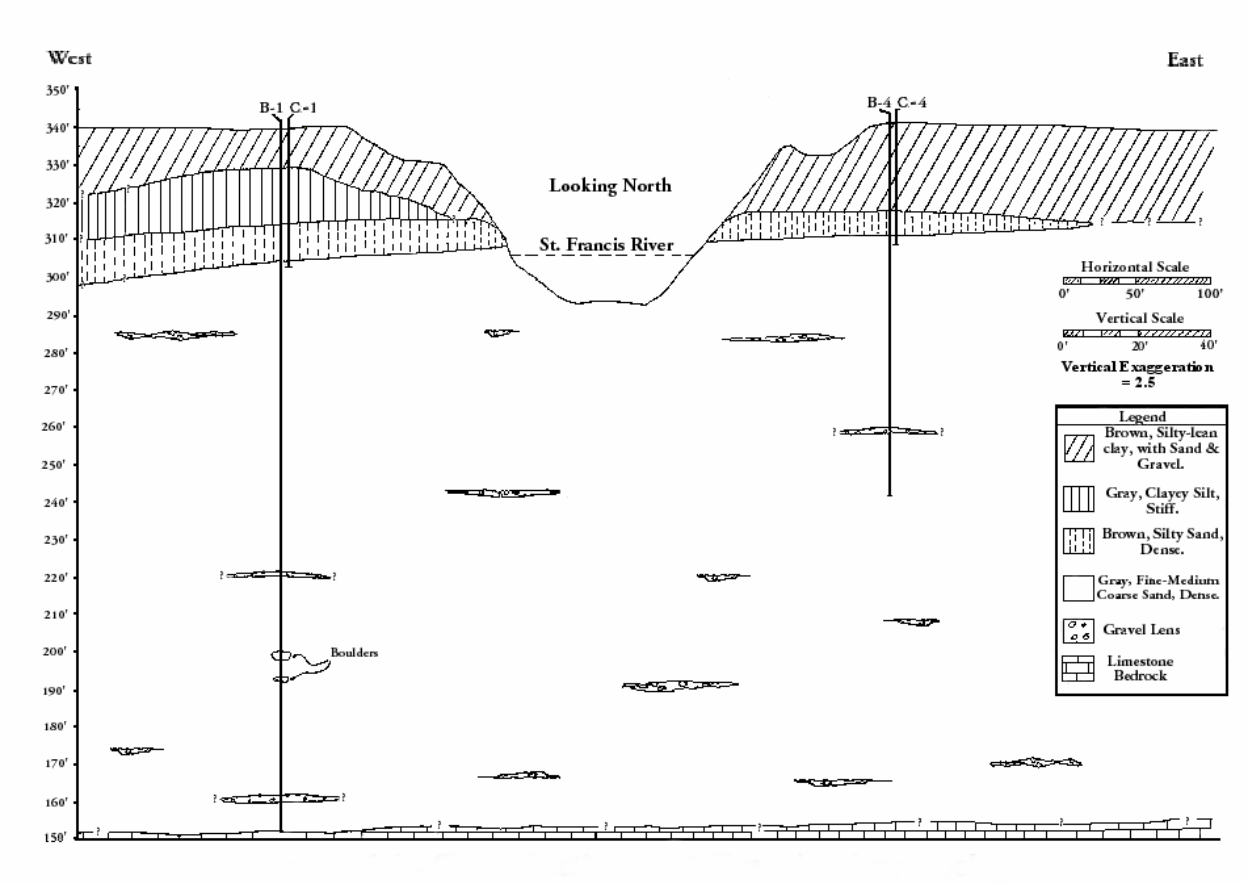

Figure 8.2 Cross-Section of St. Francis River Site Geology

The calculated peak ground accelerations at each soil level from the wave propagation analysis were plotted against depth. Figures 8.5a and b show the peak acceleration for PE 10% in 50 years for M6.2 and M7.2 respectively. Figures 8.6a and b show the peak acceleration for PE 2% in 50 years for M6.4 and M8.0 respectively

For PE 10 % in 50 years and M6.2 and M7.2 respectively, the peak accelerations at the soil surface are higher than those at the base-rock. However, for PE 2 % in 50 years, the peak accelerations at the soil surface of this site are smaller than those at the base rock.

8.1.3.2 Resulting Ground Motion Time Histories

Table 8.2a shows the peak horizontal acceleration of design earthquake at the soil surface, bridge abutment and pier respectively for PE 10% in 50 years, Table 8.2b shows similar information for PE 2 % in 50 years.

Figures 8.7a and b contain 6-plots of surface ground acceleration for PE 10 % in 50 years and earthquake magnitude M6.2 and M7.2. Similarly, Figures 8.7c and d

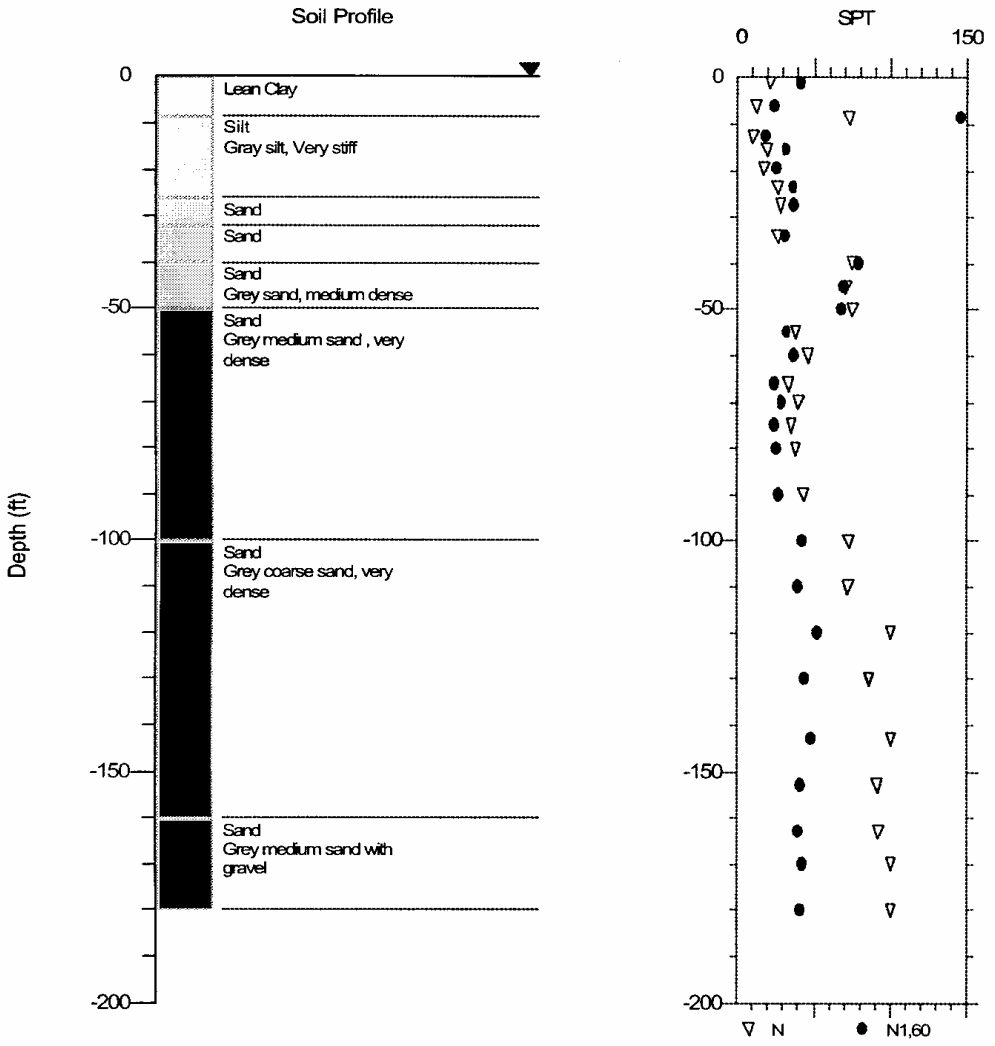


```
Notes:
     CSR analysis using SHAKE results.
     CSR File: D:\I-O SF Pe10%\SF100103\Sf100103.grf
     CRR using SPT Data and Seed et. al. Method in 1997 NCEER Workshop.
     Earthquake File for SHAKE Analysis: D:\SF\SF100103.ACC
     Earthquake Magnitude for CRR Analysis:  6.2
     Magnitude Scaling Factor (MSF):  1.62
     Depth to Water Table for CRR Analysis (ft):  0
     Depth to Water Table for Cn Calculation (ft):  0
     Depth to Base Layer for CSR Analysis (ft):  219.6
     MSF Option: I.M. Idriss (1997)
     Cn Option: Liao & Whitman (1986)
     Ksigma Option: L.F. Harder & R. Boulanger (1997)
     SPT Energy Ratio: USA/Safety/Rope: 0
```

Figure 8.3 Soil Profile St. Francis River Site Boring B-1

Table 8.1 Detail of Synthetic Ground Motion at the Rock Base of St. Francis River Site with Corresponding Maximum Peak Horizontal Ground Acceleration

a. PE 10% in 50 Years

Name (1)	Mw (2)	R (km) (3)	Max acc. at rock-base(g) (4)	Max acc. at soil-surface(g) (5)
SF100101	6.2	40	0.105	0.135
SF100102	6.2	40	0.095	0.128
SF100103*	6.2	40	0.106	0.146
SF100104*	6.2	40	0.100	0.146
SF100105*	6.2	40	0.107	0.151
SF100201*	7.2	100	0.113	0.203
SF100202*	7.2	100	0.136	0.196
SF100203	7.2	100	0.154	0.163
SF100204	7.2	100	0.117	0.173
SF100205*	7.2	100	0.153	0.187

Mw = Magnitude R = Epicentral distance
* Used in further analysis

b. PE 2 % in 50 Years

Name (1)	Mw (2)	R (km) (3)	Max acc. at rock-base(g) (4)	Max acc. at soil-surface(g) (5)
SF020101*	6.4	10	1.069	0.497
SF020102	6.4	10	1.018	0.399
SF020103*	6.4	10	0.845	0.428
SF020104	6.4	10	1.068	0.376
SF020105*	6.4	10	1.089	0.473
SF020201*	8	40	0.604	0.447
SF020202	8	40	0.655	0.362
SF020203*	8	40	0.693	0.453
SF020204	8	40	0.609	0.378
SF020205*	8	40	0.596	0.391

Mw = Magnitude R = Epicentral distance
* Used in further analysis

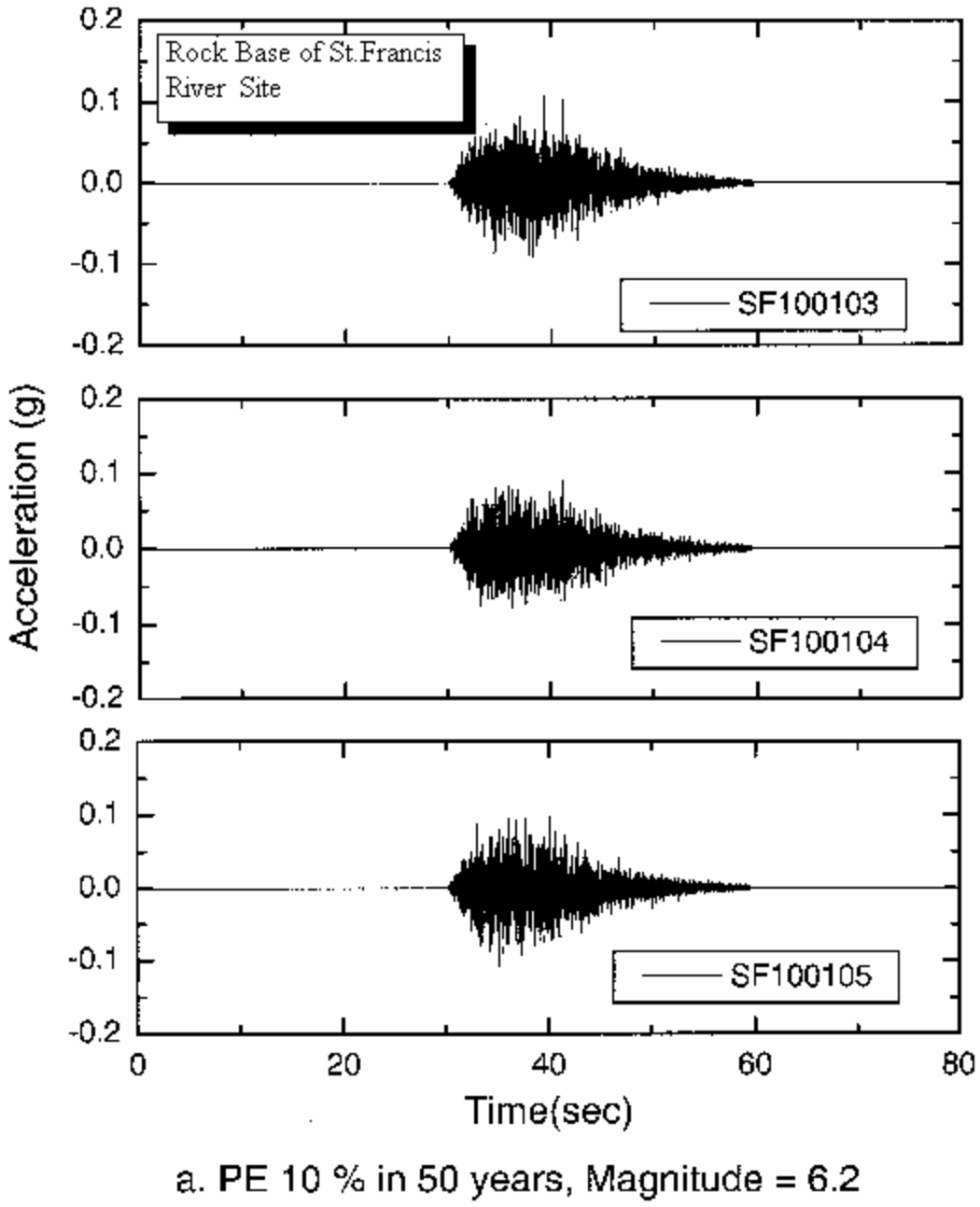

Figure 8.4a Acceleration Time Histories for St. Francis River Site, PE 10% in 50 Years, Magnitude = 6.2

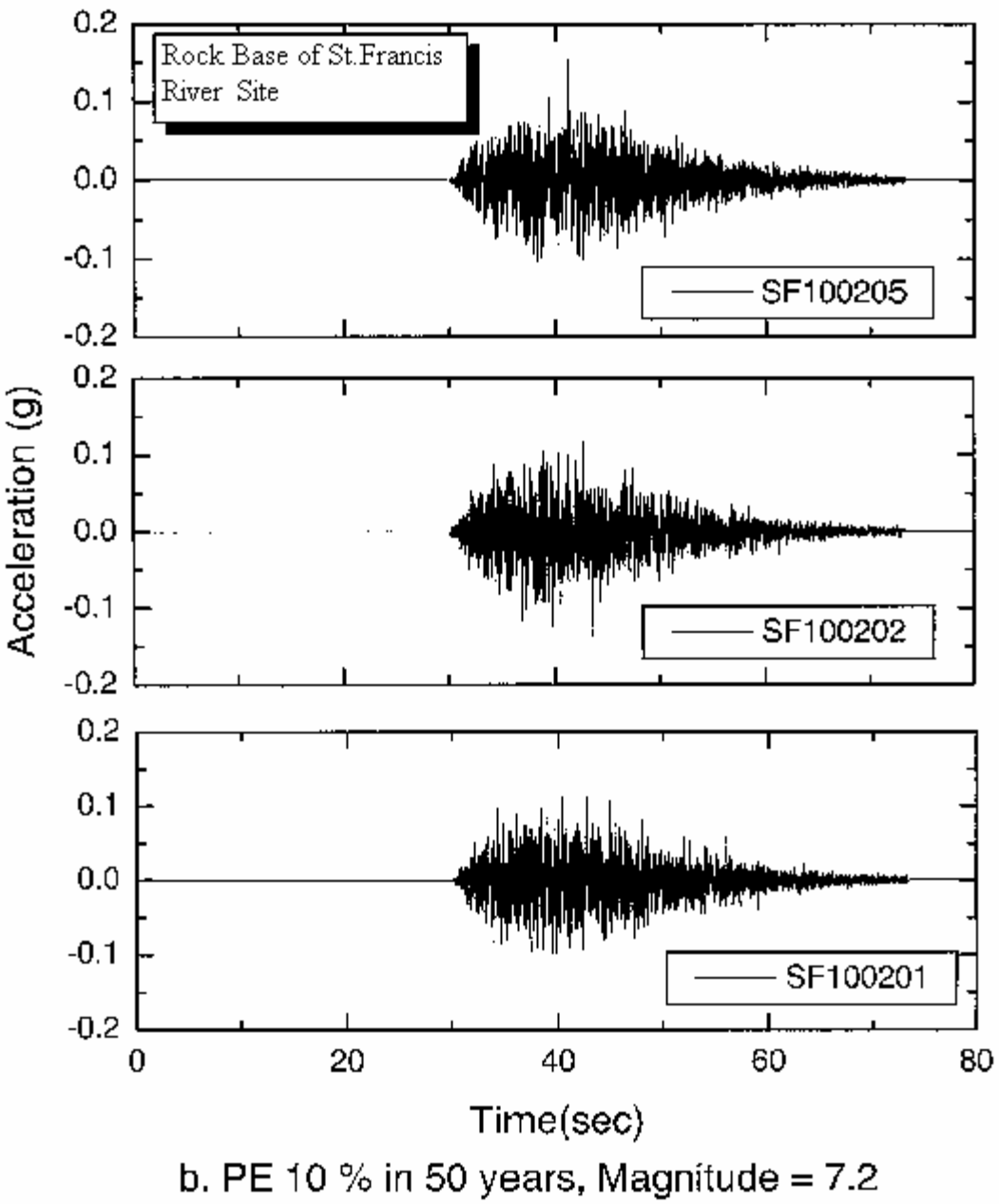

Figure 8.4b Acceleration Time Histories for St. Francis River Site, PE 10% in 50 Years, Magnitude = 7.2

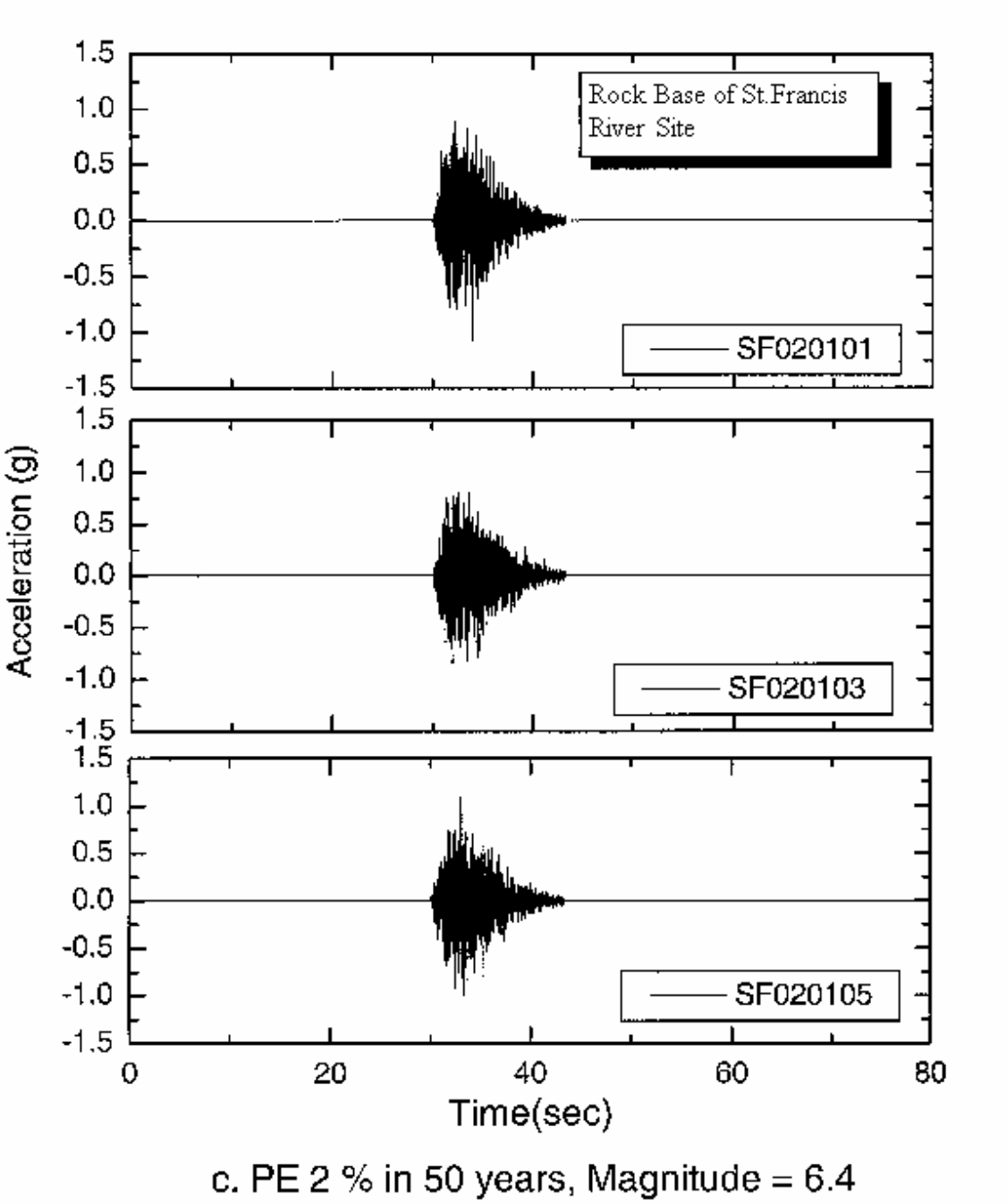

Figure 8.4c Acceleration Time Histories for St. Francis River Site, PE 2% in 50 Years, Magnitude = 6.4

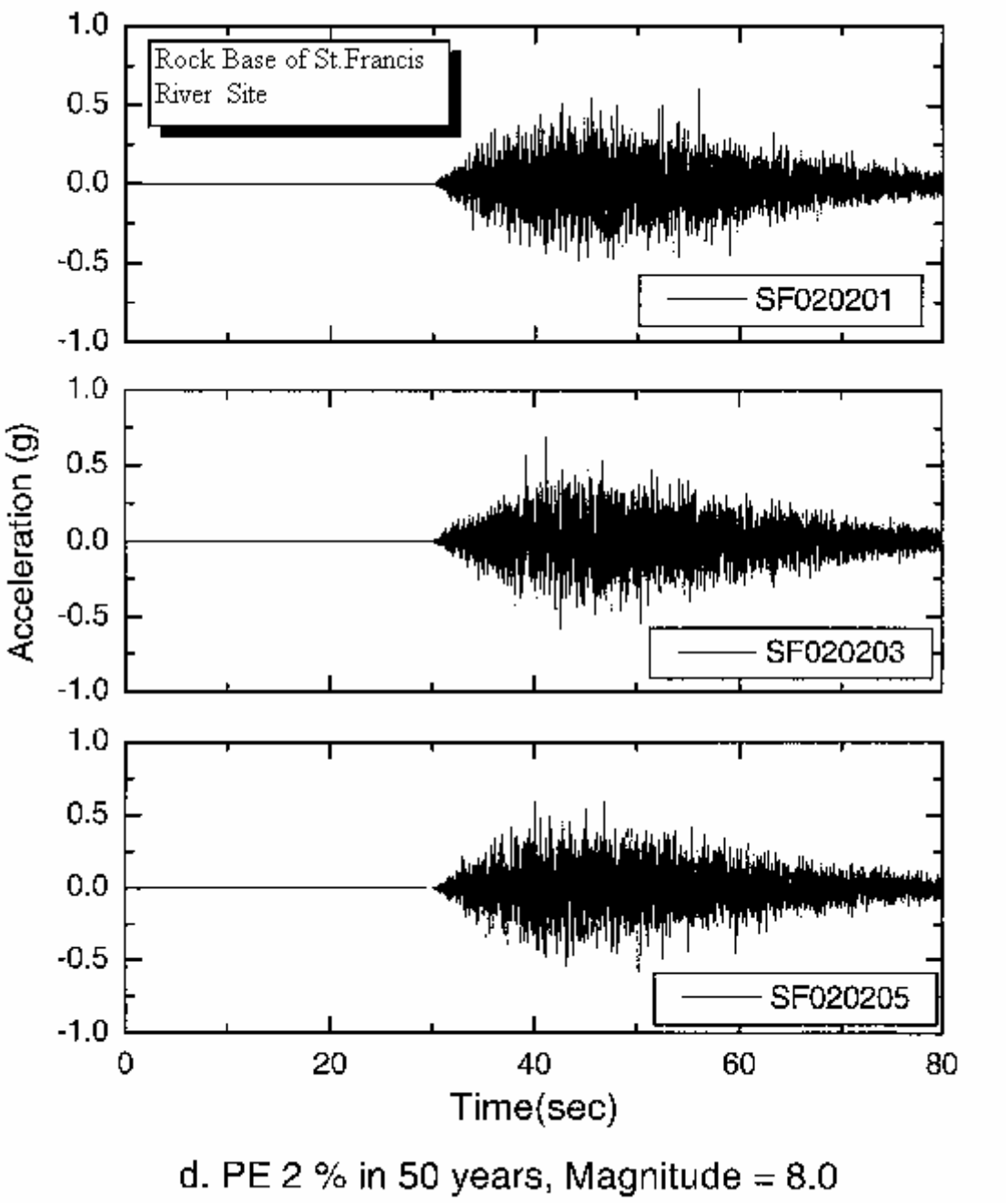

Figure 8.4d Acceleration Time Histories for St. Francis River Site, PE 2% in 50 Years, Magnitude = 8.0

contain plots of surface acceleration for PE 2% in 50 years and M6.4 and M8.0 respectively Figures 8.8a, b, c, and d show plots of design acceleration time history at the bridge abutment for (a) PE 10 % in 50 years M6.2. (b) PE 10 % in 50 years M7.2, (c) PE 2% in 50 years M6.4 and (d) PE 2% in 50 years M8.0.

Similarly Figures 8.9a, b, c and d contain plots of design acceleration time histories at the bridge pier.

8.1.3.3 Vertical Seismic Response of Soil

Herrmann (2000) also recommended that vertical rock motion is of the same order as the horizontal rock motion. *SHAKE91* is used to transmit the horizontal rock motion to the soil surface and/or any other depth. No such solution is available for transmission of vertical motion. Therefore the following procedure was adopted to transfer vertical rock motion to desired elevation.

1. Use *SHAKE* to transfer the P-wave.
2. Adjust peak vertical ground motion to be 2/3 of the peak horizontal ground motion.
3. Adjust the time history to reflect adjustment in (2) above.

The calculated vertical time histories of acceleration at the soil surface, the base of bridge abutment and at the bridge pier were also modified as above.

The time histories of the modified vertical acceleration at the soil surface, the base of the bridge abutment and the base of the pier of each site are presented in Appendix D. It appears that for the horizontal and vertical time histories of any one event:

1. (k_v)max and (k_h)max do not occur at the same instant of time.
2. Frequency contents of these two-motions are quite different.

8.1.4 Liquefaction Potential Analysis

The liquefaction potential of St. Francis sites are evaluated by Seed and Idriss (1971) simplified method as modified by Youd and Idriss (1997). The procedure to obtain liquefaction potential was explained in Section 5.

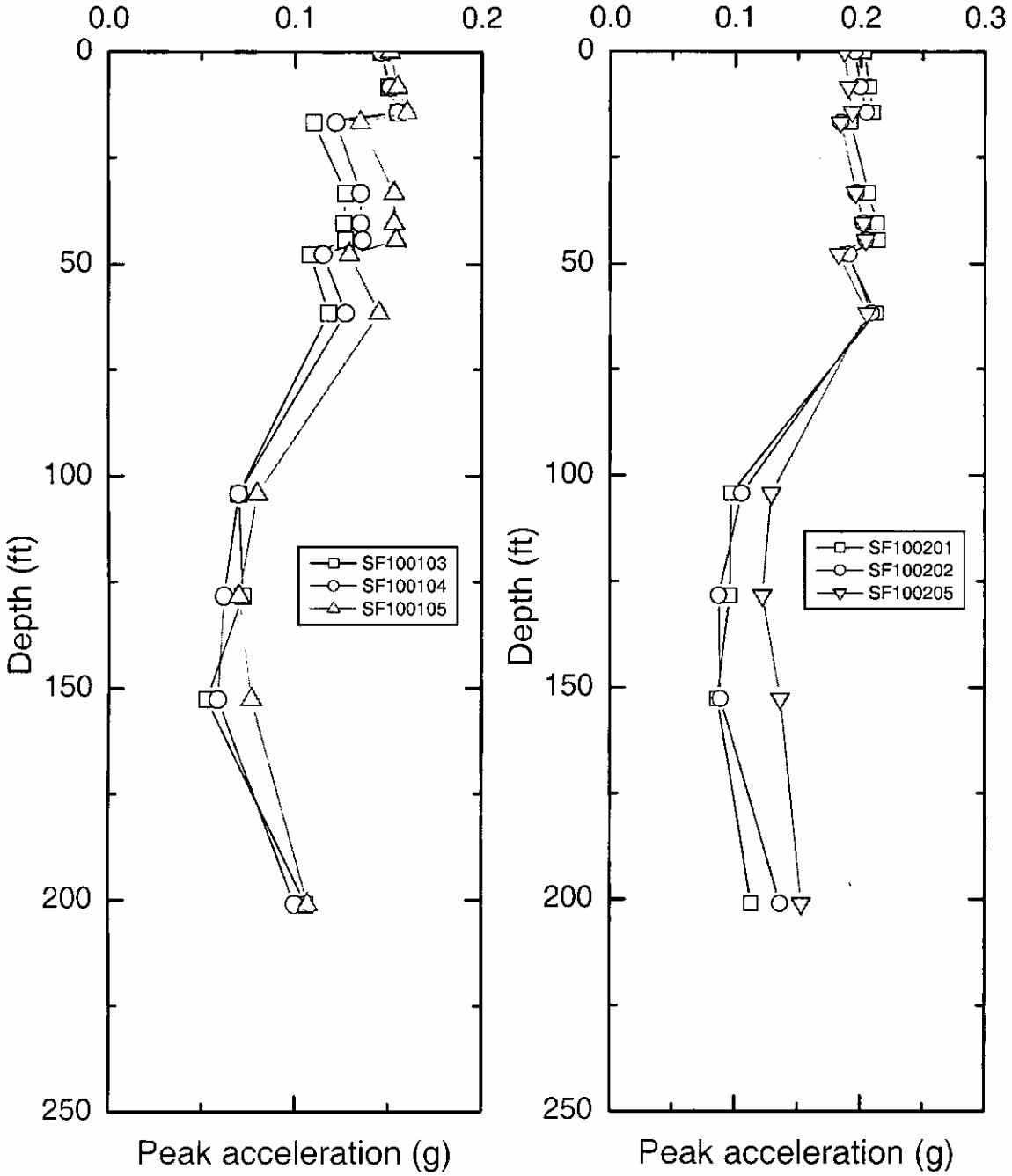

a. Magnitude = 6.2 **b.** Magnitude = 7.2

Figure 8.5 Peak Ground Acceleration vs. Depth for PE 10% in 50 Years Magnitudes 6.2 and 7.2 St. Francis River Site

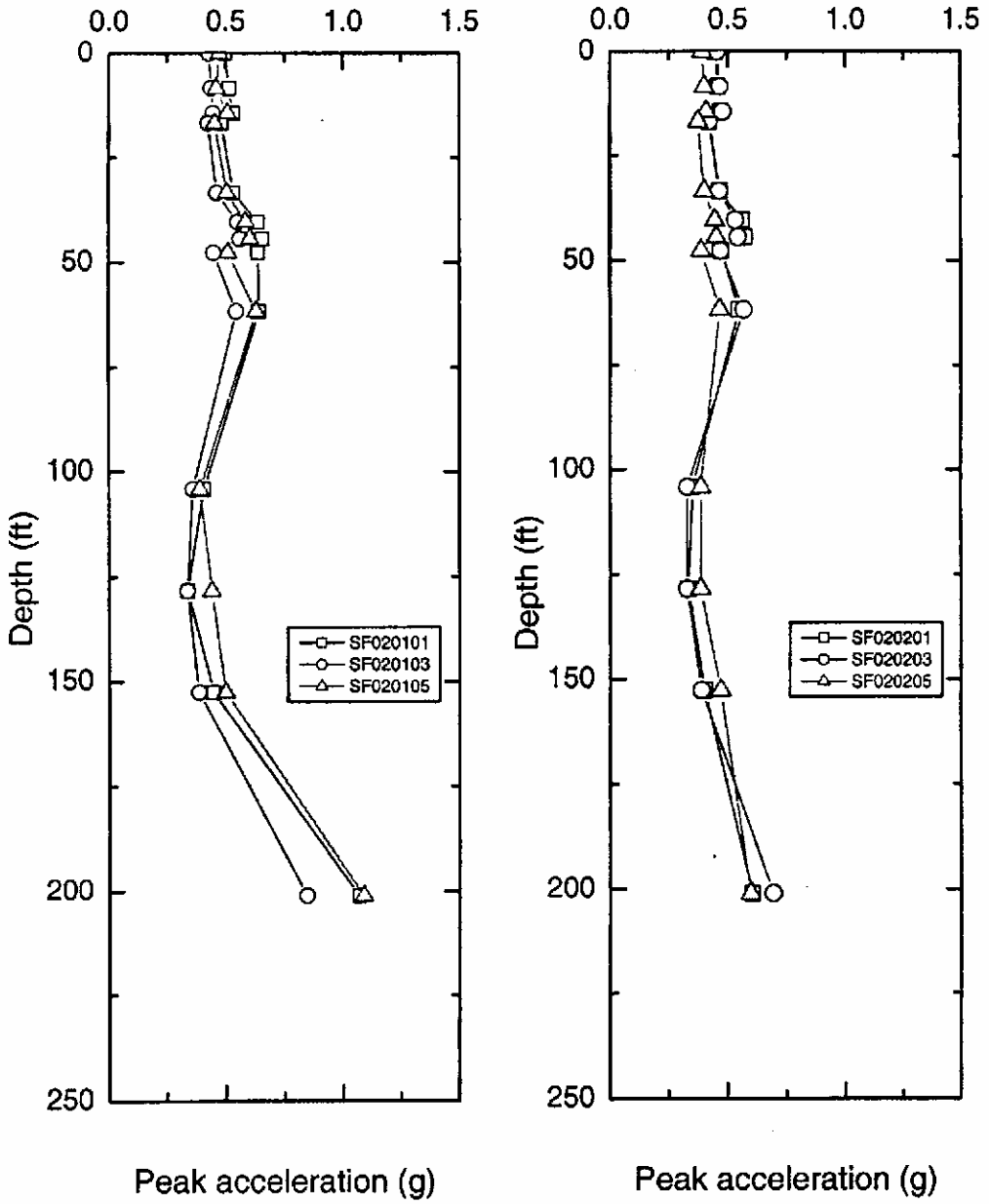

a. Magnitude = 6.4 **b.** Magnitude = 8.0

Figure 8.6 Peak Ground Acceleration vs. Depth for PE 2% in 50 Years Magnitudes 6.4 and 8.0 St. Francis River Site

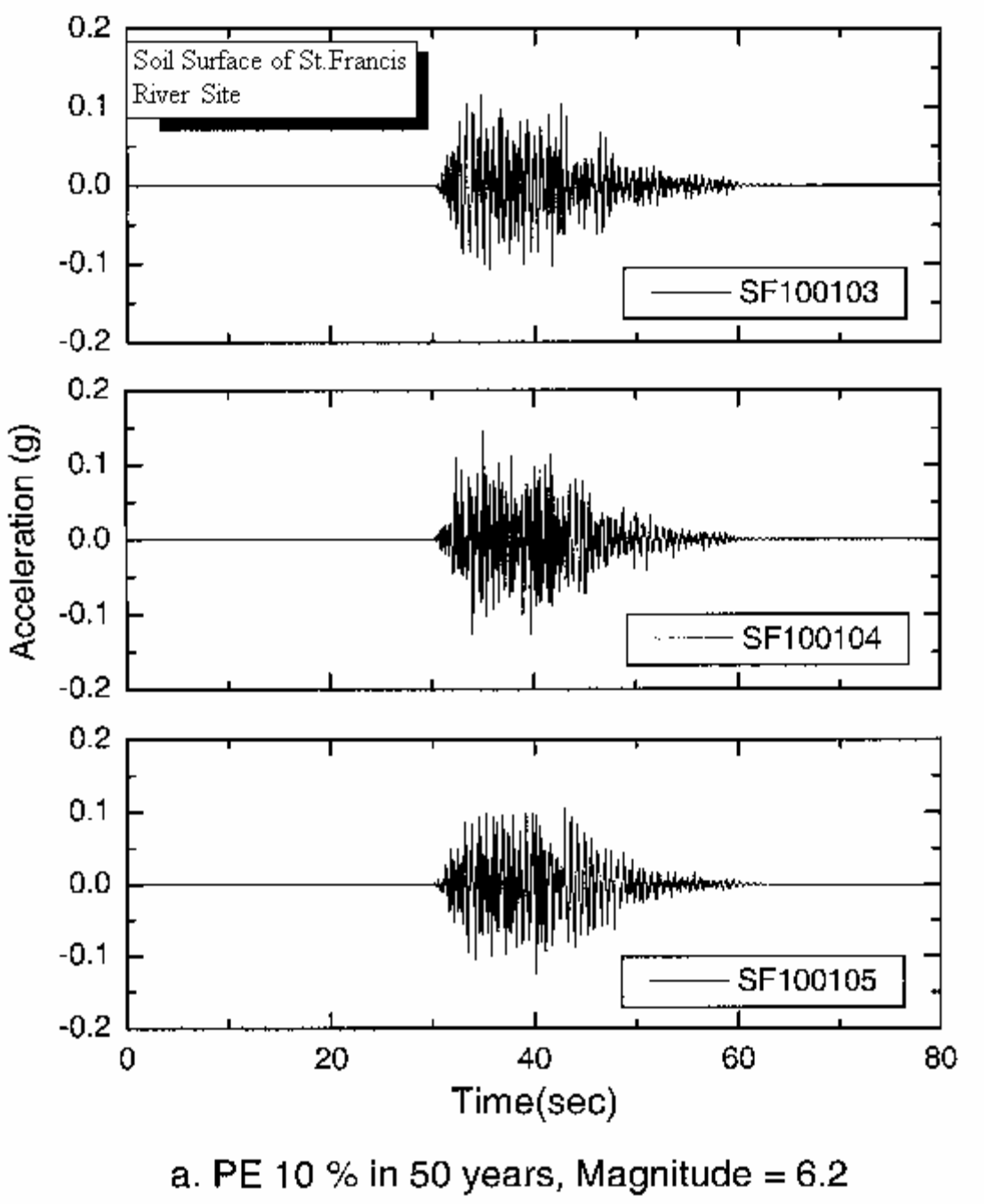

Figure 8.7a Ground Acceleration at the surface of the St. Francis River Site, PE 10% in 50 years, Magnitude = 6.2

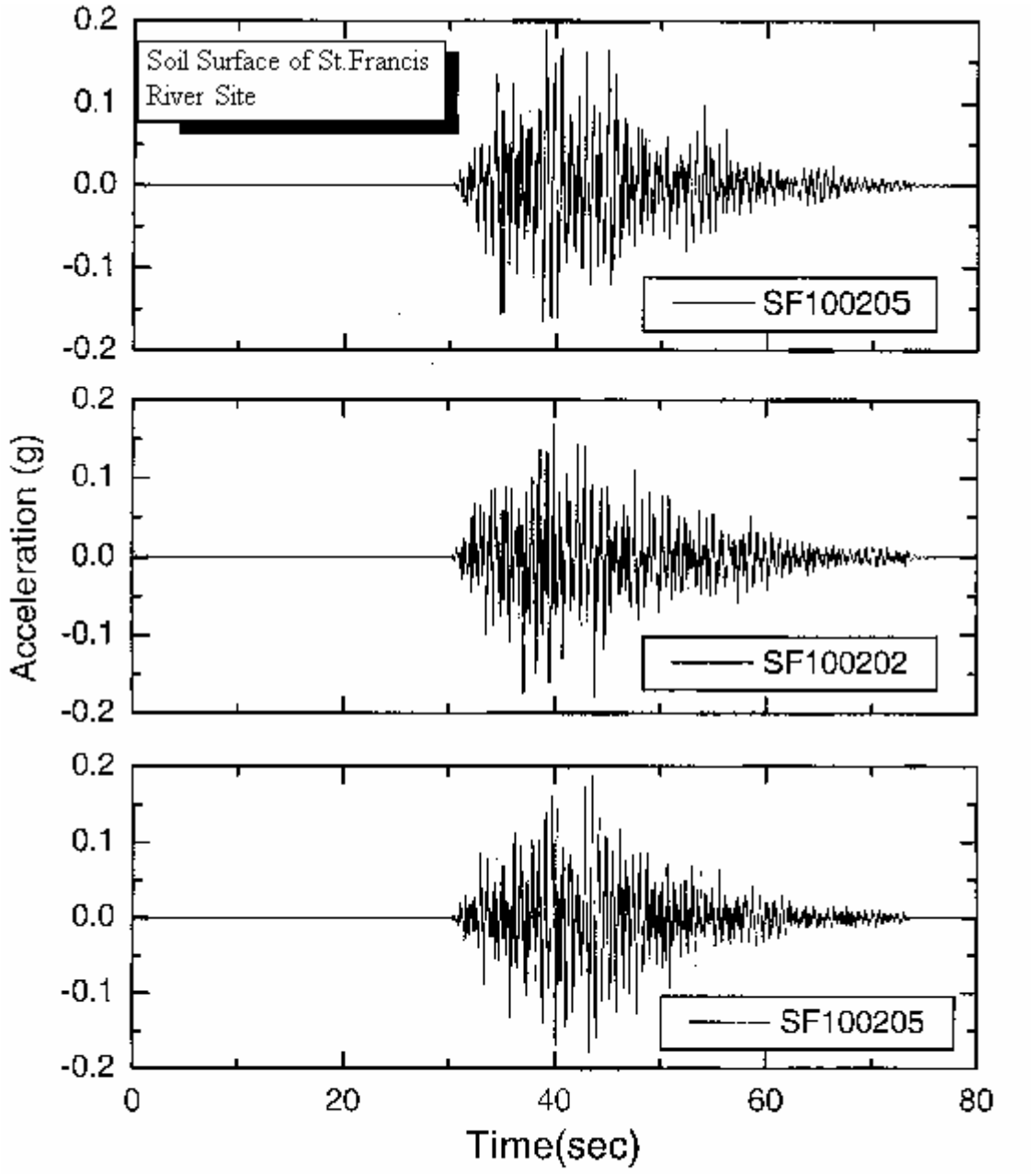

b. PE 10 % in 50 years, Magnitude = 7.2

Figure 8.7b Ground Acceleration at the surface of the St. Francis River Site, PE 10% in 50 years, Magnitude = 7.2

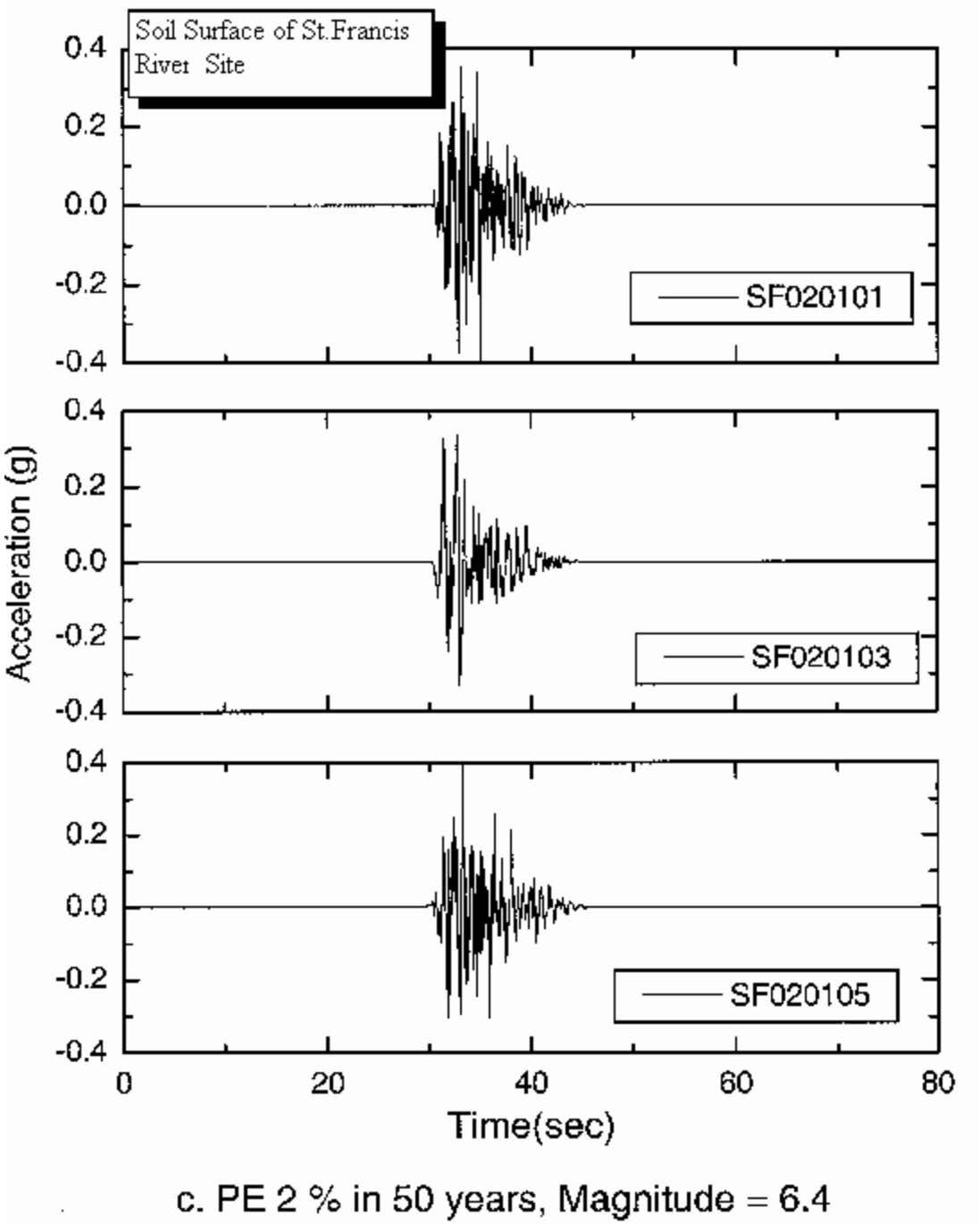

Figure 8.7c Ground Acceleration at the surface of the St. Francis River Site, PE 2% in 50 years, Magnitude = 6.4

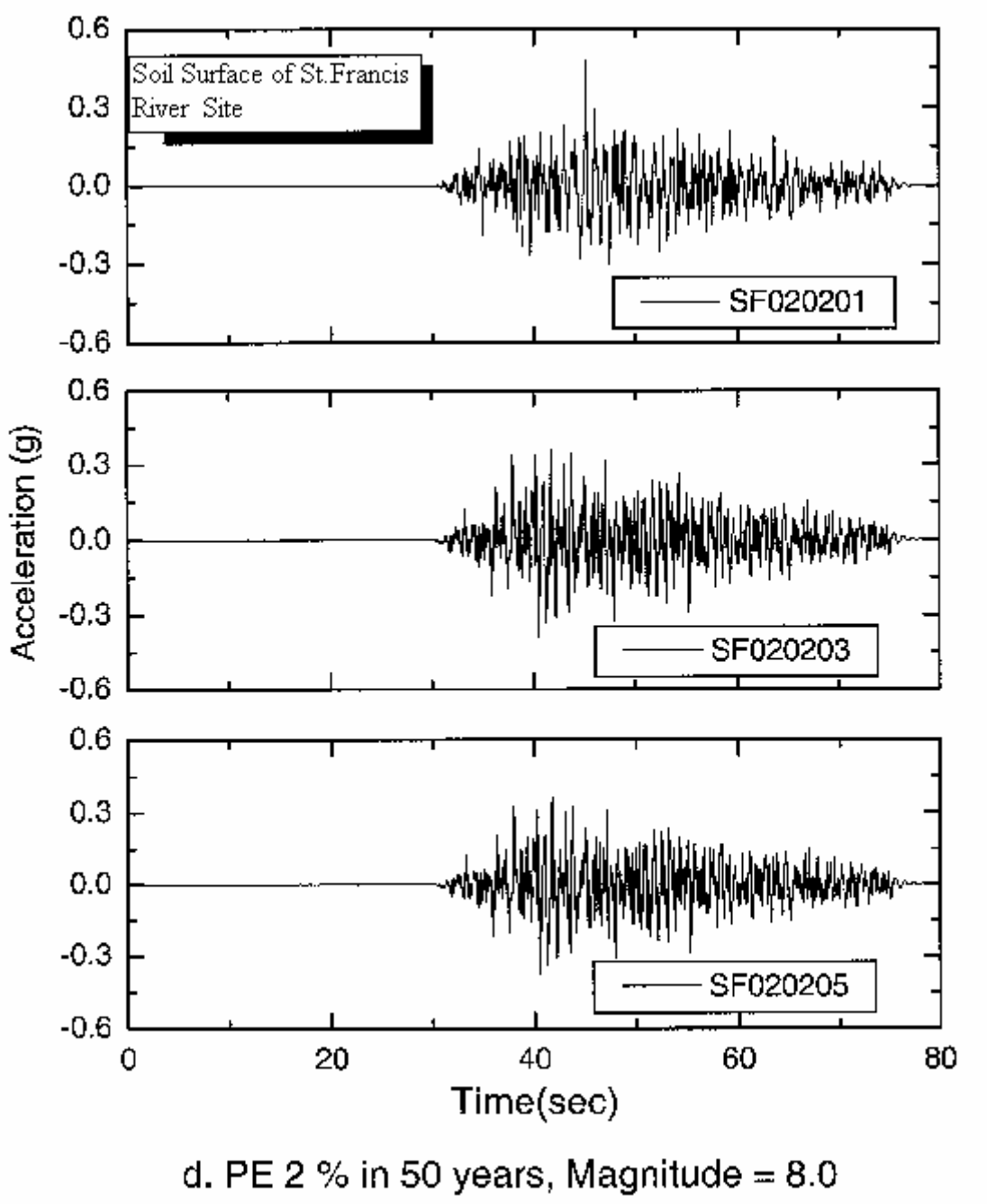

Figure 8.7d Ground Acceleration at the surface of the St. Francis River Site, PE 2% in 50 years, Magnitude = 8.0

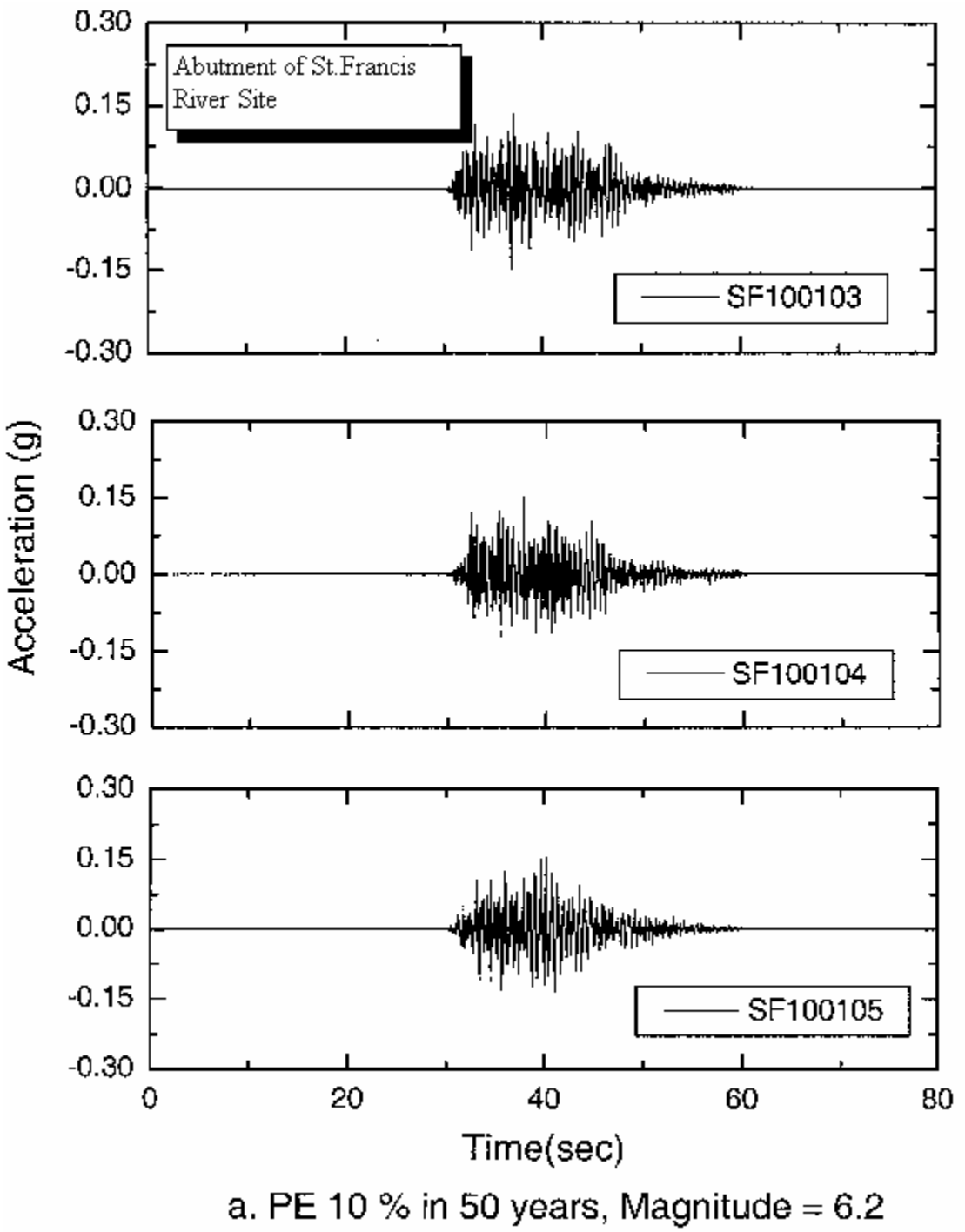

Figure 8.8a Ground Acceleration at the abutment of the St. Francis River Site, PE 10% in 50 years, Magnitude = 6.2

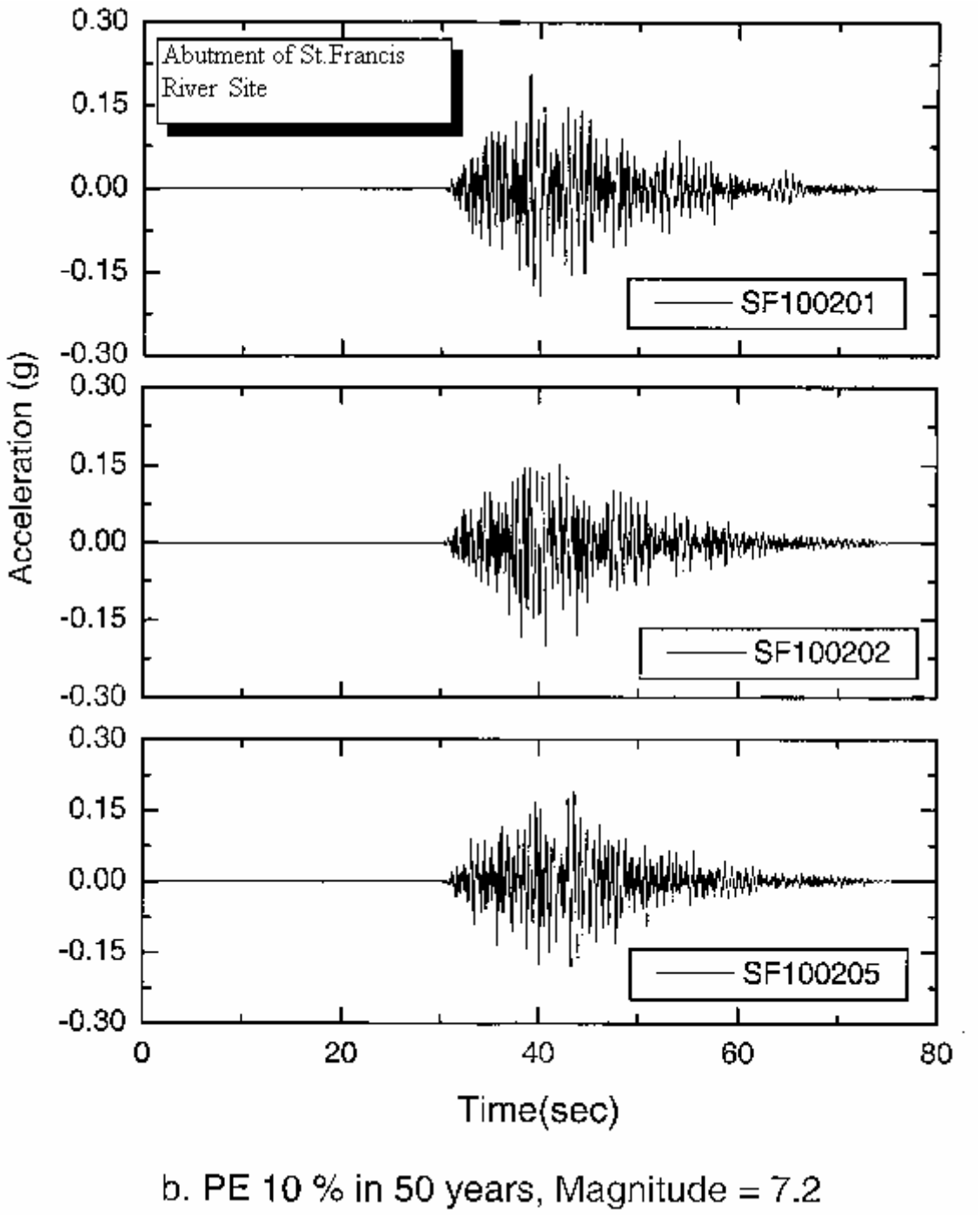

b. PE 10 % in 50 years, Magnitude = 7.2

Figure 8.8b Ground Acceleration at the abutment of the St. Francis River Site, PE 10% in 50 years, Magnitude = 7.2

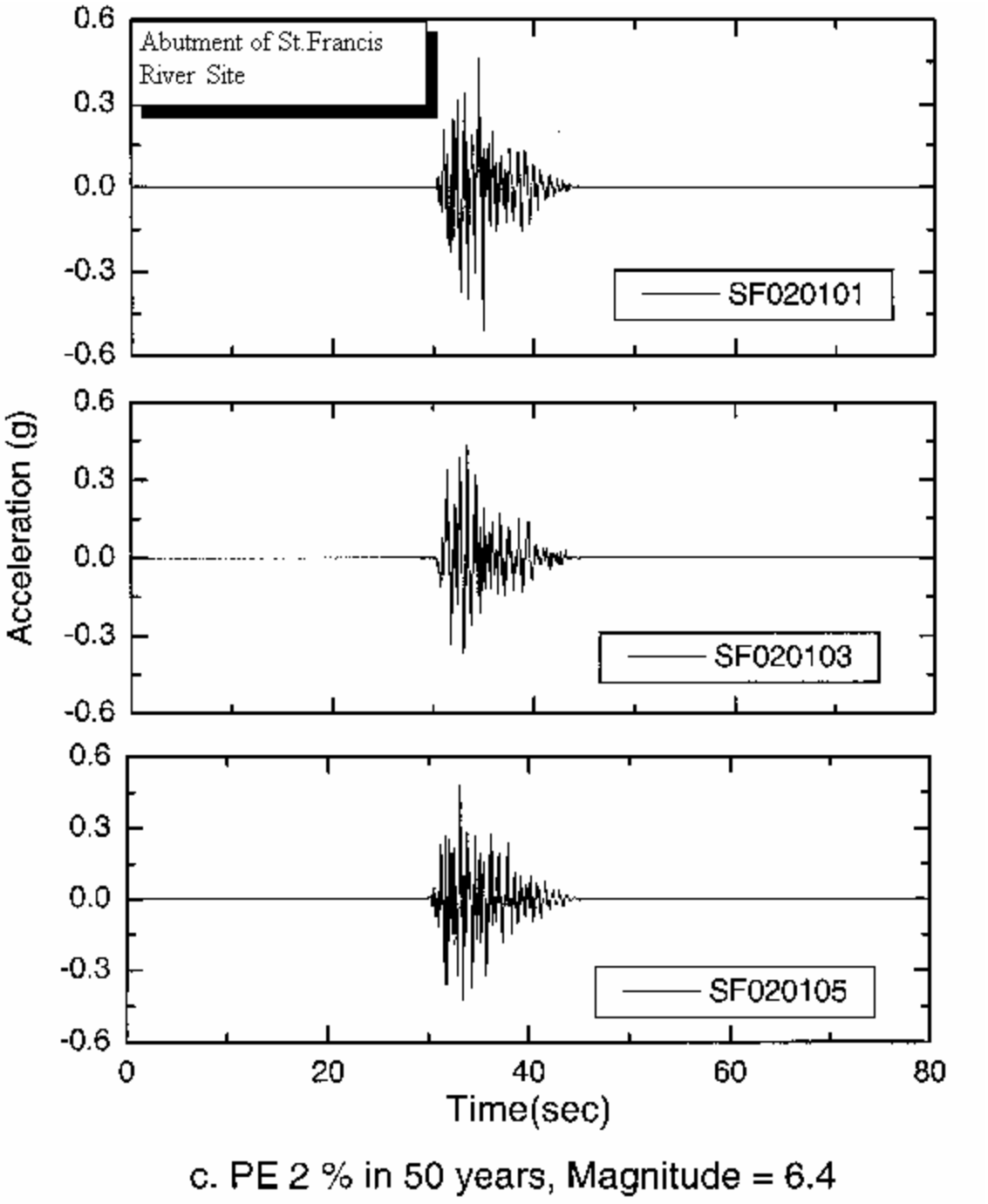

c. PE 2 % in 50 years, Magnitude = 6.4

Figure 8.8c Ground Acceleration at the abutment of the St. Francis River Site, PE 2% in 50 years, Magnitude = 6.4

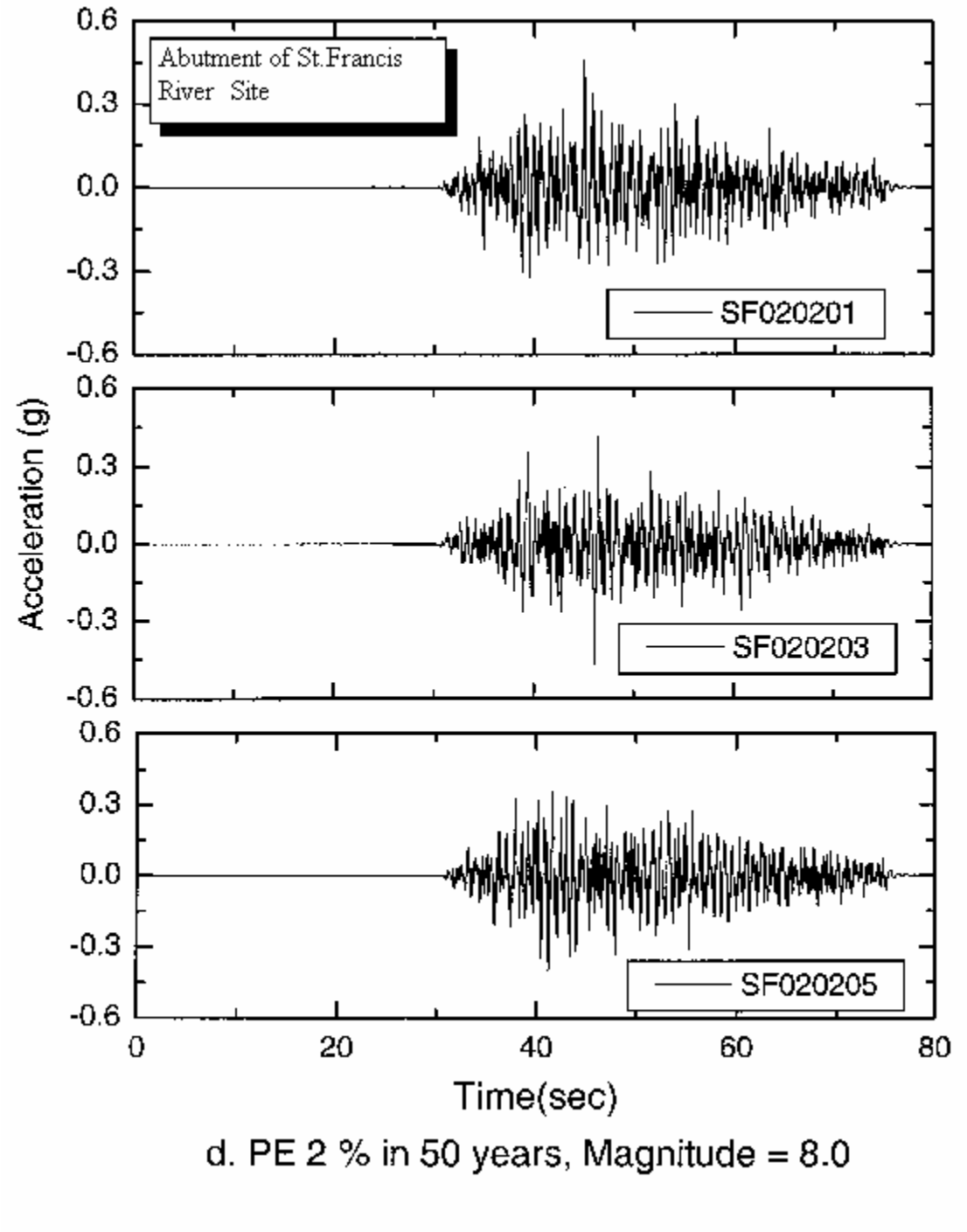

Figure 8.8d Ground Acceleration at the abutment of the St. Francis River Site, PE 2% in 50 years, Magnitude = 8.0

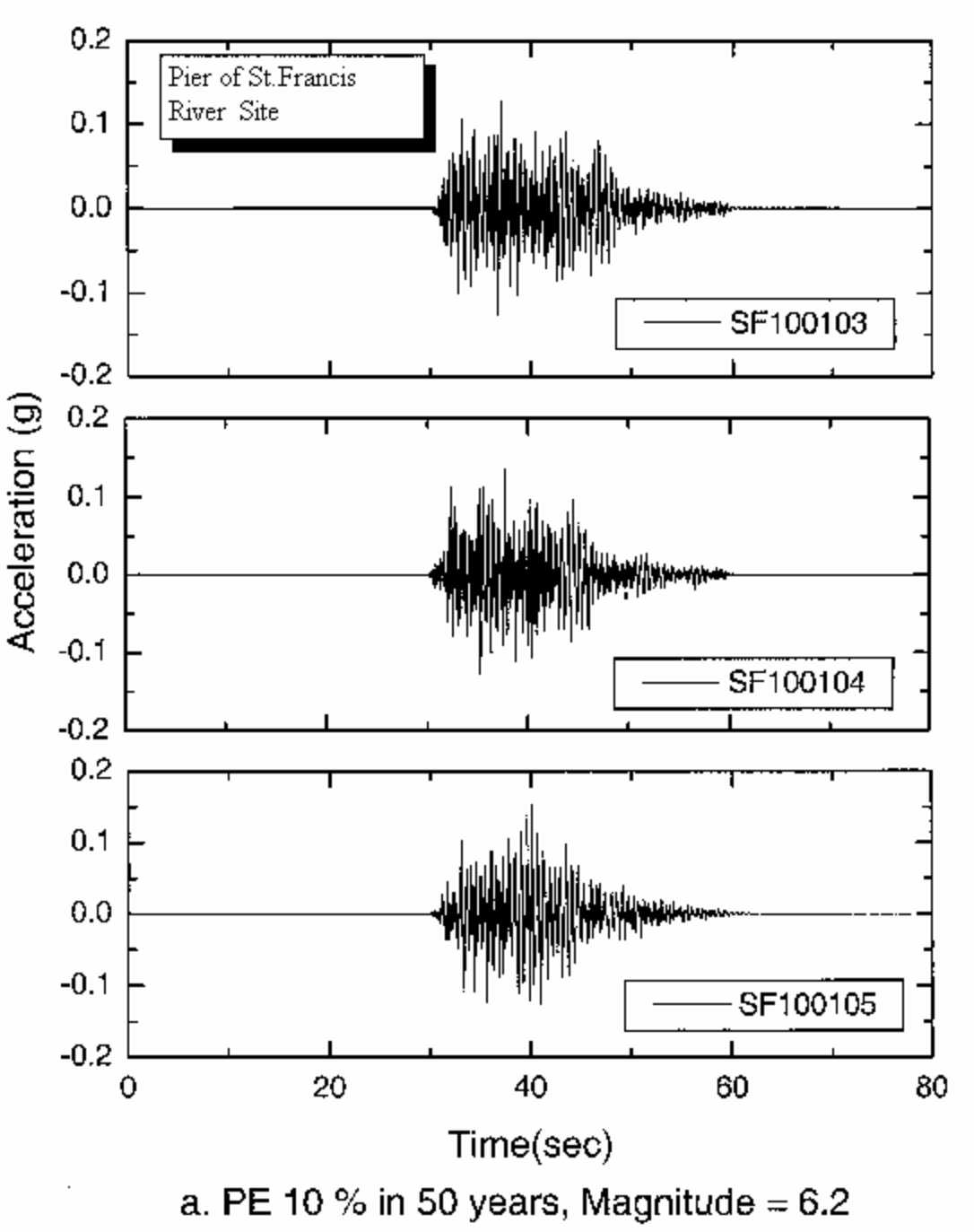

Figure 8.9a Ground Acceleration at the pier of the St. Francis River Site, PE 10% in 50 years, Magnitude = 6.2

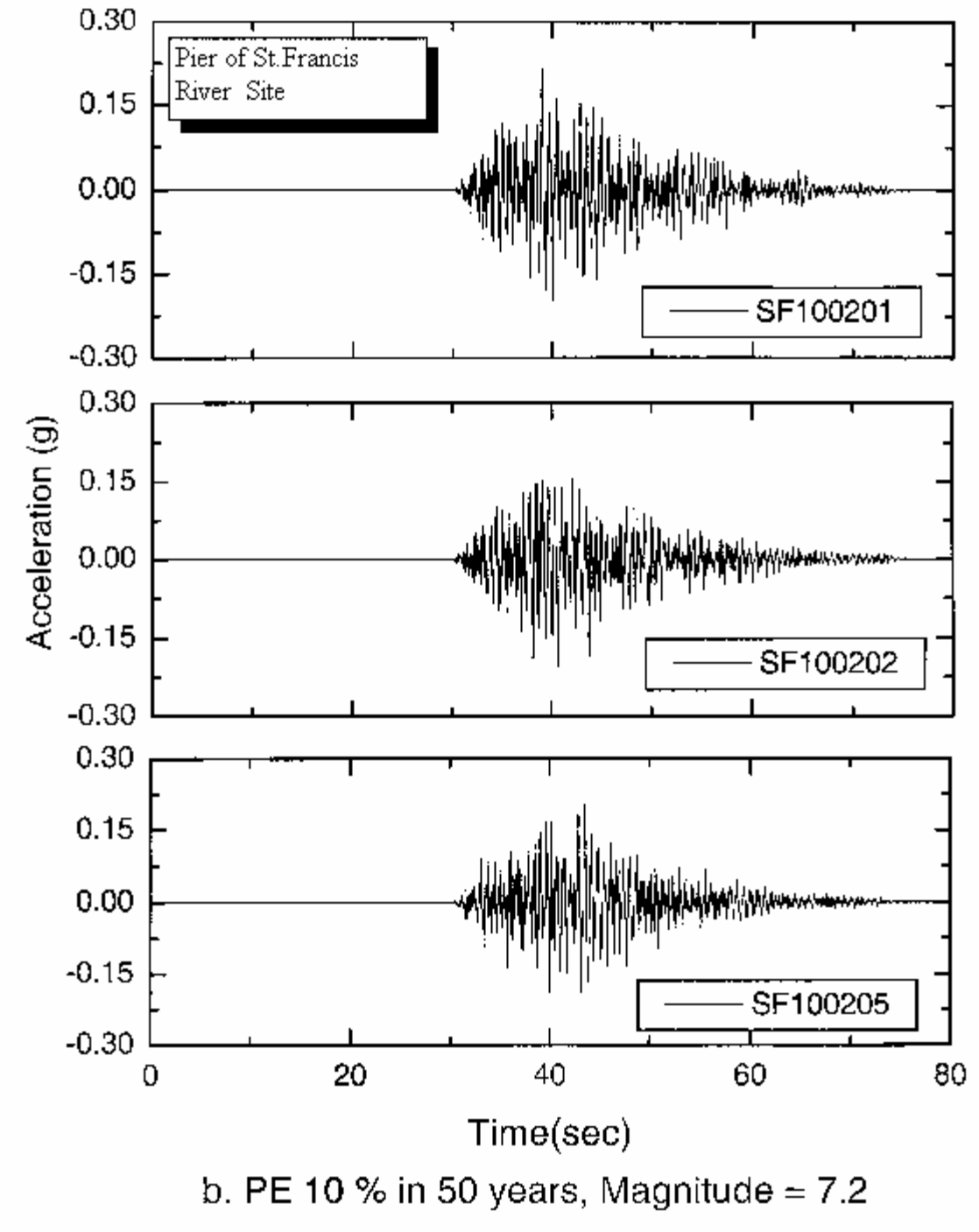

Figure 8.9b Ground Acceleration at the pier of the St. Francis River Site, PE 10% in 50 years, Magnitude = 7.2

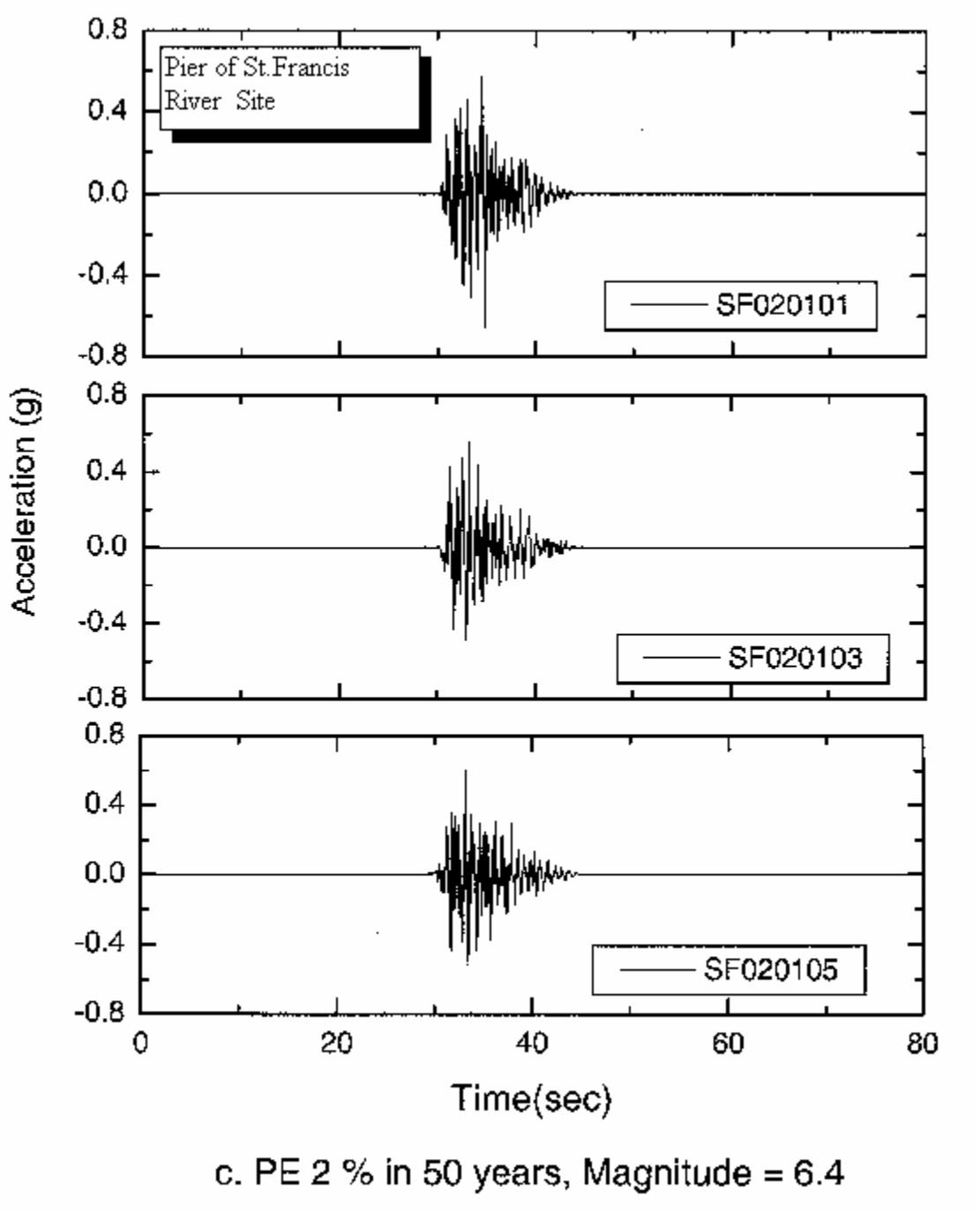

Figure 8.9c Ground Acceleration at the pier of the St. Francis River Site, PE 2% in 50 years, Magnitude = 6.4

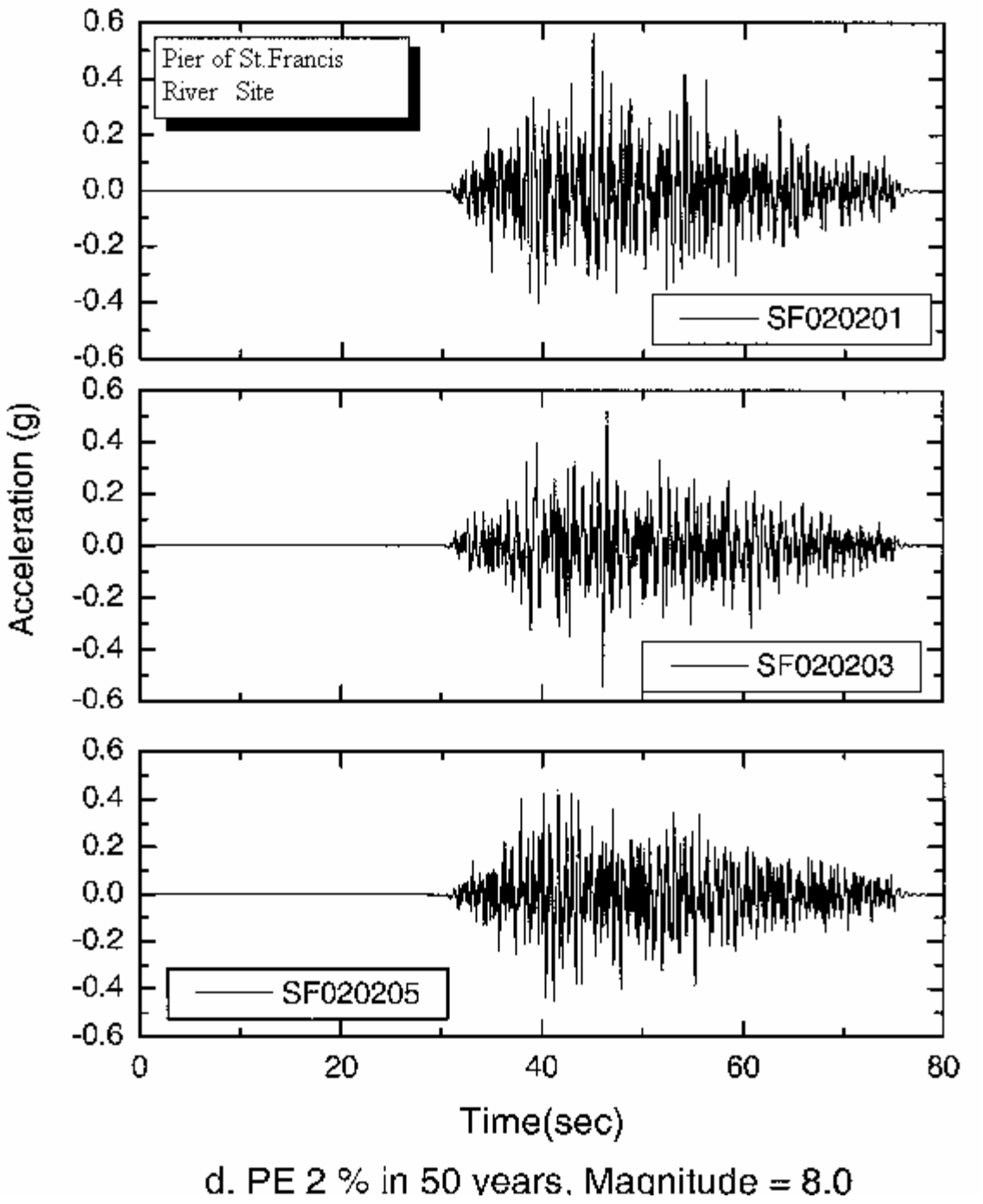

Figure 8.9d Ground Acceleration at the Pier of the St. Francis River Site, PE 2% in 50 years, Magnitude = 8.0

Table 8.2 Detail of Peak Ground Motion Used at the St. Francis River Site Rock Base, Ground Surface, Bridge Abutment and Pier.

a. PE 10% In 50 Years

Name	Max. acc. at rock-base EL. 149.8. (g)	Max acc. at soil-surface EL341.8 (g)	Max acc. at bridge abutment EL 333.4 (g)	Max acc. at bridge pier EL 301.4. (g)
SF100103*	0.106	0.146	0.160	0.126
SF100104*	0.100	0.146	0.160	0.134
SF100105*	0.107	0.151	0.155	0.154
SF100201*	0.113	0.203	0.206	0.214
SF100202*	0.136	0.196	0.200	0.204
SF100205*	0.153	0.187	0.190	0.204

b. PE 2 % In 50 Years

Name	Max. acc. at rock-base EL. 149.8. (g)	Max acc. at soil-surface EL341.8 (g)	Max acc. at bridge abutment EL 333.4 (g)	Max acc. at bridge pier EL 301.4. (g)
SF020101*	1.069	0.497	0.514	0.655
SF020103*	0.845	0.428	0.437	0.560
SF020105*	1.089	0.473	0.490	0.602
SF020201*	0.604	0.447	0.457	0.571
SF020203*	0.693	0.453	0.465	0.544
SF020205*	0.596	0.391	0.400	0.452

8.1.4.1 Cyclic Stress Ratio (CSR), Cyclic Resistant Ratio (CRR) and Factor of Safety (FOS)

Figure 8.10 shows the soil profile and N-values with depth, used for liquefaction analysis. A plot of factor of safety (FOS), CSR and CRR with depth for PE 10% in 50 years and Magnitude 6.2 is plotted as well. It can be seen that the soil does not liquefy for PE 10% in 50 years for Magnitude 6.2. However, for a PE of 10% in 50 years, magnitude 7.2, and for PE 2 % in 50 years and Magnitude 6.4 and 8.0, the soil liquefies to different depths as given in Table 8.4. This table lists the depths of liquefaction for each earthquake magnitude.

8.1.5 Slope Stability of Abutment Fills

Slope stability analyses were completed for seven cross-sections for the St. Francis River Site. Each cross-section was analyzed for both low and high ground-water conditions under static analysis and under three sets of pseudo-static earthquake accelerations. Cross-section locations are shown on Figure 8.1. The soil properties used for the analysis are given in Table 8.4.

An example analysis output for Cross-Section C-C' is shown on Figure 8.11. A summary of the St. Francis River Site analyses is included in Table 8.5. In general, the site slopes appear to be

stable under static conditions, with both low and high ground-water tables, with factors of safety ranging from 1.93 to 3.96. When subjected to an earthquake with a 10% exceedance probability in 50 years (10%PE), slopes continue to show stability, with factors of safety ranging from 1.19 to 3.91. When subjected to an earthquake with a 2% PE, factors of safety less than or approximately equal to one are calculated for all cross-sections except G-G' for low water conditions, and all section for high water conditions. The analysis set 2, using adjusted PHGA with corresponding adjusted PVGA showed the lowest factors of safety. Expected failure planes pass through both the roadway and bridge piers.

Table 8.3 The Different Zones of Soil Liquefaction for Different Factors of Safety, St. Francis River Site

Factor of Safety	Zones of Soil Liquefaction			
	PE 10% in 50 years		PE 2% in 50 years	
	M6.2	M7.2	M6.4	M8.0
< 1.0	No	10-12.5	8-22, 64-68, 71-85	6-110
< 1.1	No	9-13	8-24, 64-68, 70-91	6-145
< 1.2	No	8–14, 19-20	8-32, 61-93	6-180
< 1.3	No	8–15, 18–20	8-44, 61-94	5-180
< 1.4	No	8–16, 18–20, 64–65, 75-80	8-94	5-180

Table 8.4 Soil Properties Used for the Slope Stability Analysis, St. Francis River Site

Soil Characteristics*				
Class	γ_{moist} (pcf)	$\gamma_{saturated}$ (pcf)	c (psf)	ϕ (deg.)
CL	121.3	133.5	860	30
ML	106.0	122.5	450	34
SM	115.0	127.0	50	35
SP	134.9	141.9	0.0	40

* Soil characteristics obtained from slope stability procedures, Section (5.5.1)

These results indicate that slopes at the St. Francis River Site are expected to be stable under small earthquake shaking (10% PE), and unstable at higher levels of shaking (2% PE), regardless of the ground-water level.

8.1.6 Flood Hazard Analysis Results

Flood hazards were estimated assuming that an earthquake caused catastrophic failure of waterway levees in the vicinity of US 60 or failure of the Wappapello Dam, located approximately eight miles north of US 60. Hazards were estimated based solely on relative elevations of land and waterways, assuming complete failure of either levees or of the dam. The likelihood of such failure during an earthquake was not calculated, so the flood hazard analysis is considered a worst-case scenario. However, levee or dam failure was assumed to occur during moderate flow conditions and not during flood or elevated water conditions in the waterways.

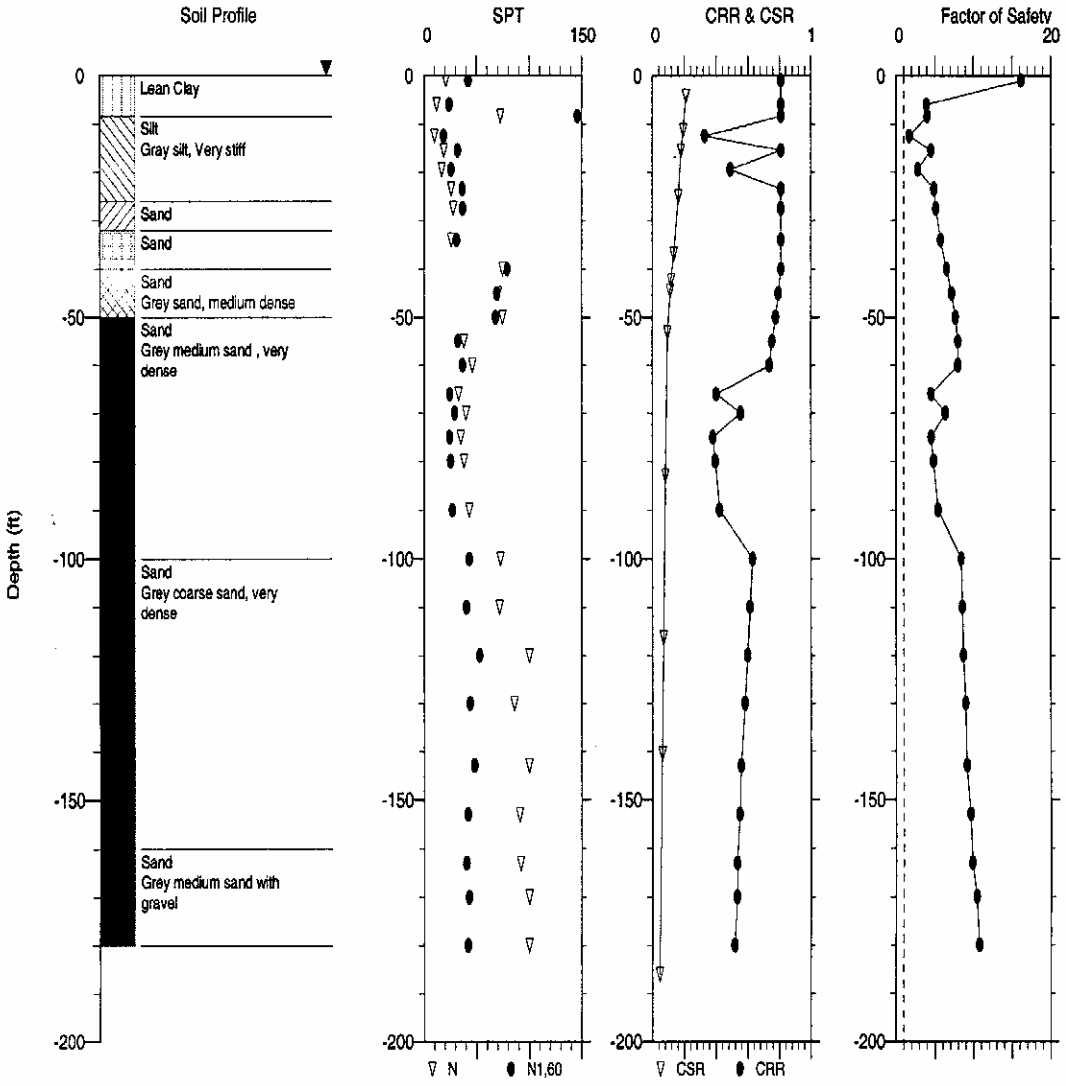

Notes:
CSR analysis using SHAKE results.
CSR File: D:\I-O SF Pe10%\SF100103\Sf100103.grf
CRR using SPT Data and Seed et. al. Method in 1997 NCEER Workshop.
Earthquake File for SHAKE Analysis: D:\SF\SF100103.ACC
Earthquake Magnitude for CRR Analysis: 6.2
Magnitude Scaling Factor (MSF): 1.62
Depth to Water Table for CRR Analysis (ft): 0
Depth to Water Table for Cn Calculation (ft): 0
Depth to Base Layer for CSR Analysis (ft): 219.6
MSF Option: I.M. Idriss (1997)
Cn Option: Liao & Whitman (1986)
Ksigma Option: L.F. Harder & R. Boulanger (1997)
SPT Energy Ratio: USA/Safety/Rope: 0

Figure 8.10 Soil Profile, CSR, CRR and Factor of Safety Against Liquefaction at the St. Francis River Site for PE 10% in 50 years and Magnitude = 6.2

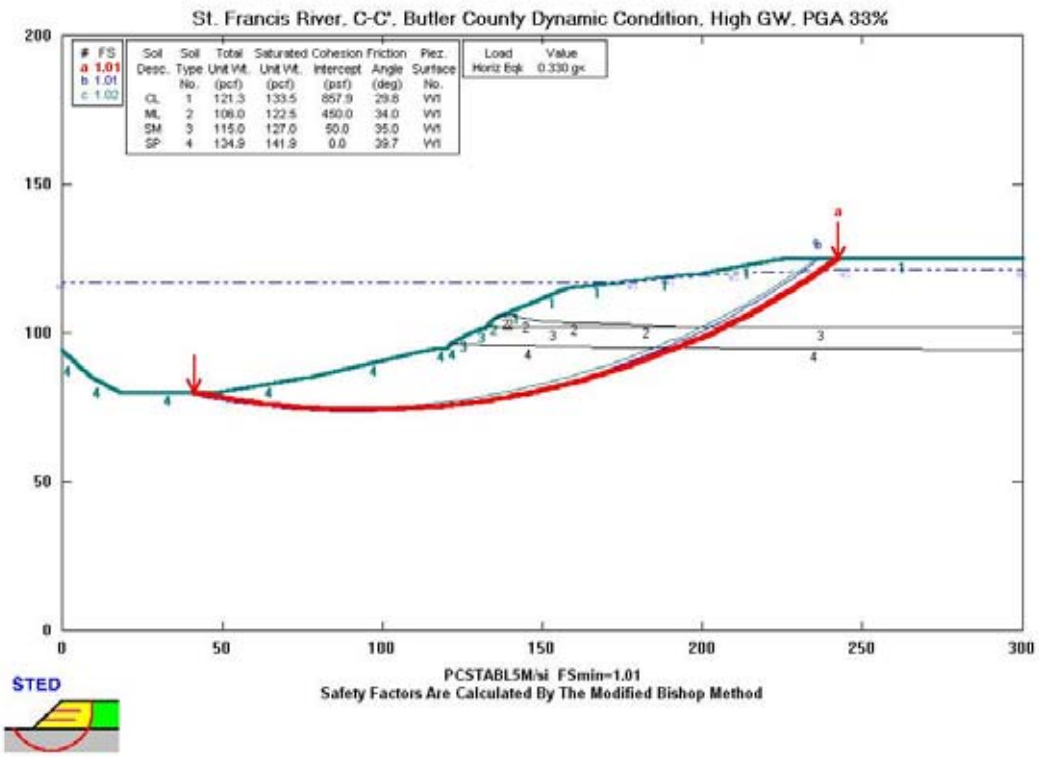

Figure 8.11 Example Slope Stability Results for St. Francis River Site

Evaluation of the effects of catastrophic failure of the Wappapello Dam was completed by USACE (1985). In general, they concluded that the peak flooding elevation in the vicinity of US 60 would be 340.0, cresting approximately two hours after failure. The estimated flooded zone is shown on Figure 8.12. This zone includes 5.7 miles of roadway from the St. Francis River eastward to approximately 0.4 miles west of Highway WW/TT (which leads to Dudley), and 3.4 miles of roadway from approximately 0.3 miles east of Highway WW/TT eastward to Highway ZZ. Highway WW/TT runs along the Dudley Ridge, which is slightly higher in elevation than the surrounding land.

Evaluation of the effects of flooding due to failure of levees was based on a series of topographic maps covering the entire study section of US 60 (Figure 8.13). This evaluation was field checked by visual observation of the elevation of the roadway compared to surrounding land. Some of the maps were as old as 1962 vintage without photo revision, so the estimate of the limits of potential flooding should be considered tentative. Furthermore, the roadway elevation was shown only to 5-foot accuracy, and slight elevations or depressions in the roadway could significantly

Table 8.5 Slope Stability Results for the St. Francis River Site

Factor of Safety for Most Sensitive Potential Failure Plane							
Cross-Section	A - A'	**B – B'**	**C – C'**	**D –D'**	**E – E'**	**F – F'**	**G – G'**
Static							
Low GW	2.63	2.76	2.88	2.71	2.52	1.93	3.96
High GW	3.06	3.14	3.48	3.23	2.87	2.02	2.67
Pseudo-Static Set 1* 10% PE in 50 years							
Low GW (0.135)	1.73	1.74	1.82	1.79	1.59	1.41	2.60
High GW (0.135)	1.61	1.68	1.78	1.72	1.64	1.23	1.74
2% PE in 50 years							
Low GW (0.331)	1.31	1.10	1.17	1.18	1.08	0.98	1.71
High GW (0.331)	0.93	0.97	1.01	1.00	0.94	0.74	1.08
Pseudo-Static Set 2 10% PE (HGA, VGA)							
Low GW (0.135,+0.048)	1.68	1.64	1.76	1.74	1.55	1.39	2.59
Low GW (0.135,-0.048)	1.77	1.75	1.87	1.83	1.62	1.43	2.62
High GW (0.135,+0.048)	1.55	1.61	1.71	1.66	1.54	1.19	1.64
High GW (0.135,-0.048)	1.67	1.73	1.84	1.77	1.63	1.26	1.75
2% PE (HGA, VGA)							
Low GW (0.331,+0.170)	0.95	0.91	0.97	0.99	0.92	0.84	1.58
Low GW (0.331,-0.170)	1.28	1.26	1.33	1.32	1.20	1.08	1.82
High GW (0.331,+0.170)	0.70	0.74	0.78	0.78	0.74	0.57	0.88
High GW (0.331,-0.170)	1.10	1.14	1.20	1.17	1.09	0.86	1.25
Pseudo-Static Set 3 10% PE (HGA, VGA)							
Low GW (0.012,+0.090)	2.50	2.50	2.71	1.80	2.21	1.89	3.91
Low GW (0.012,-0.090)	2.57	2.61	2.81	1.95	2.24	1.89	3.74
High GW (0.012,+0.090)	2.89	2.98	3.29	3.08	2.74	1.95	2.50
High GW (0.012,-0.090)	2.87	2.94	3.25	3.02	2.70	1.91	2.62
2% PE (HGA, VGA)							
Low GW (0.014,+0.221)	2.39	2.37	2.58	2.49	2.14	1.88	4.06
Low GW (0.014,-0.221)	2.59	2.66	2.86	2.66	2.23	1.89	3.65
High GW (0.014,+0.221)	2.90	2.46	3.28	3.11	2.78	1.95	2.34
High GW (0.014,-0.221)	2.85	2.91	3.21	2.96	2.68	1.88	2.67

* Peak ground acceleration values calculated with the computer program *SHAKE* Section 5.4.
HGA – Horizontal Ground Acceleration
VGA – Vertical Ground Acceleration
PE – Probability of Exceedance in 50 years

change the degree of anticipated flooding. In general, the following conditions are expected for each waterway along the study section, presented in order from west to east:

1. Blue Spring Slough – Failure of the levee could potential flood a 1-mile section of the roadway flanking the slough and a 0.25 section of the roadway 1 mile west of Highway FF.

2. St. Francis River – The river is entrenched within a levee, and then flanked by a natural floodplain bounded by a second levee to the west and higher ground to the east. Failure of the levees could potentially flood two 0.25-mile sections of roadway near Highway 51 slightly less than a mile east of the river.

1. Mingo, Cypress Creek Lateral, and Prairie Creek Ditches – Failure of the levees for these ditches could potentially flood the same two sections of roadway at risk from the St. Francis River, as well as a 0.25-mile section of roadway located 0.75 miles west of the Cypress Creek Lateral Ditch. Flooding would be limited by levees that did not fail.

2. Lick Creek – The roadway appears to be elevated above the surrounding land in this area, and flooding is not anticipated.

3. Unnamed Creek 1 mile West of Essex – Failure of levees could potentially flood a 0.1-mile section of roadway.

4. Bess Slough – It appears that the roadway is elevated in the vicinity of this waterway, except for a 0.5 mile section located 0.5 to 1 mile west of Highway FF, which may possibly flood in the event of a levee failure.

5. Six Unnamed Ditches Between Bess Slough and the Castor River – The roadway and surrounding fields appear to be elevated between Highways FF and N to the west. Areas to the east which may potentially flood include a 0.5 mile section located 0.5 to 1 mile east of Highway N, 2 sections 100 to 300 feet in length located 1 to 1.25 miles east of Highway N, and a 1 mile section located 1.5 to 2.5 miles east of Highway N.

6. Castor River – The river appears to be separated from the original flow source and is expected to have a limited flowing length and flooding potential.

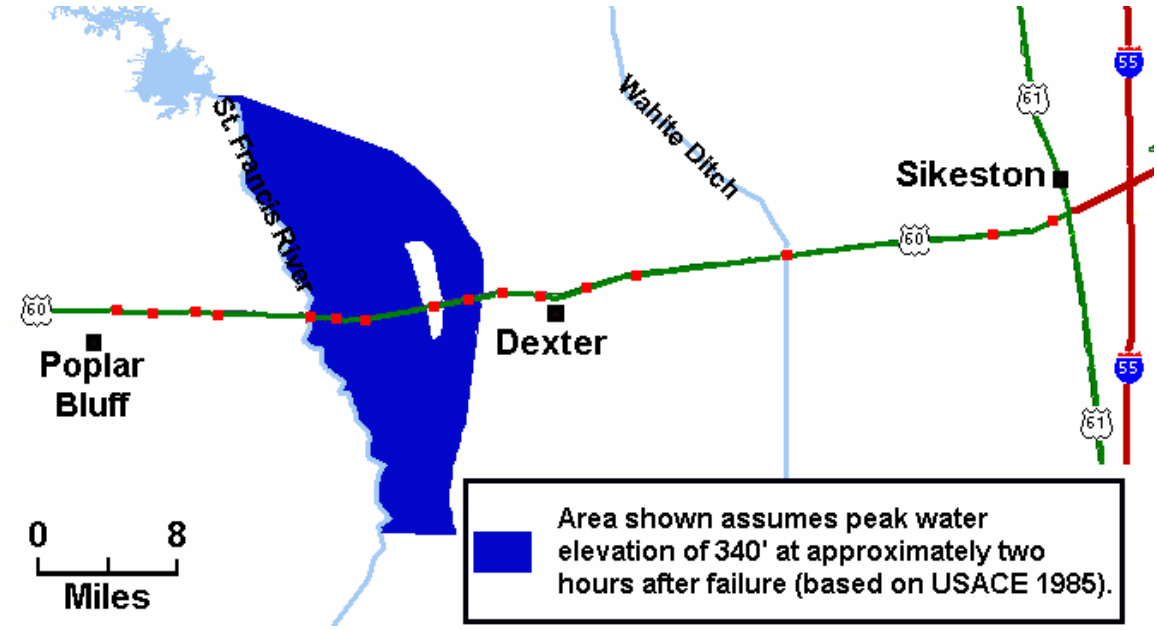

Figure 8.12 Estimated Flooding Zone Due to Wappapello Dam Failure

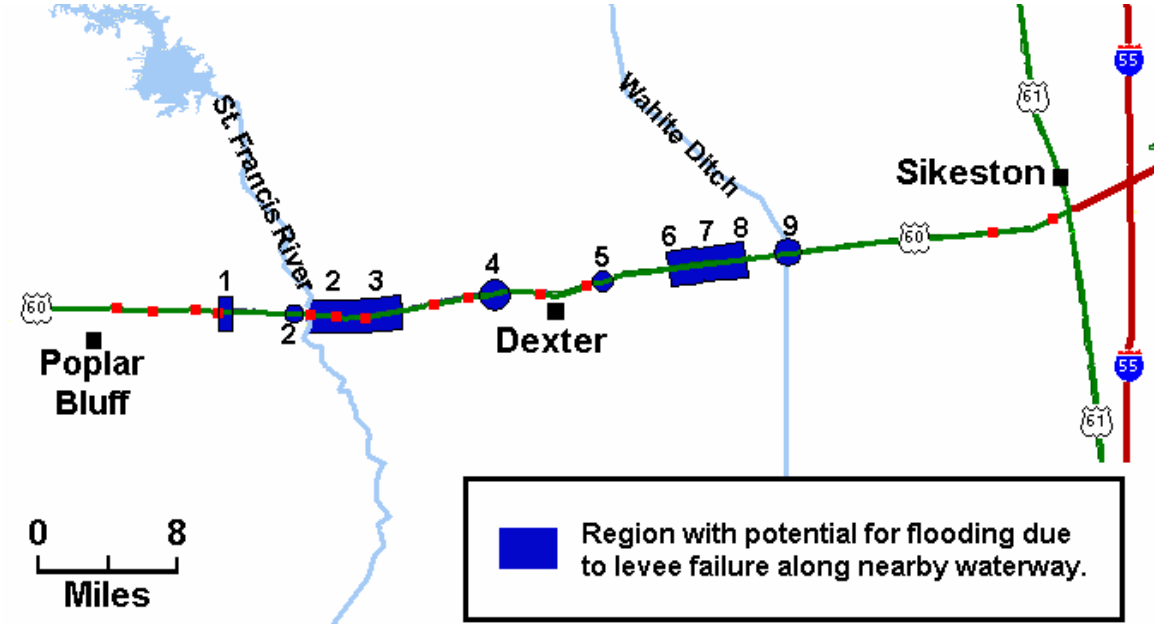

Figure 8.13 Region of Potential Flooding

8.1.7 Structure Response of Bridges and Abutments

8.1.7.1 New St. Francis River Bridge

The bridges of interest for this project are located near the New Madrid seismic zone in southeastern Missouri. These bridges were modeled in order to determine their susceptibility to earthquake damage under various ground motions. They were of particular concern for the Missouri Department of Transportation, as they are located on a key emergency route that must be kept open in the event of an earthquake.

8.1.7.1.1 Bridge Description

The bridge discussed in this section is denoted as Bridge A-3709, located in Butler-Stoddard County on US 60 where it crosses the St. Francis River. It was designed with seismic considerations according to the 1992 AASHTO Specifications. This 292 foot 8 inch bridge consists of three continuous spans supported by steel plate girders, as shown in Figure 8.14. The dimensions of these plate girders varied slightly within a span depending on the location of the tension flange. The interior diaphragms and the cross-frames each consist of two L 3x3x5/16 crossed over one another. The top and bottom horizontal members on the diaphragms and cross-frames were L 4x4x5/16. All interior diaphragms were placed perpendicular to the girders. The bridge, however, was placed at a 20^{o} skew angle, so the ends of the girders were offset from one another at the ends of the bridge. The cross-frames were constructed differently than the diaphragms in that they were placed parallel to the abutments, and therefore were not perpendicular to the girders.

The bridge superstructure is supported by two intermediate bents through fixed neoprene elastomeric pads and two integral abutments at its ends. Each bent consists of a reinforced concrete cap beam and three reinforced concrete columns. Deep pile foundations support both bents and abutments. There are 20 piles for each column footing and 11 piles for each abutment footing.

8.1.7.1.2 Bridge Model and Analysis

In order to later analyze this bridge for susceptibility to earthquake damage, the structure was modeled with the finite element method in the *SAP2000* structural analysis program. In this program, the bridge can be modeled in three dimensions, and earthquake input data can be used to simulate how the bridge would respond in the event of an earthquake.

All of the components of the structure were included in the bridge model. These components include the girders, diaphragms, cross-frames, interior bents and columns, and the bridge deck. The deck was represented by 241 shell elements with a thickness of 8.5 inches. All girders, cross-frames, and diaphragms were modeled as 927 frame members. Each frame section was then assigned member properties, such as material type and cross-section dimensions. The model also included 792 nodes.

To further assist in modeling ground soil conditions, springs were used at the base of each column (six columns total, three on each interior bent). Also, springs were placed at the ends of the bridge on each abutment. The stiffness constants of the springs were taken from Appendix F.

Rigid elements were used to model the abutments in *SAP2000*. Because of their presence, the bridge is relatively stiff and is expected to experience small displacements during earthquakes. Therefore, a linear time-history analysis was used for the bridge model. For each analysis with one directional earthquake excitation, 30 Ritz-vectors were considered associated with the earthquake direction. In Table 8.6, a sampling of five of the significant vibration modes are listed with its period in seconds and a brief description of the motion represented within the given mode. It should be noted that the fundamental period of the bridge is 0.2519 seconds. In Figures 8.15-8.19, visual representations of the mode shapes described above are shown.

The bridge was analyzed under a total of twelve earthquake ground motions described in Section 8.1.3. Six of the twelve motions correspond to a 10% PE level while the others to a 2% PE level. At each PE level of earthquakes, three were considered as near-field and the other three as far-field. The internal loads such as shear and moments and the abutment displacements were obtained at various critical locations. They will be presented together with the vulnerability evaluation of structural members in the next section. It is noted that one bridge analysis was conducted for

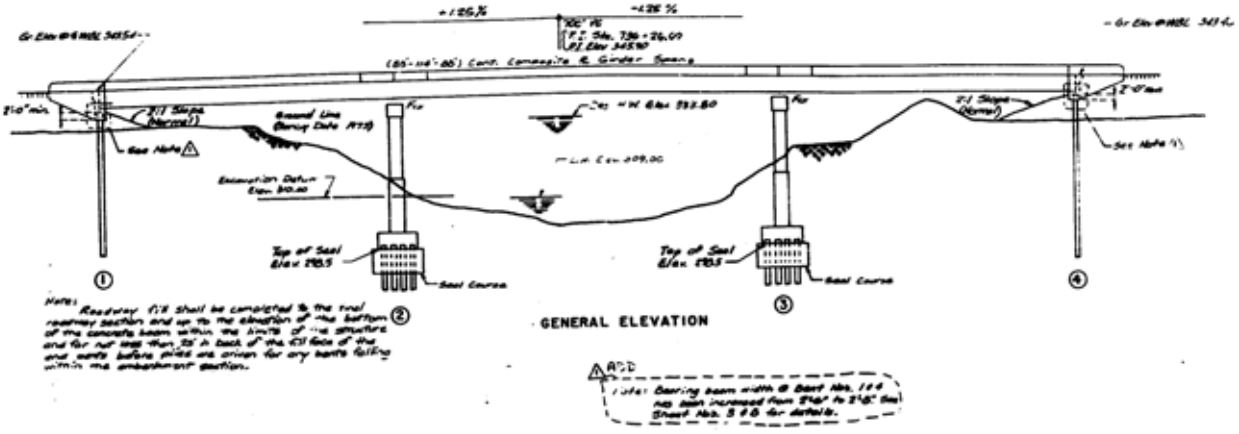

Figure 8.14 Bridge General Elevation (New St. Francis River Bridge)

Table 8.6 Natural Periods and Their Corresponding Vibration Modes (New St. Francis River Bridge)

Mode Number	Period (seconds)	Motion Description
1	0.2519	Transverse
2	0.2295	Transverse
3	0.1421	Vertical
4	0.0901	Longitudinal
5	0.0896	Longitudinal

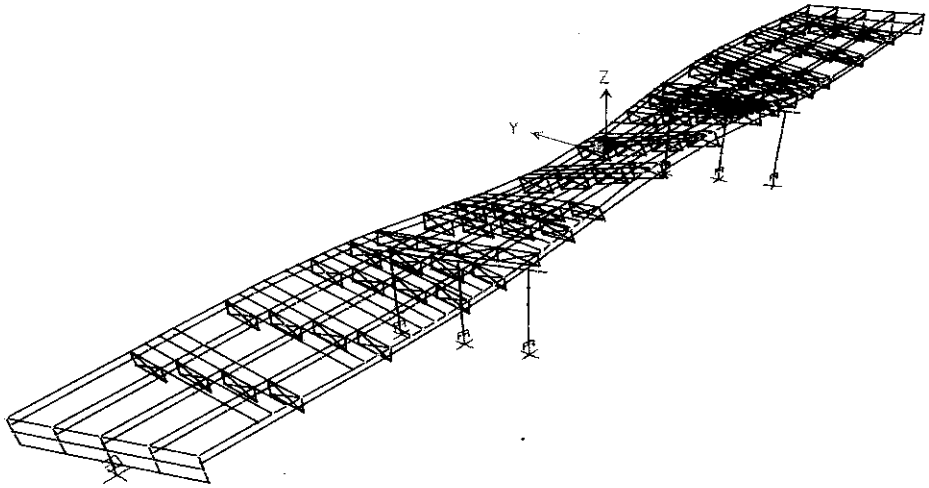

Figure 8.15 Mode 1, Period 0.2519 Seconds (New St. Francis River Bridge)

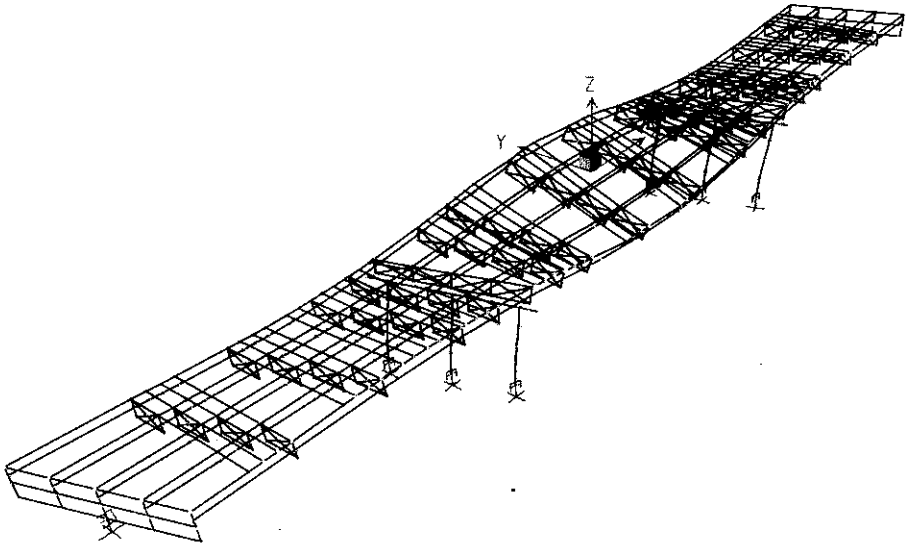

Figure 8.16 Mode 2, Period 0.2295 Seconds (New St. Francis River Bridge)

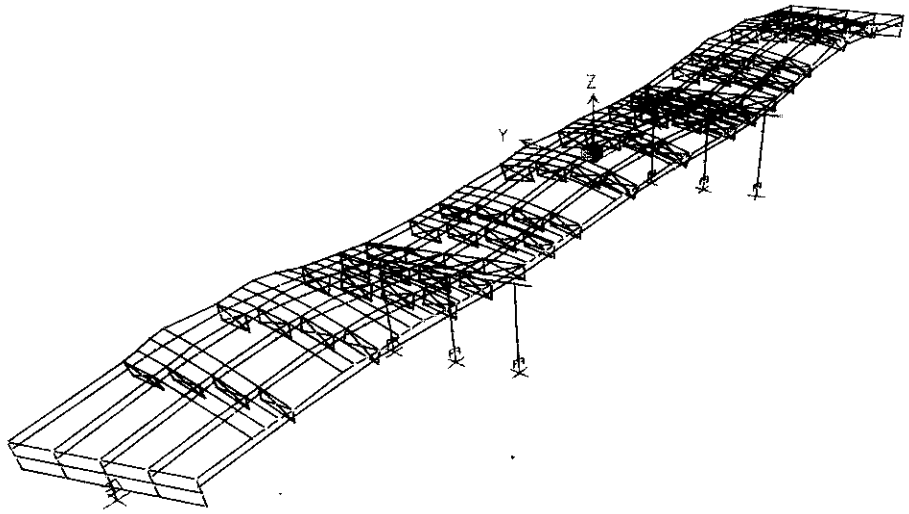

Figure 8.17 Mode 3, Period 0.1421 Seconds (New St. Francis River Bridge)

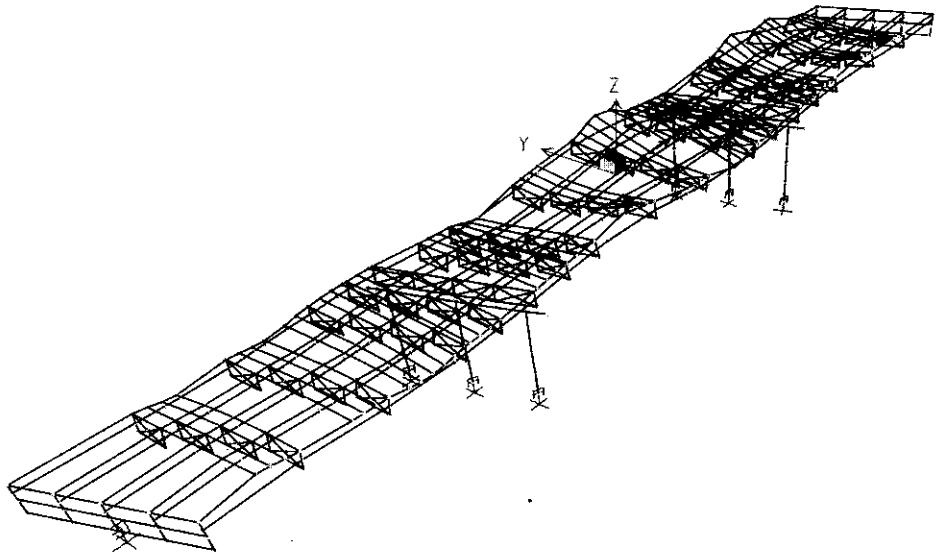

Figure 8.18 Mode 4, Period 0.0901 Seconds (New St. Francis River Bridge)

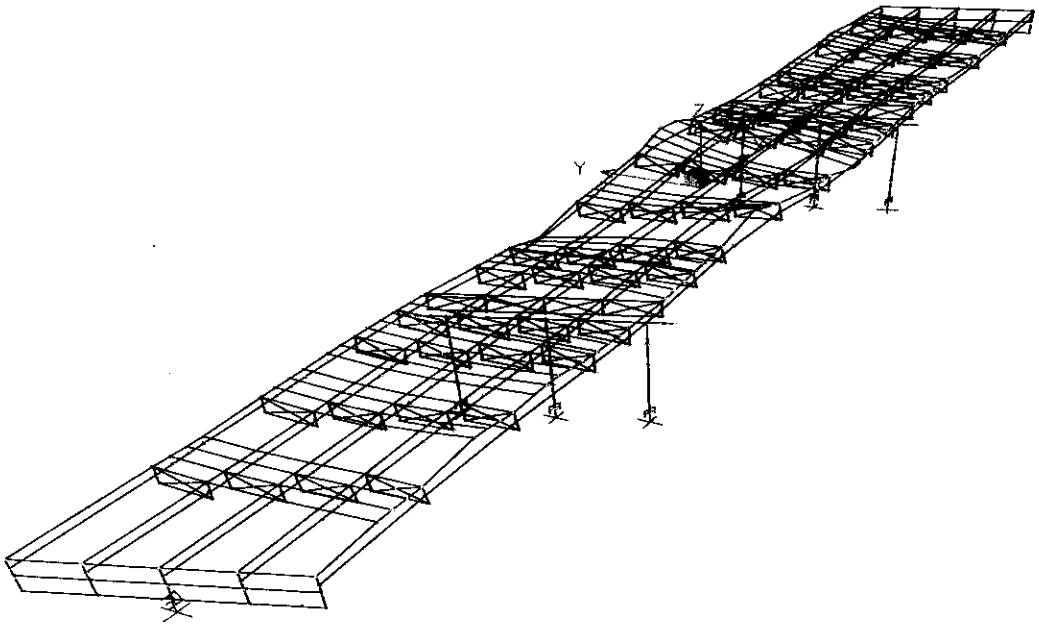

Figure 8.19 Mode 5, Period 0.0896 Seconds (New St. Francis River Bridge)

each directional earthquake excitation due to the special directional combination rule specified in the AASHTO Specifications (1996). Consequently, a total of 36 runs were completed.

8.1.7.1.3 Detailed Description of Bridge Evaluation

This section is delineated according to the various sections labeled on the spreadsheet of analysis and results. Each section explains the method and reasoning behind the calculations. The methods outlined here are mainly taken from the FHWA Seismic Retrofitting Manual for Highway Bridges (1995) with necessary modifications based on engineering judgment.

The purpose of the analysis was to form a quantitative summary of which components "pass" and which "fail" due to earthquake motions. To do this, the FHWA Manual outlined a method for determining Capacity / Demand ratios, which will further be referred to as C/D ratios. The concept is relatively simple, with the goal to determine whether a component's capacity is greater than its demand. If so, the ratio will be greater than one, indicating that there should be no problems associated with that component. If the capacity is less than the demand, the ratio will be less than one, indicating that problems may arise with that component in the event of an earthquake. Although no method is foolproof, these ratios do yield a reasonably accurate measure of the performance of the structure.

8.1.7.1.3.1 Load Combination Rule

For all force (moment, shear, axial) and displacement C/D ratios in this analysis, the 30% Combination Rule was used (AASHTO Division I-A, Section 3.9, 1996) for the effect of two horizon-

tal ground motions that are perpendicular to each other. This rule states that the forces/displacements due to transverse and longitudinal earthquake motions are added as follows:

CASE I: $0.3*(\text{force/displacement}_{\text{due to transverse}}) + 1.0*\text{force/displacement}_{\text{due to longitudinal}}$

CASE II: $0.3*(\text{force/displacement}_{\text{due to longitudinal}}) + 1.0*\text{force/displacement}_{\text{due to transverse}}$

The above relationship would be used for forces/displacements in both the longitudinal and transverse directions. The larger of CASE I and II would then be combined with the force/displacement due to the vertical earthquake motion, using a square-root-of-the-sum-of-the-squares relationship (SRSS).

This combination rule was used in several instances throughout these calculations for various types of demands on the structure (shear, moment, and axial forces, as well as transverse and longitudinal displacements).

8.1.7.1.3.2 Minimum Support Length and C/D Ratio for Bearing

Because this bridge has integral abutments, there are no expansion joints, and therefore there is no need to calculate this capacity/demand ratio. This C/D ratio is only applicable for bridges with seat-type abutments, which are susceptible to the dropping of exterior spans during earthquake motion.

8.1.7.1.3.3 C/D Ratios for Shear Force at Bearings

The first C/D ratios calculated in this section define the behavior of the bolts located at the neoprene elastomeric pads on the cap beams at the interior bents. In both the transverse and the longitudinal directions, there are two bolts for capacity. From the bridge analysis the shear demand at each of these points was determined and the maximum demand among these points was used to compute the C/D ratio for the "worst case". Before these shear values were used in determining the C/D ratios, the values were compared to 20% of the axial dead load at that location (FHWA, 1995). The greater of these two values were used in the subsequent calculations.

The second set of C/D ratios in this section involves the embedment length and edge distance requirements for the bolts discussed in the previous paragraph. First, the required embedment length was found from Table 8-26 of the LRFD AISC Manual (1998). This length, for the 2.5-inch diameter rods that were used on this bridge, is 42.5 inches. From the plans, it is noted that the rods only extend 25 inches into the concrete. With the check, this results in a C/D ratio less than one, which would indicate a possible failure due to axial forces acting on the bolts.
.

Finally, the edge distance was checked using another C/D ratio. From the same AISC table that provided the embedment lengths, allowable edge distances were also provided. For the rods used here, the required distance is 17.5 inches. The actual edge distance was estimated from the

plans to be approximately 20 inches. This indicates that there should be no problems with the edge distance provided for the bolts.

Figure 8.20 shows that the combination rule in Section 8.1.7.1.3.1 was used to combine the shear demands from all directions.

8.1.7.1.3.4 C/D Ratios for Columns/Piers

In this section, the C/D ratios were calculated for all circular columns on the interior bents. Both the moment demand and capacity are determined below.

Elastic Moment Demand. The first step was to note the elastic moment demands for the top and bottom of each column in the transverse and longitudinal directions due to transverse, longitudinal, and vertical earthquake motions. They are listed in Tables 8.7, 8.8, and 8.9. The moments were then combined as per the rule discussed in Section 8.1.7.1.3.1. The resulting moments from the combination were algebraically combined with the moment due to the dead load. Finally, the total transverse moment demand and the total longitudinal moment demand are combined by squaring each term, summing them, and then taking the square root to get the final resulting moment demand. This final calculation yields the value that is ultimately used in C/D ratio calculations. These final moment demands are shown in Table 8.10.

Moment Capacity. To determine the capacities of these columns, the P-M interaction diagram for the given column cross-section was used. Given an axial compressive force due to the dead load (found from the bridge analysis), a moment capacity was found from the interaction diagram. From these moment capacities, column shear forces were found. From these shear forces, axial forces due to overturning were found. These axial forces due to overturning were combined with the axial dead loads to give new axial totals. From these new axial forces, new moment capacities were found from the interaction diagrams. These moments were then used to find new column shear forces. These shear forces were compared to the ones found previously (using the axial forces which did not include the overturning effect). If these shear forces were within 10% of the originals, no further iterations would be required. Otherwise, the cycle would need to be repeated until the shear forces were within the 10% limit (AASHTO, 1996). Refer to Figure 8.21 for this procedure. In this case, the shears were within the 10% limit, so no iterations were required. However, the final capacities used for the C/D ratios reflect the use of the newest shear values to obtain updated axial forces. The change was very minimal, but the final moment capacities do include the change.

Finally, the maximum demand from the possible combinations was then used in conjunction with the determined capacity for the column to determine a C/D ratio for the columns. In most cases, the C/D ratios were well below one, indicating insufficient column strength for elastic seismic demand. However, when the columns experience inelastic deformation, the seismic demand reduces due to energy dissipation. To account for the above effect, the ductility indicator was used with these ratios (FHWA, 1995). Since the two interior bents each had multiple columns, ductility of 5 was applied to each ratio (AASHTO, 1996). In all cases, this multiplier increased the ratios to values above one. Table 8.11 summarizes the moment C/D ratios. As noted above, the capacities in this table are slightly different than those in Figure 8.21, as they reflect the change

due to the updated shear and axial forces. This note was made simply for the sake of explaining the origin of the capacity values. Within the section where column moment capacities were examined, FHWA (1995) also outlined guidelines for examining capacities for the footings of the columns as well. Assuming a fixed pile cap, the moment and axial compressive strength for each pile foundation are both determined approximately by the vertical pile capacity. Using simple geometry concepts and forming relationships between axial compressive loads, moments, rotations of the footing (denoted as θ), and displacements due to these rotations (denoted as δ), capacities of the footings were calculated.

The procedure involved first determining moments corresponding to various θ values. A moment-rotation curve was then plotted for a constant value of axial load (such as zero). The footing capacity corresponding to the case of P = 0 kips was calculated for this bridge. Assuming that P = 0, various values of θ were examined. For each different θ, pile displacements were determined, and using these displacements multiplied by the pile stiffness, axial loads were found. These axial loads were then used in a basic summation of moment equation. It was from this summation of moments equation that the moment value was taken for the moment-rotation plot. The plateau of this curve is taken as the moment capacity

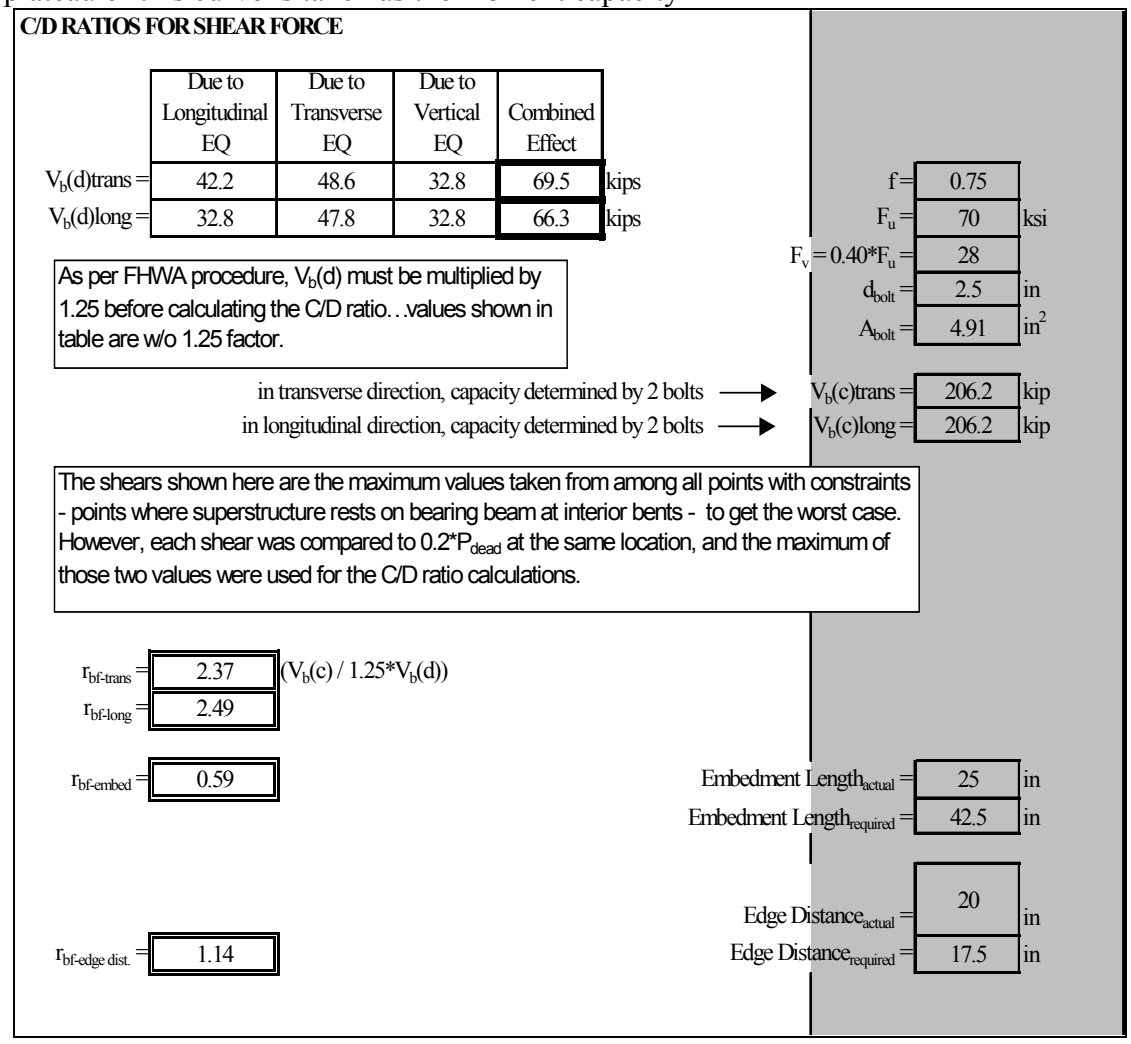

Figure 8.20 Shear Force Calculations

for the corresponding P value. It is well known that the moment capacity would increase with increasing P values so long as they are less than the balanced axial force. Because it was noted that the moment capacity for the case of P = 0 is considerably higher than the capacities of the columns (several orders of magnitude greater), it was deemed unnecessary to proceed with the entire process of determining C/D ratios for these footings, as they would clearly be more than adequate. The moment versus rotation relation for the case of axial load equal to zero is plotted in Appendix H.

Table 8.7 Elastic Moments Due to Transverse Acceleration

(kip-inch units)			Transverse Moment, $M_T^{(T)}$	Longitudinal Moment, $M_L^{(T)}$
SAP fr. #	**Location**	**Component**	**EQ**	**EQ**
21	Bent 2, top	column 1	28416	8768
24	bottom	column 1	-53652	-12804
30	Bent 2, top	column 2	33884	12241
42	bottom	column 2	-56823	13912
52	Bent 2, top	column 3	27290	11790
64	bottom	column 3	-52163	-16809
16	Bent 3, top	column 4	27171	11744
96	bottom	column 4	-52043	-16778
103	Bent 3, top	column 5	33781	12191
216	bottom	column 5	-56689	-15938
300	Bent 3, top	column 6	28131	8663
529	bottom	column 6	-53427	-12698

Table 8.8 Elastic Moments Due to Longitudinal Acceleration

(kip-inch units)			Transverse Moment, $M_T^{(L)}$	Longitudinal Moment, $M_L^{(L)}$
SAP fr. #	**Location**	**Component**	**EQ**	**EQ**
21	Bent 2, top	column 1	-699	-263
24	bottom	column 1	1618	2227
30	Bent 2, top	column 2	790	303
42	bottom	column 2	1792	2136
52	Bent 2, top	column 3	-806	-306
64	bottom	column 3	1697	2074
16	Bent 3, top	column 4	-795	316
96	bottom	column 4	1717	2094
103	Bent 3, top	column 5	-922	296
216	bottom	column 5	1817	2136
300	Bent 3, top	column 6	-680	-245
529	bottom	column 6	1644	2207

Table 8.9: Elastic Moments Due to Vertical Acceleration

(kip-inch units)			Transverse Moment, $M_T^{(V)}$	Longitudinal Moment, $M_L^{(V)}$
SAP fr. #	**Location**	**Component**	**EQ**	**EQ**
21	Bent 2, top	column 1	-252	115
24	bottom	column 1	-975	-373
30	Bent 2, top	column 2	604	166
42	bottom	column 2	-1305	-463
52	Bent 2, top	column 3	940	346
64	bottom	column 3	-1532	-359
16	Bent 3, top	column 4	-865	-340
96	bottom	column 4	1438	468
103	Bent 3, top	column 5	-591	-172
216	bottom	column 5	1256	662
300	Bent 3, top	column 6	-297	115
529	bottom	column 6	900	615

Table 8.10 Summary of All Moment Demands

Elastic Moment Demands - TOTAL including combined 3 directions									
(kip-inch units)			**Transverse Moment**			**Longitudinal Moment**			
SAP fr. #	**Location**	**Component**	**EQ (from transverse & longitudinal input)**	**EQ (from vertical input)**	**DL**	**EQ (from transverse & longitudinal input)**	**EQ (from vertical input)**	**DL**	**Elastic Moment Demand**
21	Bent 2, top	column 1	28626	-252	-533	8847	115	-178	30525
24	bottom	column 1	54137	-975	543	13472	-373	-186	56370
30	Bent 2, top	column 2	34121	604	-89	12332	166	-17	36376
42	bottom	column 2	57361	-1305	258	14553	-463	-280	59513
52	Bent 2, top	column 3	27532	940	401	11882	346	114	30416
64	bottom	column 3	52672	-1532	-58	17431	-359	-348	55669
16	Bent 3, top	column 4	27410	-865	-377	11839	-340	-110	30261
96	bottom	column 4	52558	1438	25	17406	468	339	55517
103	Bent 3, top	column 5	34058	-591	116	12280	-172	17	36324
216	bottom	column 5	57234	1256	-293	16579	662	272	59961
300	Bent 3, top	column 6	28335	-297	561	8737	115	203	30249
529	bottom	column 6	53920	900	-576	13360	615	155	56158

1) Using P-M diagrams for columns from SAP2000 to create following table:

Bent	End	Axial Force (due to DL)	1.3 Mu	Mu
2	top	262	38163	29356
2	bottom	335	56690	43608
3	top	260	38151	29347
3	bottom	332	56664	43588

2) Column Shear Forces (forces are per column, so total shear for one bent = 3 * 266)

Bent 2: $V_u =$ 266 $(M_{top} + M_{bottom}) / L_{col}$ $L_{col\text{-}bent\ 2} =$ 29.7 ft

Bent 3: $V_u =$ 266 $(M_{top} + M_{bottom}) / L_{col}$ $L_{col\text{-}bent\ 3} =$ 29.7 ft

3) Axial Forces due to Overturning

Bent 2: P = 730 $(3*V_u*L_{col}) / D$ D = 32.5 ft

Bent 3: P = 729 $(3*V_u*L_{col}) / D$ (distance between columns)

4) Revision of Moment Capacity for Iterations

- Take new axial forces (P, from **3)**)
- Using P's, get new M_{top}, M_{bottom}
- Using new M_{top}, M_{bottom}, get new column shear forces
- Compare new shear forces to original ones -- are they within 10 %?
- If not, get new P's and try again, otherwise, use new shears to get new P's and move on

Bent	End	Axial Force	1.3 Mu	Mu
2	top	-468	31324	24095
2	top	992	43306	33312
2	bottom	-395	42405	32619
2	bottom	1065	63324	48711
3	top	-469	31303	24079
3	top	989	43284	33295
3	bottom	-397	42353	32579
3	bottom	1061	63283	48679

Revised Shear Capacity:

Bent 2: $V_u = (M_{top}+M_{bottom})_{min}/L_{col} + (M_{top}+M_{bottom})_{max}/L_{col}$

Vu = 759.1

Bent 3: $V_u = (M_{top}+M_{bottom})_{min}/L_{col} + (M_{top}+M_{bottom})_{max}/L_{col}$

Vu = 758.5

For each bent (2 & 3): This revised capacity accounts for 2 columns. Since the bent has 3 columns, multiply value by 1.5 to get shear for entire bent.

Compare to 266*3 (for one bent from above w/ 3 columns): 798

Check: YES - OK (within 10% - move on)

Figure 8.21 Calculations of Axial Loads and Column Shears

Table 8.11 Summary of Moment C/D Ratios for Columns

			Column			
Bent	**End**	**Axial Load**	**Demand**	**Capacity**	$r_{ec\text{-}initial}$	$r_{ec\text{-}final}$
2	top	minimum	36376	25225	0.69	3.47
2	top	maximum	36376	13462	0.37	1.85
2	bottom	minimum	59513	46083	0.77	3.87
2	bottom	maximum	59513	30952	0.52	2.60
3	top	minimum	36324	25225	0.69	3.47
3	top	maximum	36324	13462	0.37	1.85
3	bottom	minimum	59961	46083	0.77	3.84
3	bottom	maximum	59961	30952	0.52	2.58

NOTE: Capacities are *not* multiplied by 1.3

Final C/D ratios are equal to initial ratios multiplied by 5, which is the ductility indicator.

8.1.7.1.3.5 C/D Ratios for Hooked Anchorage in Columns

For both the top and bottom of the columns, the adequacy of the anchorage of longitudinal reinforcement must be checked. The capacity was determined simply by finding the length of hooked anchorage at both the top and bottom of the columns. The demand was determined from an equation outlined in the FHWA Seismic Retrofit Manual (1995).

In both the tops and the bottoms of the columns, the length of anchorage required was less than the actual length, as taken from the plans. The value for the C/D ratio was found from Figure 78 from the FHWA Manual, and this table was set up in terms of the anchorage geometry and location of the anchorage. In this case, the C/D ratio value of 1.0 was not the ratio of $l_a(c)$ to $l_a(d)$. The aforementioned figure from the FHWA Manual assigned values for C/D ratios depending on the location of the anchorage (top/bent cap or bottom/footing), as well as the relationship of the capacity length to the demand length. Based on these parameters, the value assigned for these C/D ratios is 1.0. The calculations are shown in Figure 8.22.

8.1.7.1.3.6 C/D Ratios for Splices in Longitudinal Reinforcement

In this section, a C/D ratio was determined for the adequacy of the splicing of the longitudinal reinforcement. The formula used to determine the demand was again taken from the FHWA Retrofit Manual. The capacity was also found based on the definition from the Manual. Because the C/D ratio depends on the column moment C/D ratio, r_{ec}, an adjustment needed to be made. An attempt was made to determine the actual stress in the steel due to the external moment, and then divide the yield stress of the reinforcement (60 ksi) by this actual stress to form a ratio of the stresses. This ratio would likely be greater than one, therefore increasing the C/D ratio for the splices in the longitudinal reinforcement. The method used a reinforced concrete relationship to determine steel stresses at service loads. This method did increase the C/D ratio as expected. For all cases, both for 2% and 10% ground motions, the adjusted C/D ratios were raised above one, indicating that there will likely be minimal concerns with these splices. All calculations are shown in Figure 8.23.

C/D RATIOS FOR HOOKED ANCHORAGE IN COLUMNS, $r_{ca\text{-}bottom}$					
$l_a(c)$ =	36	in		k_m =	0.7
$l_a(d)$ =	19.477	in	$1200*k_m*d_b*(f_y / (60000(f'c^{0.5}))$ or $15*d_b$	d_b =	1.27 in
$r_{ca\text{-}bottom}$ =	1.0		(choose larger)	f_y =	60000 psi
				f'_c =	3000 psi

C/D RATIOS FOR HOOKED ANCHORAGE IN COLUMNS, $r_{ca\text{-}top}$					
$l_a(c)$ =	36	in		k_m =	0.7
$l_a(d)$ =	19.477	in	$1200*k_m*d_b*(f_y / (60000(f'c^{0.5}))$ or $15*d_b$	d_b =	1.27 in
$r_{ca\text{-}top}$ =	1.0		(choose larger)	f_y =	60000 psi
				f'_c =	3000 psi

Figure 8.22: Calculations for Hooked Anchorage in Columns

8.1.7.1.3.7 C/D Ratio for Transverse Confinement

The calculations in this section were similar to those in the previous section. Again, an FHWA-defined relationship was used to determine the adequacy of the transverse confinement. The relationship defined for the transverse confinement did include a multiplier. This multiplier was dependent on adequacy of transverse confinement. Also, this C/D ratio was again dependent on the column moment C/D ratio, r_{ec} (without including the ductility indicator), several factors, including geometry of the confinement as well as properties of the column reinforcement, the concrete, and the column cross-section.

The C/D ratios for all cases were above one. This indicates that there should be minimal problems with transverse confinement. All aforementioned calculations are shown in Figure 8.24.

8.1.7.1.3.8 C/D Ratio for Column Shear

In this section, a determination was made for column shear forces. On the spreadsheet, several parameters were calculated, as per the methodology outlined in the FHWA Manual. The maximum elastic shear force in the column was determined from the bridge analysis ($V_e(d)$). The maximum column shear force, $V_u(d)$ was found earlier when determining the ultimate moment capacities in Section 8.1.7.1.3.4. The other two parameters, $V_i(c)$ and $V_f(c)$, are the initial and final shear capacities of the column, respectively. The initial shear capacity was determined using equation 11-4 from ACI 318-99. This equation was to be used to find the shear

C/D RATIOS FOR SPLICES IN LONGITUDINAL REINFORCEMENT, r_{cs}

$A_{tr}(d)$ = 0.04536 = $((s*f_y)/(l_s*f_{yt}))*A_{b,\ splice}$

$A_{tr}(c)$ = 0.2

r_{cs} = 0.74 = $(A_{tr}(c) / A_{tr}(d))*r_{ec} <= 2r_{ec}$

NOTE: r_{ec} is from the moment section - using minimum r_{ec} value to obtain "worst case"; however, the initial value was used without the ductility indicator.

s =	3	in
f_y =	60000	psi
l_s =	84	in
f_{yt} =	60000	psi
$A_{b,\ splice}$ =	1.27	in^2

NOTE: because r_{cs} depends on the moment C/D ratio, which was increased by the ductility indicator, it must be determined whether rcs can also be increased. Using the ACI equation for determining steel stress at service loads, we can form a ratio of the maximum stress in the steel to the actual stress in the steel under the given moment (output from SAP2000).

$f_s = M / A_s*j*d$

M = 23955 (from SAP2000 output -- moment from column corresponding to the r_{ec} used above)

As = 33.02 in^2

j = 0.944

d = 46.5 in

($j = 1-k/3$; $k = (2\rho n+(\rho n)2)1/2-\rho n$; $\rho = A_s/A_{concrete}$; $n = Es/Ec$ where E_s = 29000 ksi, E_c = 3120 ksi)

f_s = 16.53

r_{cs-adj} = 2.69

Figure 8.23 Calculations for Splices in Longitudinal Reinforcement

C/D RATIOS FOR TRANSVERSE CONFINEMENT, r_{cc}

r_{cc} = 3.33 = μr_{ec}

NOTE: r_{ec} is from the moment section - using minimum r_{ec} value to obtain "worst case"; however, the initial value was used without the ductility indicator.

Assume transverse steel is effectively anchored, so $k_3 = 1$

(**r(d)** according to AASHTO Specifications, Division I-A, Section 7.6)

μ =	6	
k_1 =	1	
k_2 =	1	
k_3 =	1	
$\rho(c)$ =	0.0050	
$\rho(d)$ =	0.00554	
P_c =	355	kip
f'_c =	3	ksi
A_g =	1809.6	in^2
s =	3	in
d_b =	1.27	in
b_{min} =	48	in

Figure 8.24 Calculations for Transverse Confinement

capacity of members subjected to axial compression. The final shear capacity of the column was defined in the FHWA Manual. If the axial force, which was taken as approximately 425 k (the approximate largest axial load experienced by any column), divided by the column cross-sectional area was greater than 0.1 of f'_c, then $2\sqrt{f_c'}$ was to be used (FHWA, 1995). If the axial stress was less than $0.1f'_c$, then a value of zero was to be assumed for $V_f(c)$. In this case, $V_f(c)$ was zero. In addition, by assuming a value of zero for the final capacity, the results are slightly more conservative. The procedure and formulas for these parameters are noted below. From these parameters, a "Case" needed to be chosen, based on the flow chart from Figure 81 in the FHWA Manual (1995). This flow chart outlined the process for determining the column shear C/D ratio. The original moment C/D ratios without the ductility indicator are used in these calculations.

In all cases of 2% motions, "Case B" was chosen, based on definitions from the FHWA Manual. This case was needed because at least one of the moment C/D ratios was less than one for each earthquake. This case was applicable when r_{ec} (column moment C/D ratio) was less than one and $V_i(c) > V_u(d) > V_f(c)$. When "Case B" was used, the relationship for the column shear C/D ratio was the column moment C/D ratio multiplied by an FHWA-defined multiplier. This multiplier, as shown in the spreadsheet, was based on column geometry (L_c = length of column and b_c = width of column) as well as the various shear parameters defined at the start of the section.

For the 10% motions, "Case B" did not apply because the initial C/D ratios for the columns under these earthquakes were above one. Therefore, the C/D ratios for these earthquakes were determined simply as a ratio of the initial capacity of the column to the maximum shear force in the column. All calculations are shown in Figure 8.25.

8.1.7.1.3.9 C/D Ratio for Diaphragm and Cross-Frame Members

This section examines the damage caused to the diaphragm and cross-frame members for the bridge. Both the diaphragms and the cross-frames can be analyzed using the same method because they are both composed of the same sections (each consisted of two L 3x3x5/16 crossed over each other with L 4x4x5/16 as the top and bottom horizontal members). Because of very low moments on these members, the members were analyzed based on their axial load capacity and demand.

There are two calculations shown for the same capacity/demand ratio. The first uses the full length of the member spanning diagonally from top to bottom of the diaphragm/cross-frame. However, since there is a welded connection in the center where the diagonal members meet, the second calculation uses half of the total length of the member. This was done because of the possibility of failure within this connection, thus removing the intermediate brace. It should be noted that the members were modeled as two halves put together to make a full-length diagonal member for the diaphragms and cross-frames. This was done with the hopes of more closely modeling the actual bridge conditions**.**

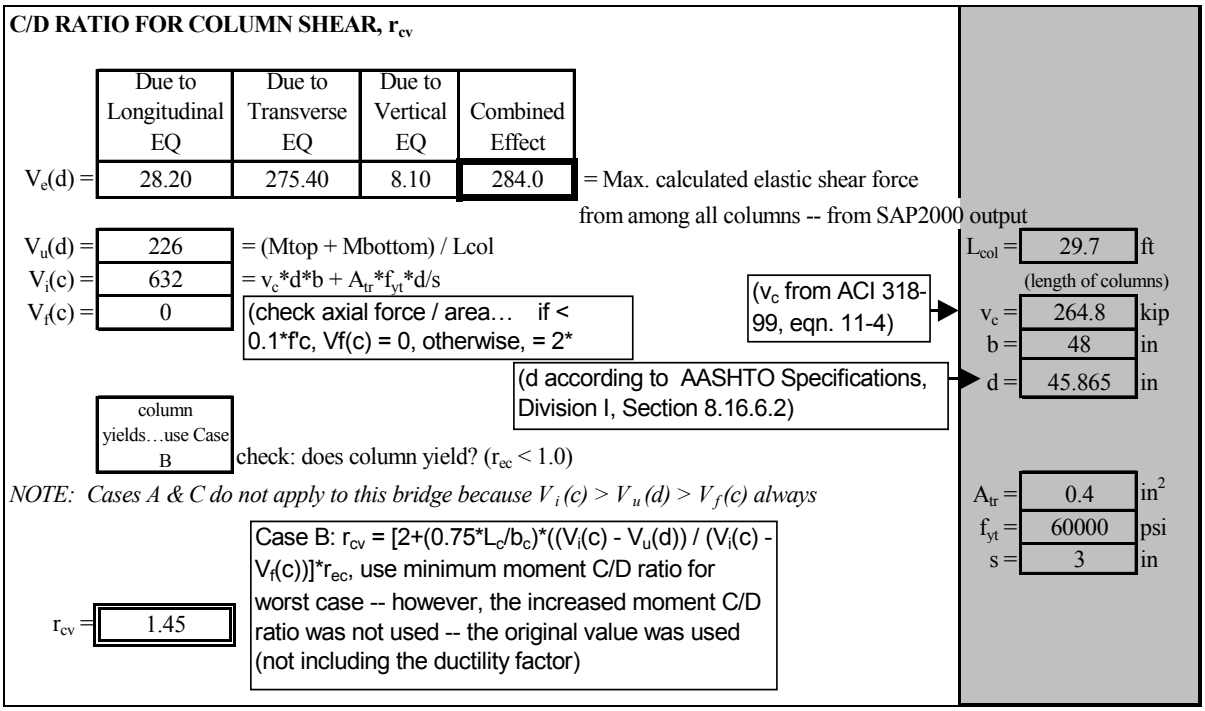

Figure 8.25 Calculations for Column Shear

The axial capacities for these members were estimated using load tables from the AISC Manual (1998). The total load demand on these members was determined using the combination rule described in Section 8.1.7.1.3.1. The calculations are shown in Figure 8.26.

8.1.7.1.3.10 C/D Ratio for Abutment Displacements

The final section of the spreadsheet outlines the check for abutment adequacy. This test involves comparing the actual abutment displacements to maximum displacement values given by FHWA. These maximum values from FHWA are based on previous experiences due to past earthquakes and engineering judgment. The values are given as three inches of allowable displacement in the transverse direction and six inches of allowable displacement in the longitudinal direction.

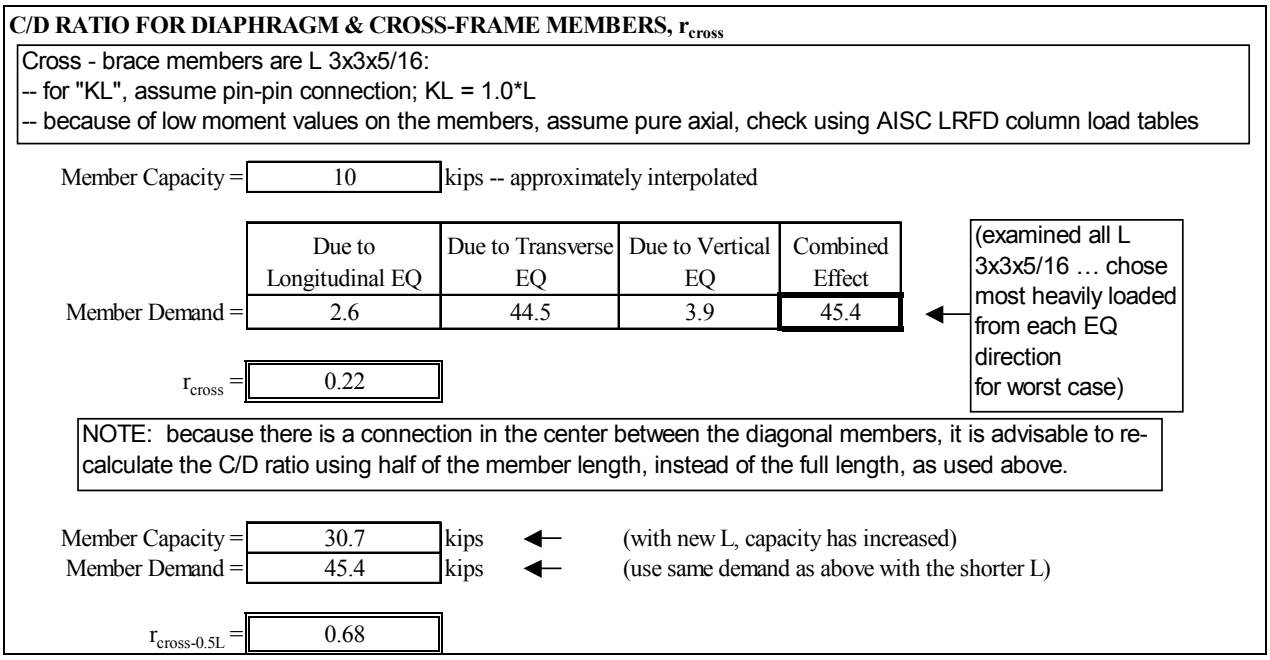

Figure 8.26 Calculations for Diaphragm and Cross-Frame Members

Similar to the determination of elastic moment demands for the columns, the abutment displacements due to all three directions of earthquake motions were also combined using the rule specified in Section 8.1.7.1.3.1. Figure 8.27 lists the maximum transverse and longitudinal abutment displacements due to the transverse, longitudinal, and vertical earthquake ground motions. The displacements were then combined as per the combination rule.

In all cases, no problems were encountered due to abutment displacements. The C/D ratios were always well over one, indicating that the abutments should remain relatively damage-free (at least due to displacement) in the event of an earthquake. Refer to Figure 8.27 for abutment displacements calculations.

8.1.7.1.4 Summary of Problem Areas

Based on the step-by-step procedure illustrated in Section 8.1.7.1.3, the bridge was evaluated under twelve ground motions that were selected in Section 8.1.3. A sample summary table of all C/D ratios for one earthquake is shown in Table 8.12. A summary of all C/D ratios for all earthquakes for this bridge is shown in Table 8.13. It can be observed from Table 8.13 that the bridge experienced minimal problems. As expected, the bridge generally performed more poorly under the influence of the 2% likelihood earthquakes, which were considerably stronger than the 10%

C/D RATIOS FOR ABUTMENTS, r_{ad}	Due to Longitudinal EQ	Due to Transverse EQ	Due to Vertical EQ	Combined Effect
maximum transverse displacements:	0.002057	0.0700	0.0009462	0.070623
maximum longitudinal displacements:	0.0523	0.1259	0.018	0.142730

$r_{ad\text{-}trans}$	42.48	(= 3" capacity in transverse direction / maximum transverse displacement from above)
$r_{ad\text{-}long}$	42.04	(= 6" capacity in longitudinal direction / maximum longitudinal displacement from above)

Figure 8.27 Calculations for Abutment Displacements

likelihood earthquakes. In some instances, C/D ratios for various components of the structure were increased by multipliers and thus indicated no problems because their values were raised above one. However, it would be advisable to pay careful attention to areas such as columns, for extensive inelastic deformations could occur at these locations.

Of main concern are the diagonal members in the cross-frames and diaphragms of the bridge. The C/D ratios for these members were raised above one in some cases by using the half-length of the member due to the presence of a weld connection between two diagonal members crossing over each other. However, for four of the 2% earthquakes, the ratios still fell below one, indicating that the members may need to be retrofitted. In the other two 2% earthquakes, the C/D ratio was raised to exactly one, indicating that the capacity is just barely enough.

The strength of the weld at the intermediate brace of the diagonals was calculated to be approximately 33.4 kips. According to the bridge analysis, several of the 2% PE motions would likely cause this weld to fail, since all the axial demands for those earthquakes are greater than 33.4 kips (range from 33 to 45 kips). However, the 10% PE motions do not appear to cause this problem, as the axial loads for those motions range from 9 to 18 kips.

8.1.7.1.5 Time History Analysis vs. Response Spectrum Analysis

In order to verify that the response spectrum analysis is as reliable as the time history analysis, several cases of the response spectrum analysis were run on SAP2000 to compare to the time history results used for this evaluation.

Tables 8.14, 8.15, and 8.16 show the average of forces or displacements at several key locations (bottom of column 2, bottom of column 5 and for the maximum abutment displacement) on the structure for four 2% motions and also for four 10% motions. The averages for the response spectrum analysis were compared to the averages for the time history analysis to give an indication as to how closely these results coincide.

Table 8.12 Summary of all C/D Ratios for New St. Francis Bridge Structure – For One 2% PE Earthquake

SUMMARY TABLE OF ALL C/D RATIOS FOR BRIDGE STRUCTURE *Bridge A3709, PR020101 -- all three acceleration directions*			
Element Description	**C/D Ratio Name**	**C/D Ratio Value**	**NOTES**
bearing	r_{bd}	---	NOT APPLICABLE TO THIS BRIDGE
shear force - transverse	$r_{bf\text{-}trans}$	2.37	satisfactory
shear force - longitudinal	$r_{bf\text{-}long}$	2.49	satisfactory
bolt/anchor rod embedment length	$r_{bf\text{-}embed}$	0.59	Unsatisfactory…demand exceeds capacity
bolt/anchor rod edge distance	$r_{bf\text{-}edge\ dist.}$	1.14	satisfactory
column top, bent 2, P_{min}	$r_{ec\text{-}final}$	3.39	satisfactory
column top, bent 2, P_{max}	$r_{ec\text{-}final}$	4.55	satisfactory
column bottom, bent 2, P_{min}	$r_{ec\text{-}final}$	2.80	satisfactory
column bottom, bent 2, P_{max}	$r_{ec\text{-}final}$	4.07	satisfactory
column top, bent 3, P_{min}	$r_{ec\text{-}final}$	3.40	satisfactory
column top, bent 3, P_{max}	$r_{ec\text{-}final}$	4.56	satisfactory
column bottom, bent 3, P_{min}	$r_{ec\text{-}final}$	2.78	satisfactory
column bottom, bent 3, P_{max}	$r_{ec\text{-}final}$	4.04	satisfactory
hooked anchorage @ column bottom	$r_{ca\text{-}bottom}$	1.00	satisfactory
hooked anchorage @ column top	$r_{ca\text{-}top}$	1.00	satisfactory
splices in longitudinal reinforcement	r_{cs}	1.11	satisfactory
splices in longitudinal reinforcement, adjusted for stresses in steel	$r_{cs\text{-}adj}$	4.03	satisfactory
transverse confinement	r_{cc}	3.33	satisfactory
column shear	r_{cv}	2.06	satisfactory
diaphragm / cross-frame members	r_{cross}	0.22	Unsatisfactory…demand exceeds capacity
diaphragm / cross-frame members, using 1/2 of total member length	$r_{cross\text{-}0.5L}$	0.68	Unsatisfactory…demand exceeds capacity
abutments - transverse displacement	$r_{ad\text{-}trans}$	42.48	satisfactory
abutments - longitudinal displacement	$r_{ad\text{-}long}$	42.04	satisfactory

Table 8.13 Summary of C/D Ratios For All Earthquakes at New St. Francis River Bridge

C/D Ratio Name	020101	020103	020105	020201	020203	020205	100103	100104	100105	100201	100202	100205
r_{bd}	---	---	---	---	---	---	---	---	---	---	---	---
$r_{bf\text{-}trans}$	2.37	3.07	2.79	3.07	3.07	2.70	3.07	3.07	3.07	3.07	3.07	3.07
$r_{bf\text{-}long}$	2.49	3.05	2.97	3.07	3.07	2.69	3.07	3.07	3.07	3.07	3.07	3.07
$r_{bf\text{-}embed}$	**0.59**	**0.59**	**0.59**	**0.59**	**0.59**	**0.59**	**0.59**	**0.59**	**0.59**	**0.59**	**0.59**	**0.59**
$r_{bf\text{-}edge\ dist.}$	1.14	1.14	1.14	1.14	1.14	1.14	1.14	1.14	1.14	1.14	1.14	1.14
$r_{ec\text{-}final}$	3.39	4.88	4.54	5.18	5.09	3.81	16.59	18.42	15.86	13.51	9.44	11.43
$r_{ec\text{-}final}$	4.55	6.55	6.10	6.94	6.83	5.11	22.25	24.71	21.28	18.12	12.66	15.34
$r_{ec\text{-}final}$	2.80	3.95	3.73	4.25	4.15	3.11	13.39	15.30	13.15	10.92	7.74	9.57
$r_{ec\text{-}final}$	4.07	5.74	5.42	6.17	6.02	4.52	19.45	22.23	19.10	15.86	11.24	13.90
$r_{ec\text{-}final}$	3.40	4.91	4.56	5.20	5.07	3.81	16.63	18.49	15.88	13.53	9.47	11.47
$r_{ec\text{-}final}$	4.56	6.58	6.12	6.97	6.80	5.12	22.32	24.80	21.30	18.15	12.71	15.39
$r_{ec\text{-}final}$	2.78	3.95	3.74	4.26	4.13	3.11	13.40	15.32	13.14	10.93	7.75	9.58
$r_{ec\text{-}final}$	4.04	5.75	5.43	6.19	6.00	4.52	19.48	22.27	19.10	15.88	11.26	13.92
$r_{ca\text{-}bottom}$	1.00	1.00	1.00	1.00	1.00	1.00	1.00	1.00	1.00	1.00	1.00	1.00
$r_{ca\text{-}top}$	1.00	1.00	1.00	1.00	1.00	1.00	1.00	1.00	1.00	1.00	1.00	1.00
r_{cs}	1.11	1.58	1.49	1.70	1.65	1.24	5.36	6.12	5.26	4.37	3.10	3.83
$r_{cs\text{-}adj}$	4.03	8.11	7.29	9.45	8.96	5.04	94.92	126.79	92.91	62.94	31.60	48.98
r_{cc}	3.33	4.74	4.48	5.10	4.96	3.73	16.07	18.37	15.77	13.11	9.29	11.48
r_{cv}	2.06	2.94	2.77	3.16	3.07	2.31	10.74	12.67	10.80	8.66	6.21	7.94
r_{cross}	**0.22**	**0.31**	**0.30**	**0.32**	**0.33**	**0.25**	1.04	1.06	**0.93**	**0.85**	**0.57**	**0.68**
$r_{cross\text{-}0.5L}$	**0.68**	**0.96**	**0.91**	1.00	1.00	**0.76**	3.19	3.24	2.85	2.61	1.74	2.08
$r_{ad\text{-}trans}$	42	59	59	67	63	48	211	262	220	171	121	162
$r_{ad\text{-}long}$	42	59	55	62	64	49	201	219	197	181	121	143

Table 8.14 Comparison of Moments for Time History and Response Spectrum Analysis for Column 2 (New St. Francis River Bridge)

Due to 2% motions

Due to Transverse EQ	transverse		longitudinal	
	time history	response spectra	time history	response spectra
Column 2, bottom	56823	58252	13912	16363
	41965	40841	11775	11470
	36840	38104	10358	10703
	37835	36107	10660	10143
average	43366	43326	11676	12170

Due to Longitudinal EQ	transverse		longitudinal	
	time history	response spectra	time history	response spectra
Column 2, bottom	1792	1958	2136	2319
	1942	1833	2249	2503
	1484	1514	2089	1950
	1356	1328	1828	1668
average	1644	1658	2076	2110

Due to Vertical EQ	transverse		longitudinal	
	time history	response spectra	time history	response spectra
Column 2, bottom	1305	1222	463	462
	1081	1040	398	408
	1133	1069	310	369
	923	1025	355	458
average	1111	1089	382	424

Due to 10% motions

Due to Transverse EQ	transverse		longitudinal	
	time history	response spectra	time history	response spectra
Column 2, bottom	9966	14924	2795	4192
	11702	13059	3285	3668
	14162	14511	3986	4075
	16160	14081	4532	3954
average	12998	14144	3650	3972

Due to Longitudinal EQ	transverse		longitudinal	
	time history	response spectra	time history	response spectra
Column 2, bottom	521	665	701	909
	500	517	593	682
	550	563	694	714
	828	619	848	838
average	600	591	709	786

Due to Vertical EQ	transverse		longitudinal	
	time history	response spectra	time history	response spectra
Column 2, bottom	244	232	124	135
	267	260	121	141
	369	324	152	153
	301	338	150	184
average	295	289	137	153

Table 8.15 Comparison of Moments for Time History and Response Spectrum Analysis for Column 5 (New St. Francis River Bridge)

Due to 2% motions

Due to Transverse EQ	transverse		longitudinal	
	time history	response spectra	time history	response spectra
Column 5, bottom	56689	58104	15938	16292
	41820	40742	11722	11427
	36708	38010	10308	10658
	37924	36104	10665	10123
average	43285	43240	12158	12125

Due to Longitudinal EQ	transverse		longitudinal	
	time history	response spectra	time history	response spectra
Column 5, bottom	1817	1965	2136	2308
	1959	1841	2248	2490
	1478	1521	2086	1940
	1354	1336	1829	1660
average	1652	1666	2075	2100

Due to Vertical EQ	transverse		longitudinal	
	time history	response spectra	time history	response spectra
Column 5, bottom	1256	1165	662	531
	1011	983	509	480
	1092	1011	419	446
	874	967	464	520
average	1058	1032	514	494

Due to 10% motions

Due to Transverse EQ	transverse		longitudinal	
	time history	response spectra	time history	response spectra
Column 5, bottom	9907	14880	2776	4171
	11663	13037	3272	3654
	14112	14475	3967	4058
	16085	14057	4507	3942
average	12942	14112	3631	3956

Due to Longitudinal EQ	transverse		longitudinal	
	time history	response spectra	time history	response spectra
Column 5, bottom	536	667	697	904
	507	518	591	678
	548	565	693	710
	837	623	848	834
average	607	593	707	782

Due to Vertical EQ	transverse		longitudinal	
	time history	response spectra	time history	response spectra
Column 5, bottom	225	220	145	145
	253	245	143	154
	343	306	156	173
	284	312	166	202
average	276	271	153	169

Table 8.16 Comparison of Displacements for Time History and Response Spectrum Analysis for Maximum Abutment Displacement (New St. Francis River Bridge)

Due to 2% motions

Due to Transverse EQ	transverse		longitudinal	
	time history	response spectra	time history	response spectra
Max. Abut. Disp.	0.07	0.069	0.1259	0.1294
	0.0506	0.0484	0.093	0.0907
	0.0442	0.0452	0.0824	0.0848
	0.047	0.0429	0.0808	0.0792
average	0.053	0.05138	0.0955	0.09603

Due to Longitudinal EQ	transverse		longitudinal	
	time history	response spectra	time history	response spectra
Max. Abut. Disp.	0.0021	0.00167	0.0523	0.0485
	0.0016	0.0013	0.05	0.0525
	0.0012	0.00117	0.0439	0.0408
	0.0012	0.00106	0.039	0.035
average	0.0015	0.0013	0.0463	0.0442

Due to Vertical EQ	transverse		longitudinal	
	time history	response spectra	time history	response spectra
Max. Abut. Disp.	0.0009	0.00126	0.018	0.0171
	0.0013	0.00098	0.0137	0.0143
	0.0011	0.0009	0.0158	0.0152
	0.0009	0.00111	0.0138	0.0138
average	0.0011	0.00106	0.0153	0.0151

Due to 10% motions

Due to Transverse EQ	transverse		longitudinal	
	time history	response spectra	time history	response spectra
Max. Abut. Disp.	0.0113	0.0177	0.0227	0.0334
	0.0135	0.0155	0.0264	0.029
	0.0174	0.0172	0.0281	0.0324
	0.0183	0.0167	0.0368	0.0312
average	0.01513	0.01678	0.0285	0.0315

Due to Longitudinal EQ	transverse		longitudinal	
	time history	response spectra	time history	response spectra
Max. Abut. Disp.	0.00044	0.00046	0.0154	0.0193
	0.00036	0.00038	0.013	0.0144
	0.00048	0.00044	0.0164	0.0151
	0.00053	0.00043	0.0161	0.0178
average	0.00045	0.00043	0.01523	0.01665

Due to Vertical EQ	transverse		longitudinal	
	time history	response spectra	time history	response spectra
Max. Abut. Disp.	0.00029	0.00029	0.0023	0.00255
	0.00032	0.00026	0.00299	0.00305
	0.0004	0.00038	0.00335	0.00422
	0.00038	0.00036	0.00401	0.00409
average	0.00035	0.00032	0.00316	0.00348

It can be observed from Tables 8.16-8.18 that the results from the response spectrum analysis agree well with those of the linear time history analysis for the bridge. Therefore the response spectrum analysis can be used to replace the time history analysis for highway bridges with integral abutments that can be described with a linear model.

8.1.7.1.6 Comparison of AASHTO Response Spectrum vs. Site-Specific Response Spectrum

A response spectrum was generated based on the 1996 AASHTO Specifications. This response spectrum was used on both of the new bridges, both at the St. Francis River site and at the Wahite Ditch site. The response spectrum was created using the following parameters: Soil Type III, which yielded an S value of 1.5, and an A value of 0.18, which represents the maximum ground motion in the area. The plot of the response spectrum that was used for the analyses is shown in Figure 8.28.

In Figure 8.28, two site specific response spectra were graphically compared to the AASHTO response spectrum. It should be noted that in the region of the structure's natural period (less than T = 0.5 seconds) all the response spectrum data are relatively close to one another.

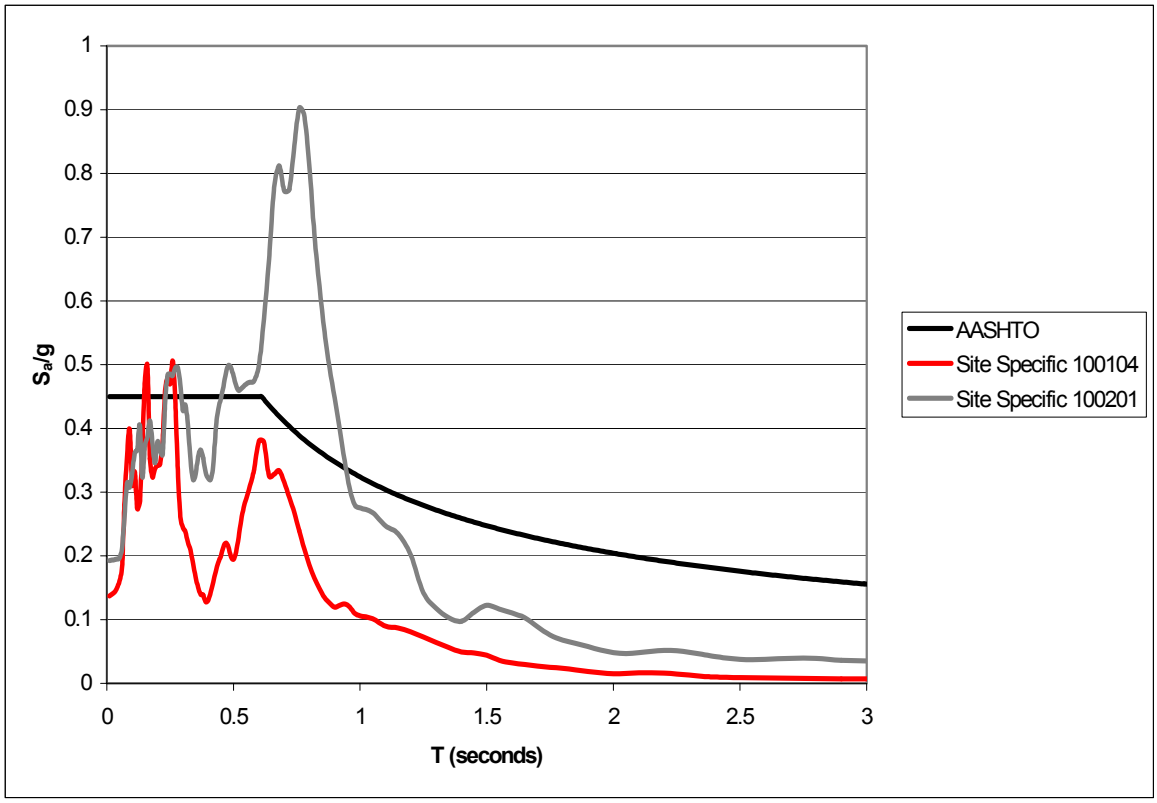

Figure 8.28 Comparison of AASHTO Response Spectrum & Site Specific Response Spectrum

Table 8.17 Comparison of AASHTO Response Spectrum vs. Site Specific Response Spectrum (New St. Francis River Bridge)

Due to Transverse EQ	transverse		longitudinal	
	response spectra	AASHTO	response spectra	AASHTO
Column 2, bottom	14924		4192	
	13059		3668	
	14511		4075	
	14081		3954	
average	14144	14574	3972	4093

Due to Transverse EQ	transverse		longitudinal	
	response spectra	AASHTO	response spectra	AASHTO
Column 5, bottom	14880		4171	
	13037		3654	
	14475		4058	
	14057		3942	
average	14112	14525	3956	4073

Due to Longitudinal EQ	transverse		longitudinal	
	response spectra	AASHTO	response spectra	AASHTO
Column 2, bottom	665		909	
	517		682	
	563		714	
	619		838	
average	591	780	786	1050

Due to Longitudinal EQ	transverse		longitudinal	
	response spectra	AASHTO	response spectra	AASHTO
Column 5, bottom	667		904	
	518		678	
	565		710	
	623		834	
average	593	786	782	1046

The results from the AASHTO response spectrum analysis were compared to several of the 10% earthquake response spectrum analyses that were run on the New St. Francis River Bridge. It was expected that these results would be reasonably close to one another. These results are summarized in Table 8.17.

8.1.7.2 Old St. Francis River Bridge

8.1.7.2.1 Bridge Description

The bridge under consideration is denoted as Bridge A-3708, located next to the new St. Francis River Bridge that was analyzed and evaluated in Section 8.1.7.1. It was designed in 1977 without seismic considerations. This 294 foot 1 inch bridge consists of three spans supported by steel plate girders, as shown in Figure 8.29. The dimensions of these plate girders varied slightly within a span depending on the location of the tension flange. The interior diaphragms and the cross-frames each consists of two L 3x2½x5/16 crossed over each other. The top and bottom horizontal members on the diaphragms and cross-frames were L 4x4x5/16. All interior diaphragms and cross-frames were placed parallel to the abutments of the bridge. The bridge, however, was skewed at a 20^{o} angle, so the ends of the girders were offset from one another at the ends of the

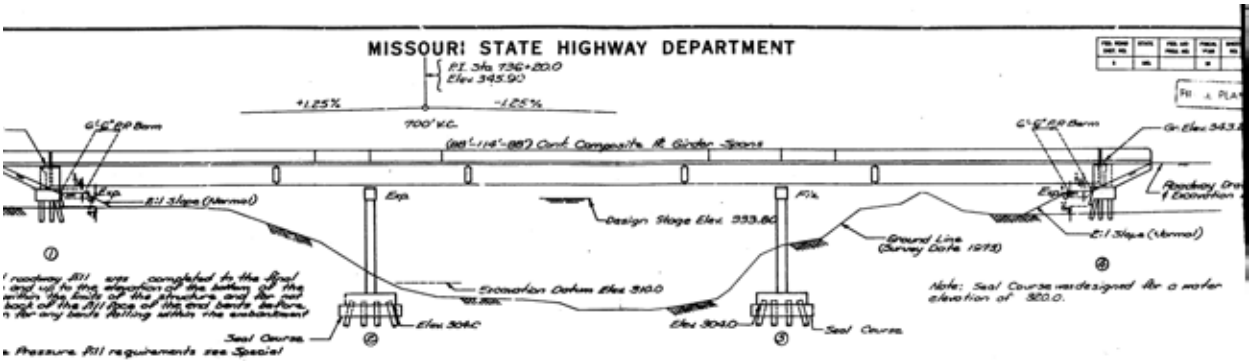

Figure 8.29 Bridge General Elevation (Old St. Francis River Bridge)

bridge. Therefore, these diaphragms and cross-frames were not perpendicular to the girders because of the angle of the structure.

The bridge superstructure is supported by two intermediate bents through one fixed bearing and one expansion bearing, along with seat-type abutments at its ends. Each bent consisted of a reinforced concrete cap beam and three reinforced concrete columns. Deep pile foundations support both bents and abutments. There are 12 piles for each column footing and 16 piles for each abutment footing. Two expansion joints were constructed at the ends of the bridge.

8.1.7.2.2 Bridge Model and Analysis

The bridge was modeled with the finite element method in the SAP2000 structural analysis program to analyze this bridge for susceptibility to earthquake damage.

All of the components of the structure were included in the bridge model. These components include the girders, diaphragms, cross-frames, interior bents and columns, and the bridge deck. The deck was represented by 52 shell elements with a thickness of 8.5 inches. All girders, cross-frames, and diaphragms were modeled as 633 frame members. Each frame section was then assigned member properties, such as material type and cross-section dimensions. The model also included 346 nodes.

To model ground soil conditions, springs and dashpots were used at the base of each column (six columns total, three on each interior bent). To account for passive soil pressure, "gap" elements with zero gap width were placed at the ends of the bridge on each abutment. A bilinear model was considered in the computer analysis. The soil body behind each abutment is considered to be mobilized when the displacement at the top of the abutment exceeds 0.5% of the abutment height (FHWA, 1995). The stiffness constants of the soil, which were input as part of the "gap" element information, were taken from Appendix F.

Rigid elements were used to model the abutments in *SAP2000*. However, unlike the New St. Francis River Bridge, the abutment rigid elements were modeled separated from the rest of the structure to represent the expansion joints between the abutment and the bridge structure. The expansion joints were modeled with several "gap" elements. Together with other "gap" elements on the abutments and the damper at the pile foundation, the bridge structure becomes a geometri-

cally nonlinear system. Therefore, a non-linear time-history analysis was used for the bridge model.

For each separate analysis using one directional earthquake excitation, 30 Ritz-vectors were considered associated with that earthquake direction. In Table 8.18, a sampling of five of the significant vibration modes are listed with its period in seconds and a brief description of the motion represented within the given mode. The mode shapes are shown in Figures 8.30-8.34.

The bridge was analyzed under a total of twelve earthquake ground motions described in Section 8.1.3. Six of the twelve motions correspond to a 10% PE level while the others to a 2% PE level. At each PE level of earthquakes, three were considered as near-field and the other three as far-field. The internal loads such as shear and moments and the abutment displacements were obtained at various critical locations. They will be presented together with the vulnerability evaluation of structural members in the next section. It is noted that one bridge analysis was conducted for each directional earthquake excitation due to the special directional combination rule specified in AASHTO Specifications (1996) and the nonlinear effect of the expansion joints and pile foundations on the bridge responses. Consequently, a total of 36 runs were completed.

8.1.7.2.3 Bridge Evaluation

The same procedure that was used for the New St. Francis River Bridge in Section 8.1.7.1.3 was followed for Old St. Francis River Bridge, denoted bridge A-3709. Again, C/D ratios were the main factor in determining whether a structural component would likely experience problems during

Table 8.18 Natural Periods and their Corresponding Vibration Modes (Old St. Francis River Bridge)

Mode Number	Period (seconds)	Motion Description
1	1.3173	Longitudinal
2	0.4773	Transverse
3	0.3673	Transverse
4	0.2065	Vertical
5	0.1501	Longitudinal

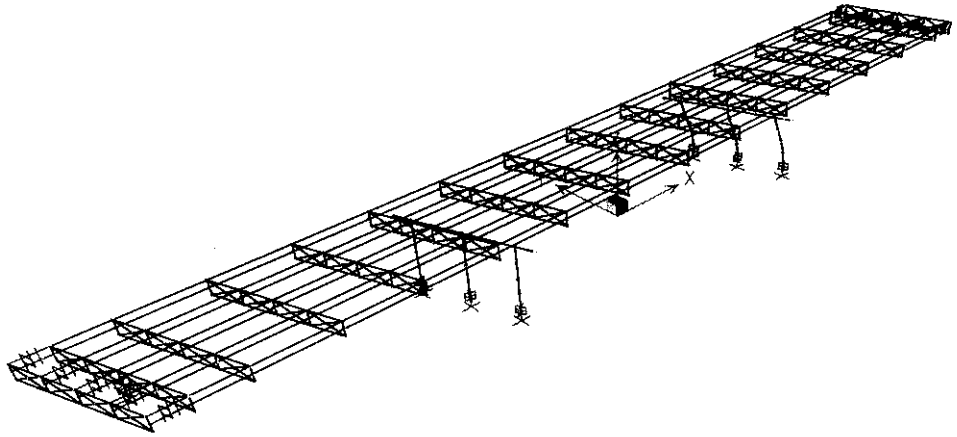

Figure 8.30 Mode 1, Period 1.3173 Seconds (Old St. Francis River Bridge)

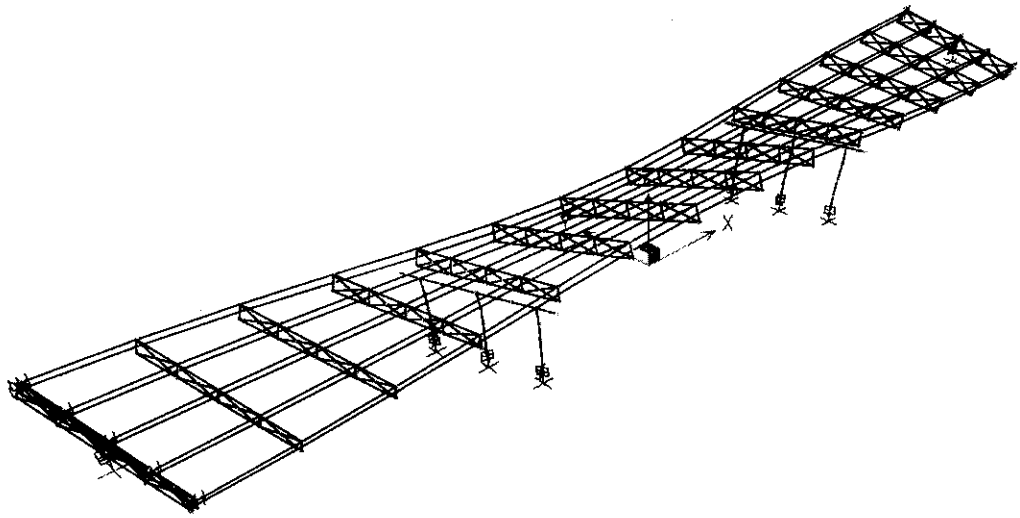

Figure 8.31 Mode 2, Period 0.4773 Seconds (Old St. Francis River Bridge)

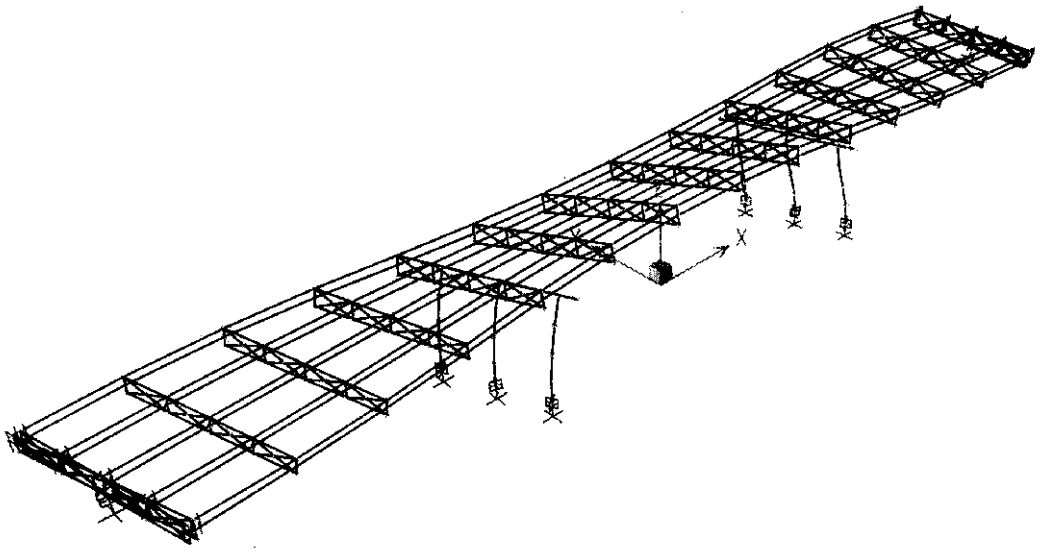

Figure 8.32 Mode 3, Period 0.3673 Seconds (Old St. Francis River Bridge)

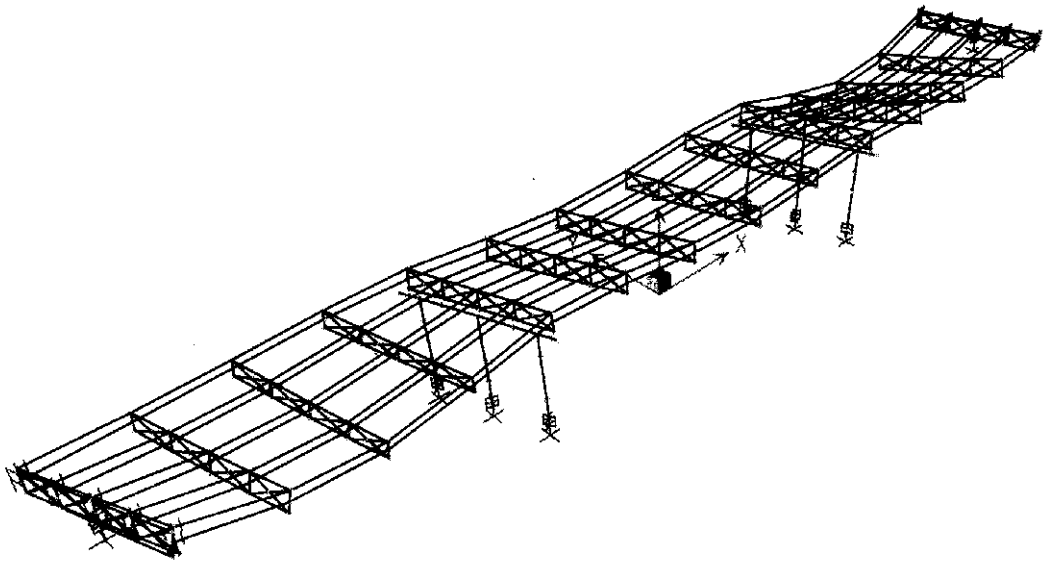

Figure 8.33 Mode 4, Period 0.2065 Seconds (Old St. Francis River Bridge)

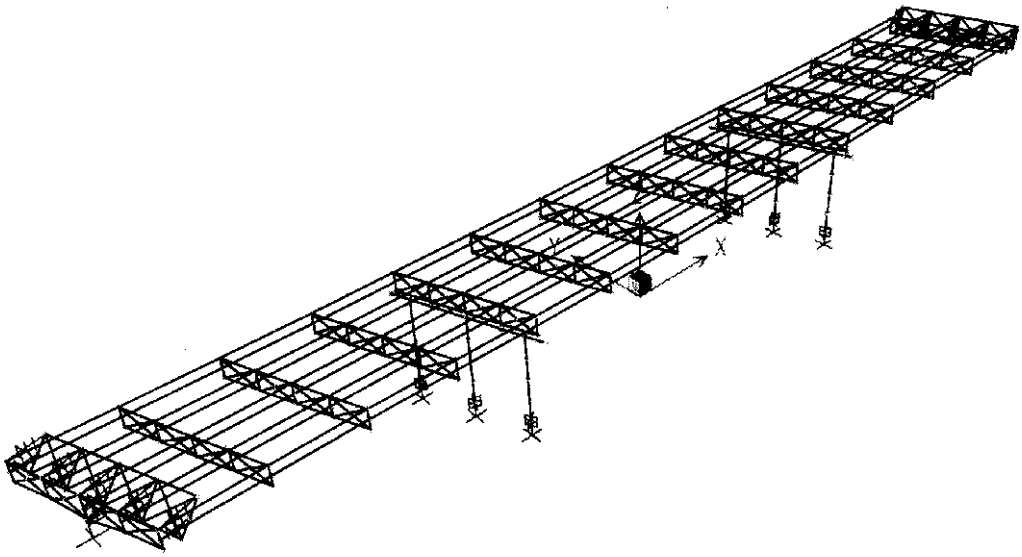

Figure 8.34 Mode 5, Period 0.1501 Seconds (Old St. Francis River Bridge)

an earthquake. Any C/D ratio equal to or greater than one would indicate that the component would probably not experience major problems during earthquake motions.

8.1.7.2.3.1 Load Combination Rule

The same load combination rule that was used for the New St. Francis River Bridge evaluation was employed for this structure as well. This combination rule was used in several instances throughout these calculations for various types of demands on the structure (shear, moment, and axial forces, as well as transverse and longitudinal displacements).

8.1.7.2.3.2 Minimum Support Length and C/D Ratio for Bearing

Because this bridge uses seat-type abutments, bearing and support length are essential components that must be examined. For this structure, the support length is a small amount short of what is required. The capacity, or actual support length for this bridge, was estimated at 23 inches. However, based on the definition of required support by FHWA, approximately 24 inches of length was needed. This indicates that the capacity is slightly less than the demand, so the bearing and support length for this bridge need to be examined more closely, as it could lead to the dropping of exterior spans during an earthquake.

8.1.7.2.3.3 C/D Ratios for Shear Force at Bearings

The first C/D ratios calculated in this section define the behavior of the bolts located at the bearing pads on the cap beams at the interior bents. In both the transverse and the longitudinal directions, there are two bolts for capacity. From the output of SAP2000 the shear demand at each of these points was determined and the maximum demand among these points was used to compute the C/D ratio for the "worst case". Before these shear values were used in determining the C/D ratios, the values were compared to 20% of the axial dead load at that location (FHWA, 1995). The greater of these two values were used in the subsequent calculations.

The force demands from each of the transverse, longitudinal, and vertical earthquake motions were combined to determine their total effect. The shear demands at these locations exceeded the capacities of these bolts for all of the 2% and 10% earthquakes. This indicates possible shear failures in the areas around the connecting bolts at the bearing pads.

The second set of C/D ratios in this section involves the embedment length and edge distance requirements for the bolts discussed in the previous paragraph. First, the required embedment length was found from Table 8-26 of the LRFD AISC Manual (1998). This length, for the 1.25-inch diameter rods that were used on this bridge, is 21.25 inches. From the plans, it is noted that the rods only extend 12 inches into the concrete. With the check, this results in a C/D ratio less than one, which would indicate a possible failure due to axial forces acting on the bolts
Finally, the edge distance was checked using another C/D ratio. From the same AISC table that provided the embedment lengths, allowable edge distances were also provided. For the rods used here, the required distance is 8.75 inches. The actual edge distance was estimated from the plans to be approximately 22 inches. This indicates that there should be no problems with the edge distance provided for the bolts.

8.1.7.2.3.4 C/D Ratios for Columns/Piers

In this section, the C/D ratios were calculated for all columns on the interior bents. The first step was to note the elastic moment demands for the top and bottom of each column in the transverse and longitudinal directions due to the combined effect of transverse, longitudinal, and vertical earthquake motions. The resulting moments were algebraically combined with the moments due to the dead load. This final calculation yields the value that is ultimately used in C/D ratio calculations.

The capacities of these columns were found in the same way as for the columns of the New St. Francis River Bridge. Again, the P-M interaction diagrams were used in conjunction with the iterative method for determining the axial load due to overturning, as well as the resulting shear force.

Finally, the maximum demand from the possible combinations was then used in conjunction with the determined capacity for the column to determine a C/D ratio for the columns. In most cases, the C/D ratios were well below one, indicating insufficient column strength for elastic seismic demand. However, a multiplier of 5 was applied to each ratio for the multiple-column bents. In all cases except for one of the 2% earthquakes, this multiplier increased the ratios to values

above one. This indicates that the columns will probably not cause problems, as long as the rebars are properly detailed in the plastic hinge zone.

As was outlined in the section discussing the New St. Francis River Bridge, capacities of the footings were also examined. The method used was identical to what was used previously, with the only adjustment accounting for the different number of piles and the different pile configurations. The plot of moment versus rotation for the case of axial load equal to zero is shown in Appendix H. It was noted that the moment capacity for this case is considerably higher than the capacities of the columns (several orders of magnitude greater). Therefore, it is unlikely that the footings would yield before the bottoms of the columns.

8.1.7.2.3.5 C/D Ratios for Reinforcement Anchorage in Columns

For both the top and bottom of the columns, the adequacy of the anchorage of longitudinal reinforcement must be checked. The capacity was determined simply by finding the length of anchorage at both the top and bottom of the columns. The demand was determined from an equation outlined in the FHWA Seismic Retrofit Manual.

At the tops of the columns, the anchorage was straight, whereas at the bottoms of the columns, the anchorage was hooked. However, in both cases, the actual length of the anchorage, which was estimated from the bridge plans, appeared to be less than the required lengths. These required lengths were determined from equations defined in FHWA (1995). The value for the C/D ratio was found from Figure 78 from the FHWA Manual, and this table was set up in terms of the anchorage geometry and location of the anchorage (top/bottom of the column, etc.). Because the capacity length was less than the demanded length, the resulting C/D ratio was simply the actual length divided by the required length, and then multiplied by the C/D ratio from the column. To determine the "worst-case" scenario, the minimum C/D ratio from among the columns was used without the ductility multiplier.

For this bridge, the initial C/D ratios for the columns were rather low, and this led to very low values for the C/D ratios for the reinforcement anchorage. These low ratios indicate that the anchorage of this longitudinal steel may be a component of concern.

8.1.7.2.3.6 C/D Ratios for Splices in Longitudinal Reinforcement

This section is not applicable to this structure, as the columns have no splices.

8.1.7.2.3.7 C/D Ratio for Transverse Confinement

In this section, a FHWA-defined relationship was used to determine the adequacy of transverse confinement. This C/D ratio was again dependent on the column moment C/D ratio, r_{ec}, without including the ductility indicator. The relationship defined for the transverse confinement included a multiplier as μ (FHWA, 1995). This multiplier was dependent on several factors, including geometry of the confinement as well as properties of the column reinforcement, the concrete, and the column cross-section.

The C/D ratios for all cases were above one. This indicates that there should be minimal problems with the transverse confinement.

8.1.7.2.3.8 C/D Ratio for Column Shear

In this section, column shear forces were determined following the same procedure as applied to the New St. Francis River Bridge previously. The same parameters needed to be calculated, including the maximum elastic shear in the columns, the initial shear capacity of the column, the final shear capacity of the column, and the shear demand on the column. From these parameters, "Case B" was chosen in all cases of 2% and 10% motions based on definitions from the FHWA Manual. For this case, the relationship for the column shear C/D ratio was the column moment C/D ratio multiplied by an FHWA-defined multiplier. This multiplier was based on column geometry (L_c = length of column and b_c = width of column) as well as the various shear parameters defined in Section 8.1.7.1.3.8.

8.1.7.2.3.9 C/D Ratio for Diaphragm and Cross-Frame Members

This section examines the damage caused to the diaphragm and cross-frame members for the bridge. They are both composed of two L 3x2½x5/16 crossed over each other with L 4x4x5/16 as the top and bottom horizontal members. Because of very low moments on these members, the members were analyzed based on their axial load capacity and demand.

As done for the New St. Francis River Bridge, two calculations for the same C/D ratio were exercised. The first uses the full length of the member spanning diagonally from top to bottom of the diaphragm/cross-frame. The second calculation uses half of the total length of the member. This was done because of the possibility of failure within the connection where the diagonal members meet, thus removing the intermediate brace. It should be noted that the members were modeled as two halves put together to make a full-length diagonal member for the diaphragms and cross-frames. The axial capacity was found to be less than the demand in most cases, which indicates that these members may have problems under the influences of strong earthquake motions.

The strength of the weld at the intermediate brace of the diagonals was calculated to be approximately 15 kips. According to the analysis, all of the 2% PE motions would likely cause this weld to fail, since all the axial demands for those earthquakes are greater than the weld capacity (range from 47 to 69 kips). The 10% PE motions appeared to cause this problem in two of the six examined cases, as the axial loads for those motions range from 12 to 30 kips.

8.1.7.2.3.10 C/D Ratio for Abutment Displacements

The final section of the procedure outlines the check for abutment adequacy. This test involves comparing the actual abutment displacements to maximum displacement values given by FHWA. The values are given as three inches of allowable displacement in the transverse direction and six inches of allowable displacement in the longitudinal direction.

The abutment displacements due to all three directions of earthquake motions were determined to be less than the allowable displacements in all cases. This indicates that the abutments should remain relatively damage-free in the event of an earthquake.

8.1.7.2.4 Summary of Problem Areas

The bridge experienced some serious problems that will be shown in more detail below. As expected, the bridge generally performed more poorly under the influence of the 2% likelihood earthquakes, which were considerably stronger than the 10% likelihood earthquakes.

Table 8.19 lists the C/D ratios of various components for all earthquakes. The following observations can be made from Table 8.19.

The first component of concern is the bearing length of this bridge. Because the capacity length is slightly less than the required length, this component could sustain damage in an earthquake. Next, the shear capacity at the bearing pads on the interior bents appears to be inadequate, as the demand outweighed the capacity in all cases. Also, the bolt embedment length and edge distance appear to be inadequate, indicating possible problems.

The next components of concern are the columns of this structure. Because the ductility indicator, which increases the column C/D ratios by five times, was used, all columns appeared to perform sufficiently, except at one point on two of the 2% ground motions. However, for all cases for both 2% and 10% ground motions, the longitudinal reinforcement anchorage was insufficient. This indicates that the ductile behavior of the columns may not be able to develop during a strong earthquake. Associated with the column ductility, the shear capacity of columns is also inadequate. For all of the 2% earthquakes, the column shear C/D ratio was less than one, which indicates some cause for concern.

The final components of concern are the diagonal members in the cross-frames and diaphragms of the bridge. As indicated by the C/D ratios, these members performed rather poorly.

The C/D ratios for these members were raised above one in some cases by using the half-length of the member. However, for all of the 2% earthquakes and two of the 10% earthquakes, the ratios still fell below one, indicating a problem that may warrant further investigation.

The strength of the weld at the intermediate brace of the diagonals was calculated to be approximately 15 kips. According to the analysis, all of the 2% PE motions would likely cause this weld to fail, since all the axial demands for those earthquakes are greater than the weld capacity (range from 47 to 69 kips). The 10% PE motions appeared to cause this problem in two of the six examined cases, as the axial loads for those motions range from 12 to 30 kips.

8.1.7.2.5 Time History Analysis vs. Response Spectrum Analysis

From the analysis of the New St. Francis River Bridge, it has been shown that a response spectrum analysis is reasonably accurate in the determination of elastic responses of structures. Due to the presence of the expansion joints in the Old St. Francis River Bridge, the bridge may behave in a nonlinear fashion due to the pounding effect. Therefore, it is necessary to compare the response spectrum analysis with the time history analysis again for this bridge to verify the accuracy of the spectrum analysis.

Tables 8.20, 8.21, and 8.21 show comparisons for moments and displacements at various locations on the structure (column 2, column 5 and the maximum abutment displacement). The values for the same location due to each of the 2% motions and 10% motions were averaged. The averages for time history results were then compared to those for the response spectra results. From these tables, the following observations can be made.

Bridge pounding in the longitudinal direction appears to be an issue when dealing with the 2% earthquake motions. This became apparent because of the "gap" elements that were used to model the expansion joints and the soil pressure on the back of the abutments in the non-linear time history analysis. In the response spectrum analysis, the structural model must be linear and the "gap" elements could not be used. Therefore, springs were used to model the soil stiffness behind the abutments, and the "gap" elements, which modeled the expansion joints between the abutment and the superstructure, were removed.

This caused noticeable differences on the moments and forces on the fixed interior bent (the other bent was an expansion bearing). Because this bent was fixed to the superstructure, it was allowed to move much more in the response spectra analysis, as the "gap" elements, which restrained the motion in the non-linear analysis, had been taken out. Therefore, it was noticed that the moments and forces on this bent were approximately two to three times larger than those noted from the time history analysis. This was only the case for longitudinal motion; the transverse and vertical direction earthquakes saw small variations. However, for the other bent, which was not fixed to the superstructure, the forces and moments were reasonably close to one another between the two analyses.

The above phenomenon was noticeable only on the stronger 2% earthquakes. The 10% earthquakes yielded different results. Pounding is apparently less of an issue with these motions, and therefore the moments and forces between the two analyses were closer to one another. There were some discrepancies, but these may have been attributed to differences in how damping is handled in the time history and response spectrum analyses.

Table 8.19 Summary of C/D Ratios for All Earthquakes at Old St. Francis River Bridge

C/D Ratio Name	020101	020103	020105	020201	020203	020204	100102	100104	100105	100201	100204	100205
r_{bd}	**0.96**	**0.96**	**0.96**	**0.96**	**0.96**	**0.96**	**0.96**	**0.96**	**0.96**	**0.96**	**0.96**	**0.96**
$r_{bf\text{-}trans}$	**0.60**	**0.46**	**0.47**	**0.43**	**0.45**	**0.30**	**0.73**	**0.89**	**0.77**	**0.48**	**0.54**	**0.50**
$r_{bf\text{-}long}$	**0.62**	**0.52**	**0.57**	**0.58**	**0.71**	**0.71**	**0.89**	**0.89**	**0.89**	**0.74**	**0.89**	**0.78**
$r_{bf\text{-}embed}$	**0.56**	**0.56**	**0.56**	**0.56**	**0.56**	**0.56**	**0.56**	**0.56**	**0.56**	**0.56**	**0.56**	**0.56**
$r_{bf\text{-}edge\ dist.}$	2.51	2.51	2.51	2.51	2.51	2.51	2.51	2.51	2.51	2.51	2.51	2.51
$r_{ec\text{-}final}$	1.91	2.54	1.70	2.40	2.35	2.51	8.95	12.46	9.56	5.40	5.84	5.92
$r_{ec\text{-}final}$	2.48	3.31	2.21	3.12	3.06	3.26	11.64	16.21	12.43	7.02	7.60	7.71
$r_{ec\text{-}final}$	1.34	1.33	1.16	1.53	1.43	1.63	6.48	8.19	7.27	3.34	4.09	3.24
$r_{ec\text{-}final}$	1.70	1.68	1.47	1.94	1.82	2.06	8.21	10.38	9.22	4.23	5.18	4.11
$r_{ec\text{-}final}$	1.77	1.54	1.67	1.66	2.17	2.19	5.01	7.28	5.65	2.93	3.25	2.96
$r_{ec\text{-}final}$	2.31	2.01	2.17	2.17	2.83	2.85	6.51	9.46	7.35	3.82	4.22	3.84
$r_{ec\text{-}final}$	1.24	**0.90**	1.05	1.05	1.12	**0.95**	2.13	3.18	2.46	1.28	1.40	1.31
$r_{ec\text{-}final}$	1.57	1.14	1.33	1.33	1.42	1.20	2.70	4.04	3.12	1.62	1.77	1.66
$r_{ca\text{-}bottom}$	**0.16**	**0.11**	**0.13**	**0.13**	**0.14**	**0.12**	**0.27**	**0.40**	**0.31**	**0.16**	**0.18**	**0.17**
$r_{ca\text{-}top}$	**0.27**	**0.24**	**0.25**	**0.25**	**0.33**	**0.33**	**0.76**	1.11	**0.86**	**0.45**	**0.49**	**0.45**
r_{cs}	---	---	---	---	---	---	---	---	---	---	---	---
$r_{cs\text{-}adj}$	---	---	---	---	---	---	---	---	---	---	---	---
r_{cc}	**0.90**	**0.65**	**0.77**	**0.77**	**0.82**	**0.69**	1.56	2.32	1.80	**0.94**	1.02	**0.96**
r_{cv}	**0.95**	**0.69**	**0.81**	**0.81**	**0.86**	**0.73**	1.64	2.45	1.90	**0.99**	1.08	1.01
r_{cross}	**0.17**	**0.13**	**0.14**	**0.16**	**0.19**	**0.18**	**0.59**	**0.74**	**0.63**	**0.30**	**0.37**	**0.32**
$r_{cross\text{-}0.5L}$	**0.45**	**0.34**	**0.39**	**0.42**	**0.52**	**0.48**	1.60	2.01	1.71	**0.80**	1.00	**0.86**
$r_{ad\text{-}trans}$	11.5	8.9	9.8	11.0	11.9	11.1	30.5	42.7	34.6	14.3	17.1	14.1
$r_{ad\text{-}long}$	14.9	6.7	7.9	9.4	10.9	7.4	40.8	62.9	45.6	10.1	13.3	10.0

To further check the response spectrum and time history a result, a third case was run, for the longitudinal direction only. This third case used the same model as from the response spectrum case (which had no "gap" elements on the abutments), but it was analyzed using a linear time history analysis. This case was run for four earthquakes, two each of the 2% and 10% motions. For the most part, the results lined up reasonably well with the response spectrum results. The only discrepancies were similar to the ones mentioned above due to the different ways of treating the damping matrix of the structure.

8.1.7.2.6 Structure Response of Abutments

The Old St. Francis River Bridge abutment (13.0 m x 2.1 m) is supported on 8 vertical piles and 8 battered piles. All piles are cylindrical concrete with 0.406 m (16 inch) diameter and 10.67 m (35 ft) length. The plan and cross section of the bridge abutment are shown in Figure 8.35.

The stiffness and damping factors are calculated using a pile length of 10.67 m (35 ft), a pile radius of 0.203 m (8 inch), and an elastic modulus of the pile material of 2.15×10^7 kN/m (1.47×10^6 kips/ft) (Section F.6). Stiffness and damping factors of a single batter piles are 0.8 times that of a vertical pile. (Prakash and Subramanayam, 1964)

The vertical load acting on the top of bridge abutment is obtained from an analysis of the bridge superstructure. Accordingly, a vertical load (Q) of 100 kN (22481 lb) per m of abutment was used in this analysis. The self-weight of the bridge abutment was calculated by multiplying its area by the unit weight of the bridge abutment material ($\gamma = 23.58$ kN/m^3) (150.19 pcf). This calculation is done in the program itself. The lateral earth pressure behind the bridge abutment is calculated using a unit weight of soil of 19.54 kN/m^3 (122 pcf), internal friction angle of 33^o and friction angle between soil and abutment of 33^o. All of loads were modified by a time dependent seismic coefficient.

8.1.7.2.6.1 Calculated Time Dependent Displacements of Abutment

Table 8.23 shows for different magnitudes of earthquakes (M), the largest sliding, rocking and total displacement at the top of the bridge abutment for an earthquake with a PE of 10% in 50 years and one with a PE of 2 % in 50 years, respectively.

Figures 8.36a and b show the time histories of sliding, rocking and total permanent displacement of the Old St. Francis River Bridge abutment for a PE 10% in 50 years for earthquake magnitudes of M6.2 and M7.2 respectively. Figures 8.37a and b show the time histories of sliding, rocking and total permanent displacement of the Old St. Francis River Bridge abutment for a PE 2% in 50 years and magnitudes of M6.4 and M8.0 respectively.

Figure 8.36a shows a plot of magnitude and significant number of cycles. Table 8.22 also shows displacement in one significant cycle.

Table 8.20 Comparison of Moments for Time History and Response Spectrum Analysis for Column 2 (Old St. Francis River Bridge)

Due to 2% motions

Due to Transverse EQ	transverse		longitudinal	
	time history	response spectra	time history	response spectra
Column 2, bottom	17677	16607	16125	18257
	19718	18457	19877	19745
	16591	16544	13460	15270
	13982	15119	17486	16400
average	16992	16682	16737	17418

Due to Longitudinal EQ	transverse		longitudinal	
	time history	response spectra	time history	response spectra
Column 2, bottom	6155	7495	14430	13499
	6630	6385	15559	14420
	5183	6486	10537	9923
	6367	6925	12146	12032
average	6084	6823	13168	12469

Due to Vertical EQ	transverse		longitudinal	
	time history	response spectra	time history	response spectra
Column 2, bottom	866	879	527	596
	539	565	339	408
	695	611	376	426
	636	623	506	508
average	684	670	437	485

Due to 10% motions

Due to Transverse EQ	transverse		longitudinal	
	time history	response spectra	time history	response spectra
Column 2, bottom	2927	3158	2303	3448
	3544	3332	2371	3449
	7148	7225	3441	6399
	5827	7142	4743	7574
average	4862	5214	3215	5218

Due to Longitudinal EQ	transverse		longitudinal	
	time history	response spectra	time history	response spectra
Column 2, bottom	1794	1150	1564	2629
	2234	1148	1648	2490
	3599	1917	4908	4035
	3879	2509	6069	5466
average	2877	1681	3547	3655

Due to Vertical EQ	transverse		longitudinal	
	time history	response spectra	time history	response spectra
Column 2, bottom	135	146	146	149
	116	148	141	152
	166	211	211	193
	164	208	191	215
average	145	178	172	177

Table 8.21 Comparison of Moments for Time History and Response Spectrum Analysis for Column 5 (Old St. Francis River Bridge)

Due to 2% motions

Due to Transverse EQ	transverse: time history	transverse: response spectra	longitudinal: time history	longitudinal: response spectra
Column 5, bottom	18491	18216	3457	5687
	20032	20271	4515	5021
	19006	18621	3816	5466
	14708	16619	4097	5286
average	18059	18432	3971	5365

Due to Longitudinal EQ	transverse: time history	transverse: response spectra	longitudinal: time history	longitudinal: response spectra
Column 5, bottom	2834	8448	22867	75473
	3810	6334	27989	54678
	3423	7719	29099	69563
	3432	7909	28826	70868
average	3375	7603	27195	67646

Due to Vertical EQ	transverse: time history	transverse: response spectra	longitudinal: time history	longitudinal: response spectra
Column 5, bottom	755	816	298	279
	489	529	167	171
	631	577	221	201
	668	578	272	222
average	636	625	240	218

Due to 10% motions

Due to Transverse EQ	transverse: time history	transverse: response spectra	longitudinal: time history	longitudinal: response spectra
Column 5, bottom	3532	3395	1698	865
	4168	3667	2097	921
	7735	8136	4182	1870
	6815	7879	4772	1991
average	5563	5769	3187	1412

Due to Longitudinal EQ	transverse: time history	transverse: response spectra	longitudinal: time history	longitudinal: response spectra
Column 5, bottom	610	1120	10821	9580
	730	1170	14160	10161
	4153	2015	27024	17573
	4116	2563	26333	22335
average	2402	1717	19585	14912

Due to Vertical EQ	transverse: time history	transverse: response spectra	longitudinal: time history	longitudinal: response spectra
Column 5, bottom	157	135	181	66
	124	141	230	73
	217	229	305	138
	182	207	261	114
average	170	178	244	98

Table 8.22 Comparison of Displacements for Time History and Response Spectrum Analysis for Maximum Abutment Displacement(Old St. Francis River Bridge)

Due to 2% motions

Due to Transverse EQ	transverse		longitudinal	
	time history	response spectra	time history	response spectra
Max. Abut. Disp.	0.2193	0.1805	0.1393	0.0858
	0.1982	0.2239	0.0582	0.1246
	0.1915	0.2121	0.0428	0.0837
	0.1647	0.1614	0.0358	0.0841
average	0.1934	0.19448	0.069	0.09455

Due to Longitudinal EQ	transverse		longitudinal	
	time history	response spectra	time history	response spectra
Max. Abut. Disp.	0.0514	0.1037	0.3877	0.1741
	0.2477	0.1117	0.7396	0.26
	0.2147	0.0983	0.6232	0.172
	0.2023	0.1011	0.5379	0.1737
average	0.179	0.1037	0.5721	0.19495

Due to Vertical EQ	transverse		longitudinal	
	time history	response spectra	time history	response spectra
Max. Abut. Disp.	0.008	0.00761	0.006	0.0121
	0.0057	0.0085	0.003	0.00519
	0.0068	0.00841	0.0035	0.00528
	0.0068	0.00848	0.0042	0.00536
average	0.0068	0.00825	0.0042	0.00698

Due to 10% motions

Due to Transverse EQ	transverse		longitudinal	
	time history	response spectra	time history	response spectra
Max. Abut. Disp.	0.0577	0.0536	0.0211	0.0328
	0.0595	0.0485	0.0207	0.0365
	0.0956	0.1005	0.051	0.0337
	0.0795	0.0778	0.0453	0.0391
average	0.0731	0.0701	0.0345	0.03553

Due to Longitudinal EQ	transverse		longitudinal	
	time history	response spectra	time history	response spectra
Max. Abut. Disp.	0.0413	0.0309	0.0882	0.0849
	0.0688	0.0332	0.1253	0.0883
	0.1807	0.0296	0.5778	0.0715
	0.1894	0.0381	0.5865	0.087
average	0.1201	0.03295	0.3445	0.08293

Due to Vertical EQ	transverse		longitudinal	
	time history	response spectra	time history	response spectra
Max. Abut. Disp.	0.0012	0.00149	0.0018	0.0007
	0.0014	0.00135	0.0023	0.00074
	0.002	0.00177	0.0025	0.00125
	0.0017	0.00192	0.0024	0.00089
average	0.0016	0.00163	0.0023	0.0009

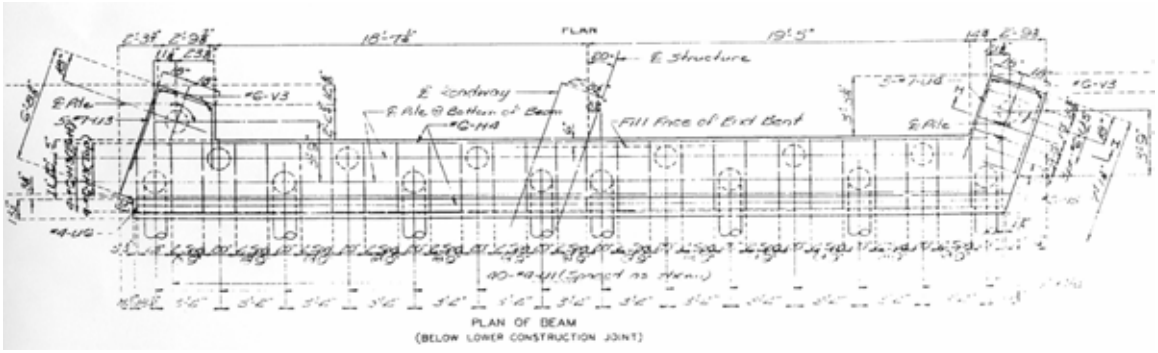

(a) Plan of bridge abutment

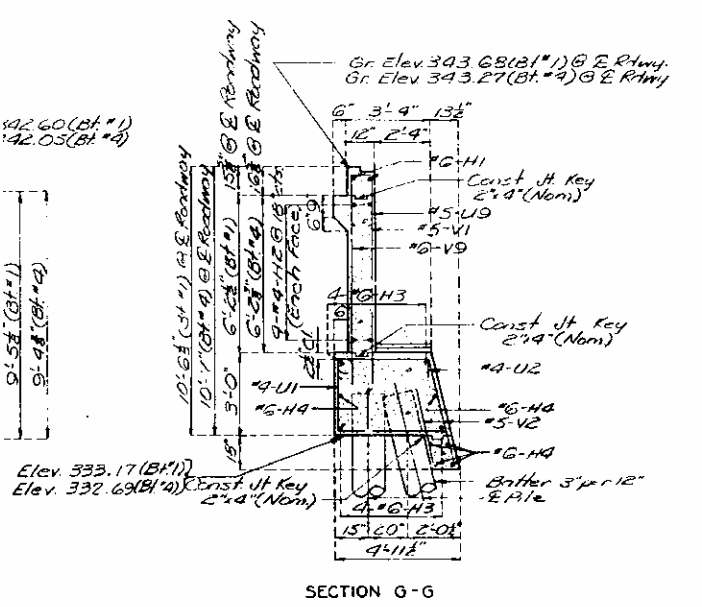

(b) Cross section of bridge abutment
Figure 8.35 Old St. Francis River Bridge Plans

8.2 Wahite Ditch Site

8.2.1 Site Geology

The following units, listed from the ground surface downward, characterize local geology at Wahite Ditch:

- Approximately 20 feet of high plasticity clay,
- Approximately 170 feet of medium sand, containing numerous thin gravel lenses, and
- Stiff clay, assumed to represent a portion of the Wilcox Group.

An example cross-section from the Wahite Ditch site is shown on Figure 8.38.

Several engineering properties of site soil units were measured in the field. These properties are recorded on the boring logs in Appendix A.

8.2.2 Selected Base Rock Motion

Herrmann, (2000) recommends 10 rock base motions for PE 10% in 50 years and another 10 for PE 2 % in 50 years. All of the 40 rock motions have been used for one-dimensional wave propagation analysis using the *SHAKE91* program. Based on wave propagation analysis, peak ground accelerations for each rock motion is obtained. Total of 12 ground motions were selected based on these peak ground acceleration values.

Table 8.24a lists 5-ground motion for PE 10% in 50 years with corresponding maximum peak ground accelerations for M6.4 with epicentral distance of 40 km. Five additional ground motions with M7.0 and epicentral distances of 65 km are given as well. Table 8.24b shows listing for PE 2 % in 50 years with different magnitudes and epicentral-distance. In these tables column 1-4 are basic data from Herrmann (2000).

As for the St. Francis River site, 12- synthetic ground motions at the rock base (six for each PE) are selected as representative of the "worst case scenarios". They are given in Table 8.25. The associated acceleration-time histories are shown in Figure 8.39a-d.

8.2.3 Seismic Response of Soil

The *SHAKE* and *SHAKEDIT* programs were used to propagate the design earthquake base rock motions to the ground surface. This resulted in peak ground motions and time histories of acceleration at the soil surface, the base of bridge abutments and the piers Figure 8.40 shows the

Table 8.23 Displacement at the Top of the Old St. Francis Bridge Abutment

Displacement at top of abutment	**PE 10% in 50 years**		**PE 2% in 50 years**	
	M6.2	**M7.2**	**M6.4**	**M8.0**
Sliding (m)	0.052	0.093	0.096	0.31
Rocking (m)	0.037	0.061	0.069	0.21
Total (m)	0.089	0.154	0.165	0.52
Significant cycles	8	11	9	20
Displacement in 1-cycle	0.011	0.014	0.018	0.026

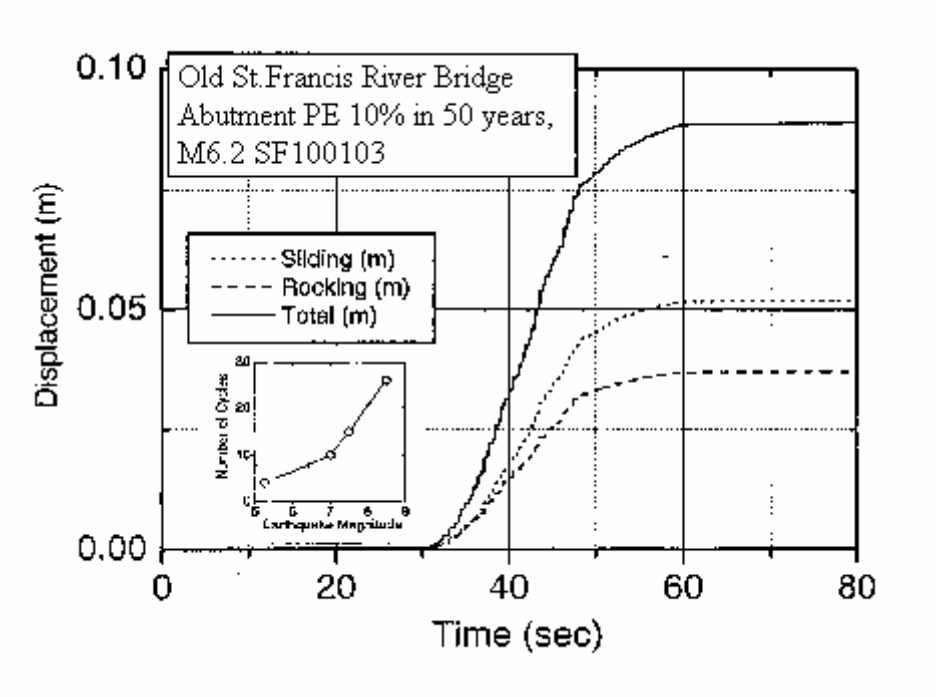

a. Magnitude 6.2

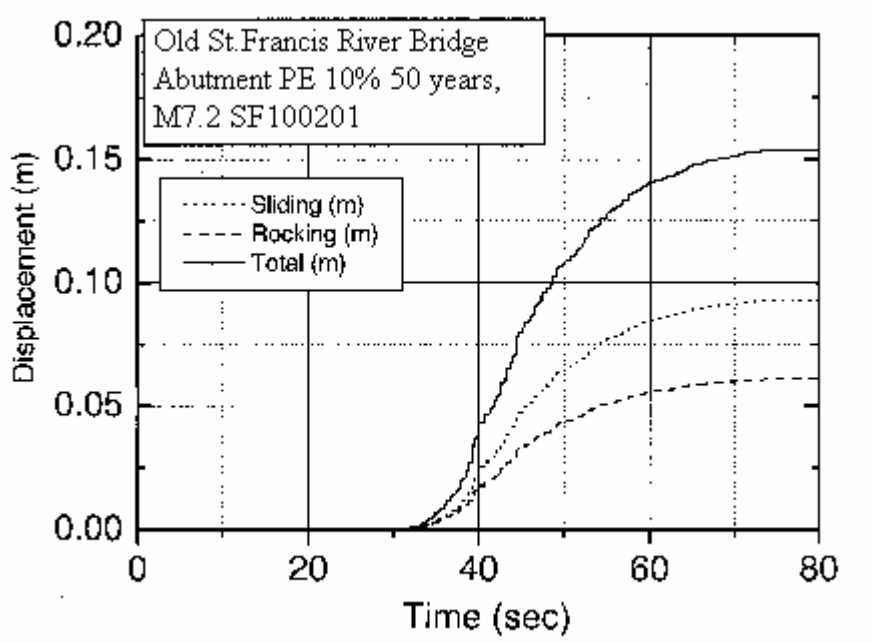

b. Magnitude 7.2

Figure 8.36 Time Histories of Sliding, Rocking and Total Permanent Displacement of the Old St. Francis River Bridge Abutment, PE 10% in 50 Years, Magnitudes 6.2 and 7.2

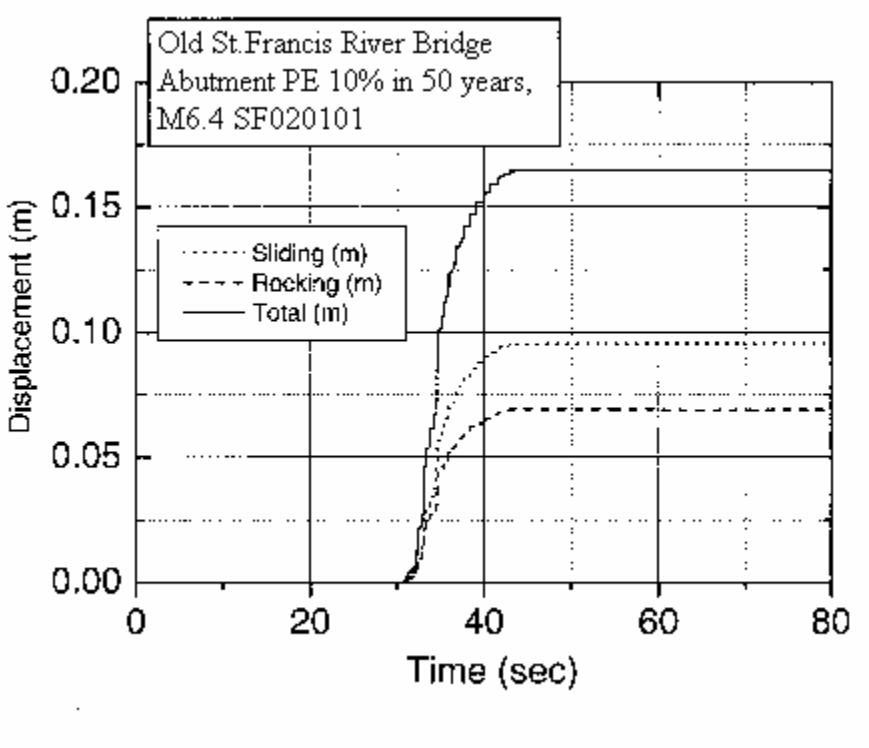

a. Magnitude 6.4

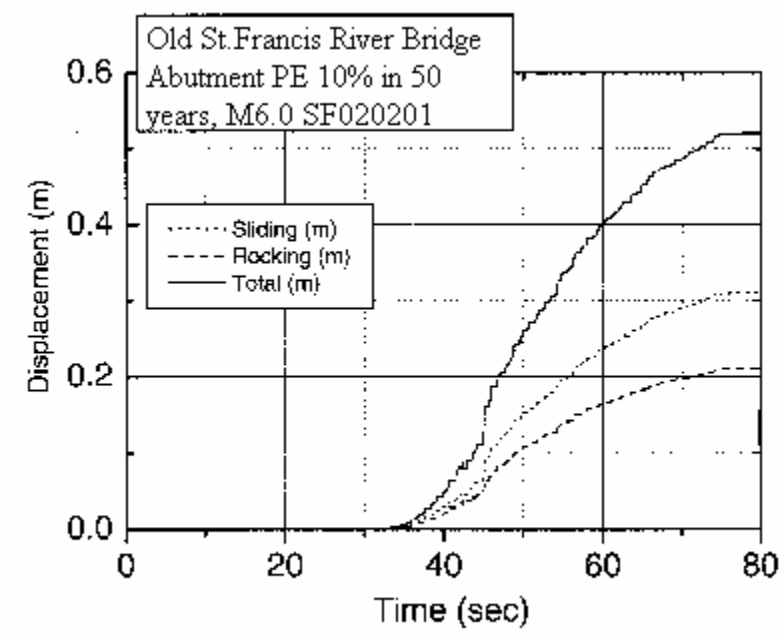

b. Magnitude 8.0

Figure 8.37 Time Histories of Sliding, Rocking and Total Permanent Displacement of the Old St. Francis River Bridge Abutment, PE 2% in 50 Years, Magnitudes 6.4 and 8.

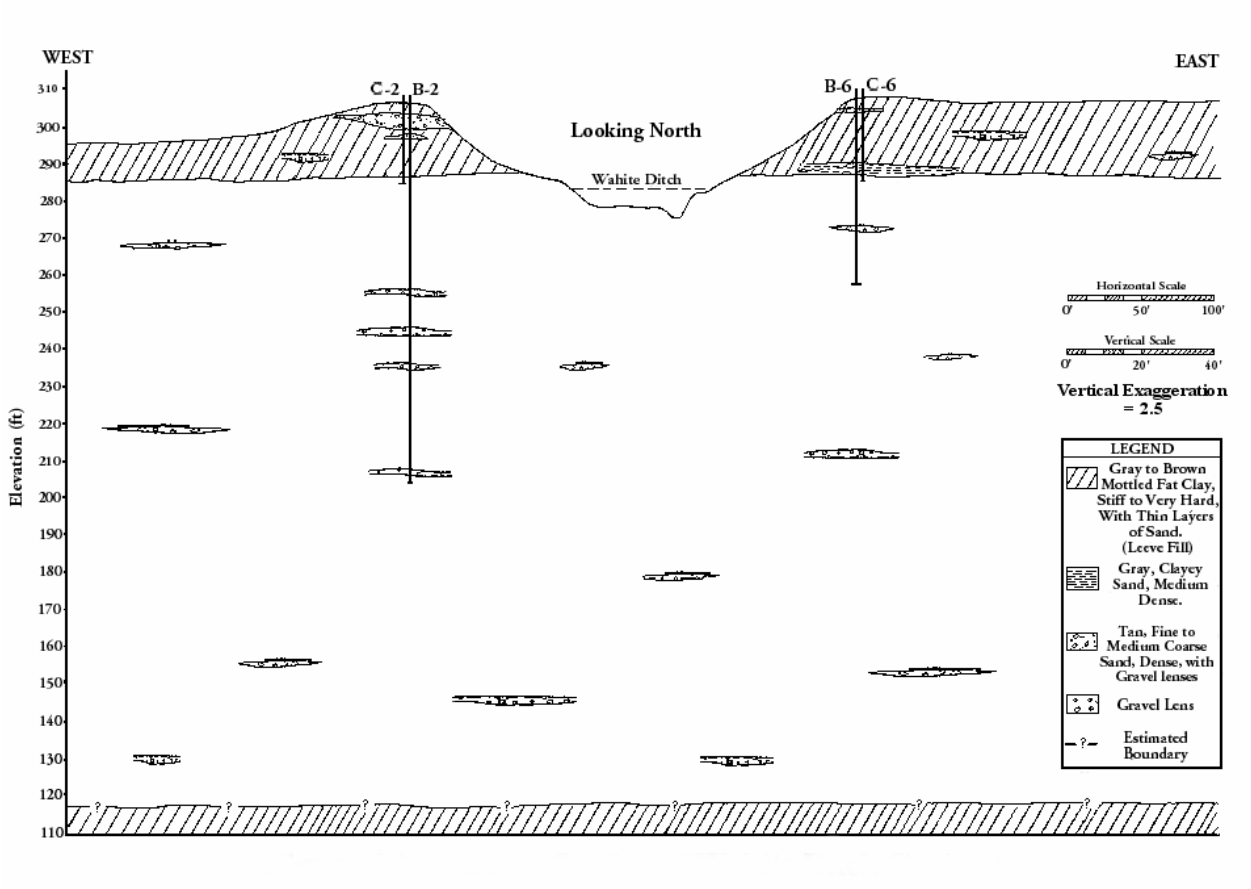

Figure 8.38 Cross-Section of Wahite Ditch Site Geology

location of the Wahite Ditch Site. A brief description of the soil profile including observed SPT (N_{obs}) and corrected $(N_1)_{60}$ values are shown in Figure 8.41. The subsurface soil consists of 20 feet of high plasticity clay overlying about 170 ft of medium sand containing numerous thin gravel lenses.

8.2.3.1 Horizontal Seismic Response of Soil

The soil profile as developed from bore hole B1 Figure 8.41), has been used in the seismic response analysis, because B1 is located close to the bridge abutment.

The initial shear modulus (G_o) was computed using the seismic cone measurements of shear wave velocity. The seismic cone could be used only to a depth of 42 feet (13 m). G_o was calculated for depths below 42 ft (13 m) based on the measured N_{spt} values. This calculation is performed in the *SHAKEDIT* program itself. The non-linear soil properties, such as modulus degradation with shear strain and material damping with shear strain, have been employed for each soil type.

Table 8.24. Detail of Synthetic Ground Motion at the Rock Base of Wahite Ditch Site with Corresponding Maximum Peak Horizontal Ground Acceleration

a. PE 10% In 50 Years

Name (1)	Mw (2)	R (km) (3)	Max acc. at rock-base(g) (4)	Max acc. at soil-surface(g) (5)
WD100101*	6.4	40	0.126	0.153
WD100102*	6.4	40	0.119	0.152
WD100103	6.4	40	0.136	0.127
WD100104	6.4	40	0.121	0.144
WD100105*	6.4	40	0.13	0.151
WD100201*	7.0	65	0.124	0.185
WD100202*	7.0	65	0.142	0.171
WD100203	7.0	65	0.173	0.171
WD100204	7.0	65	0.144	0.147
WD100205*	7.0	65	0.166	0.180
Mw = Magnitude R = Epicentral distance * Used in further analysis				

b. PE 2% In 50 Years

Name (1)	Mw (2)	R (km) (3)	Max acc. at rock-base(g) (4)	Max acc. at soil-surface(g) (5)
WD020101*	7.8	16	1.549	0.437
WD020102*	7.8	16	1.769	0.478
WD020103*	7.8	16	2.129	0.512
WD020104	7.8	16	1.996	0.415
WD020105	7.8	16	1.822	0.423
WD020201	8.0	20	1.442	0.440
WD020202	8.0	20	1.589	0.440
WD020203*	8.0	20	1.855	0.525
WD020204*	8.0	20	1.720	0.406
WD020205*	8.0	20	1.559	0.447
Mw = Magnitude R = Epicentral distance * Used in further analysis				

The calculated peak ground accelerations at each soil level, based on wave propagation analysis, were plotted against depth. Figures 8.42a and b show the peak acceleration for PE 10% in 50 years for M6.4 and M7.0 respectively. Figures 8.43a and b show the peak acceleration for PE 2% in 50 years for M7.8 and M8.0 respectively.

For PE 10 % in 50 years and M6.4 and M7.0 respectively, the peak accelerations at the soil surface are higher than those at the base-rock. However, for PE 2 % in 50 years, the peak accelerations at the soil surface are smaller than those at the base rock.

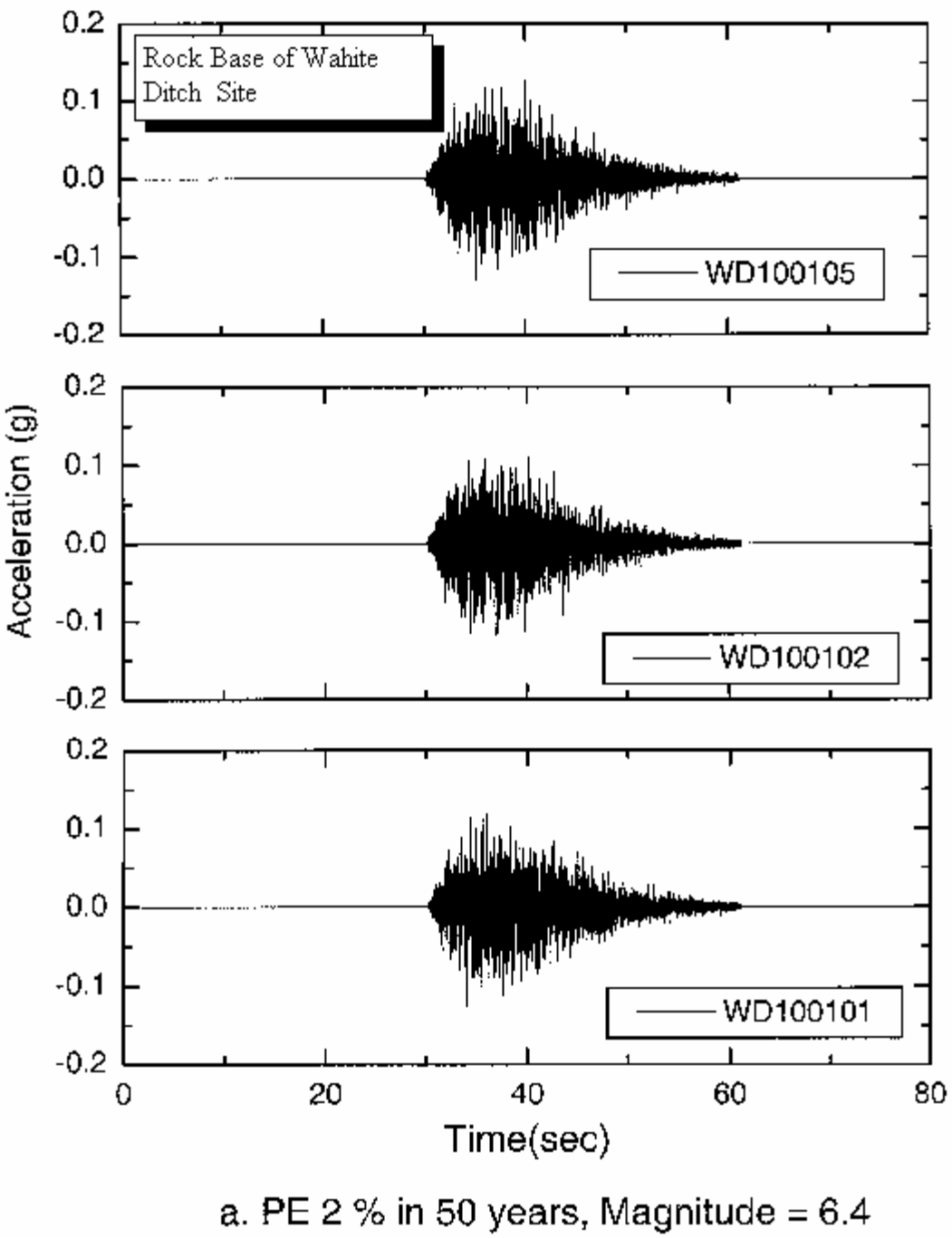

a. PE 2 % in 50 years, Magnitude = 6.4

Figure 8.39a Acceleration Time Histories for the Wahite Ditch Site, PE 2% in 50 Years, Magnitude = 6.4

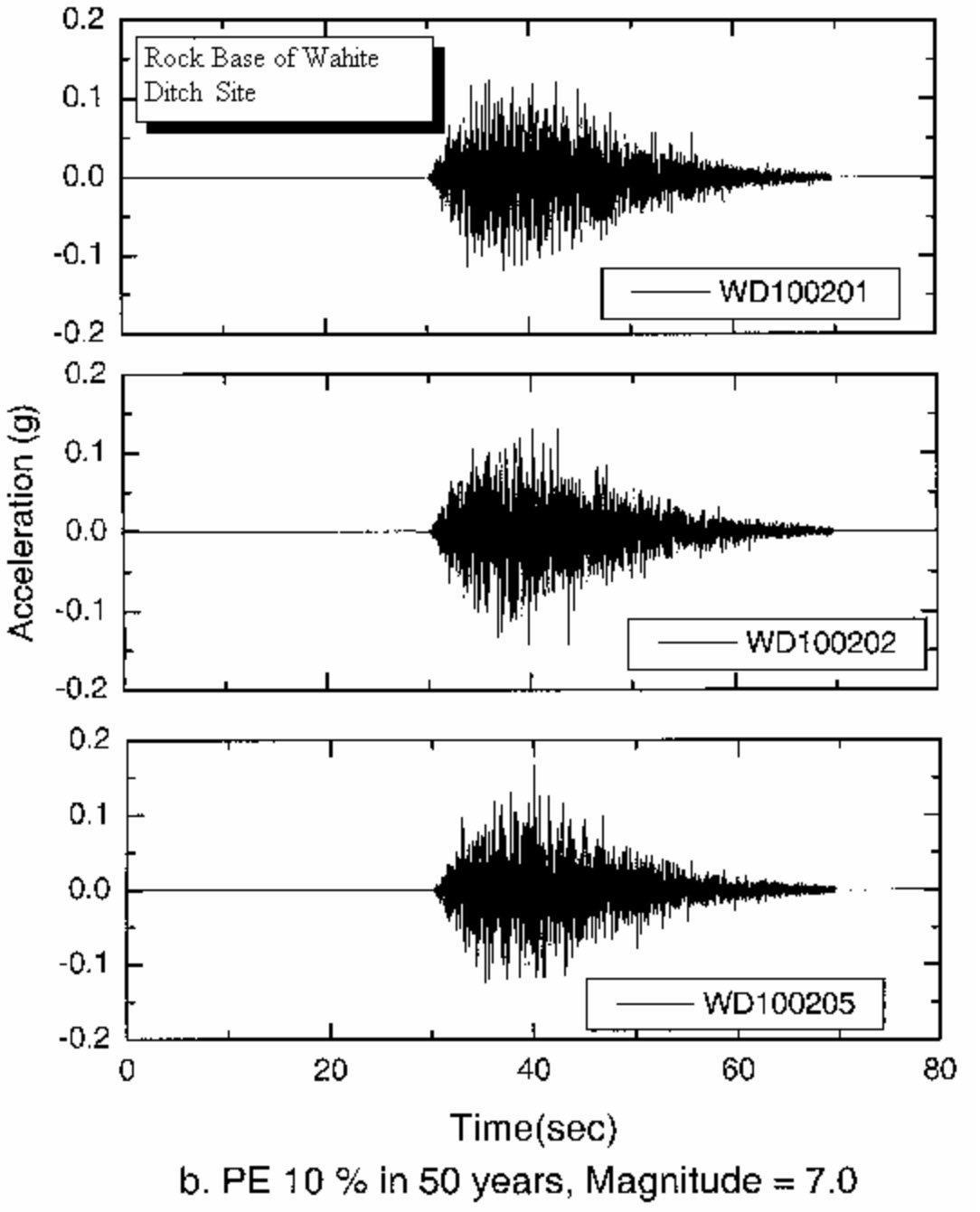

Figure 8.39b Acceleration Time Histories for the Wahite Ditch Site, PE 10% in 50 Years, Magnitude = 7.0

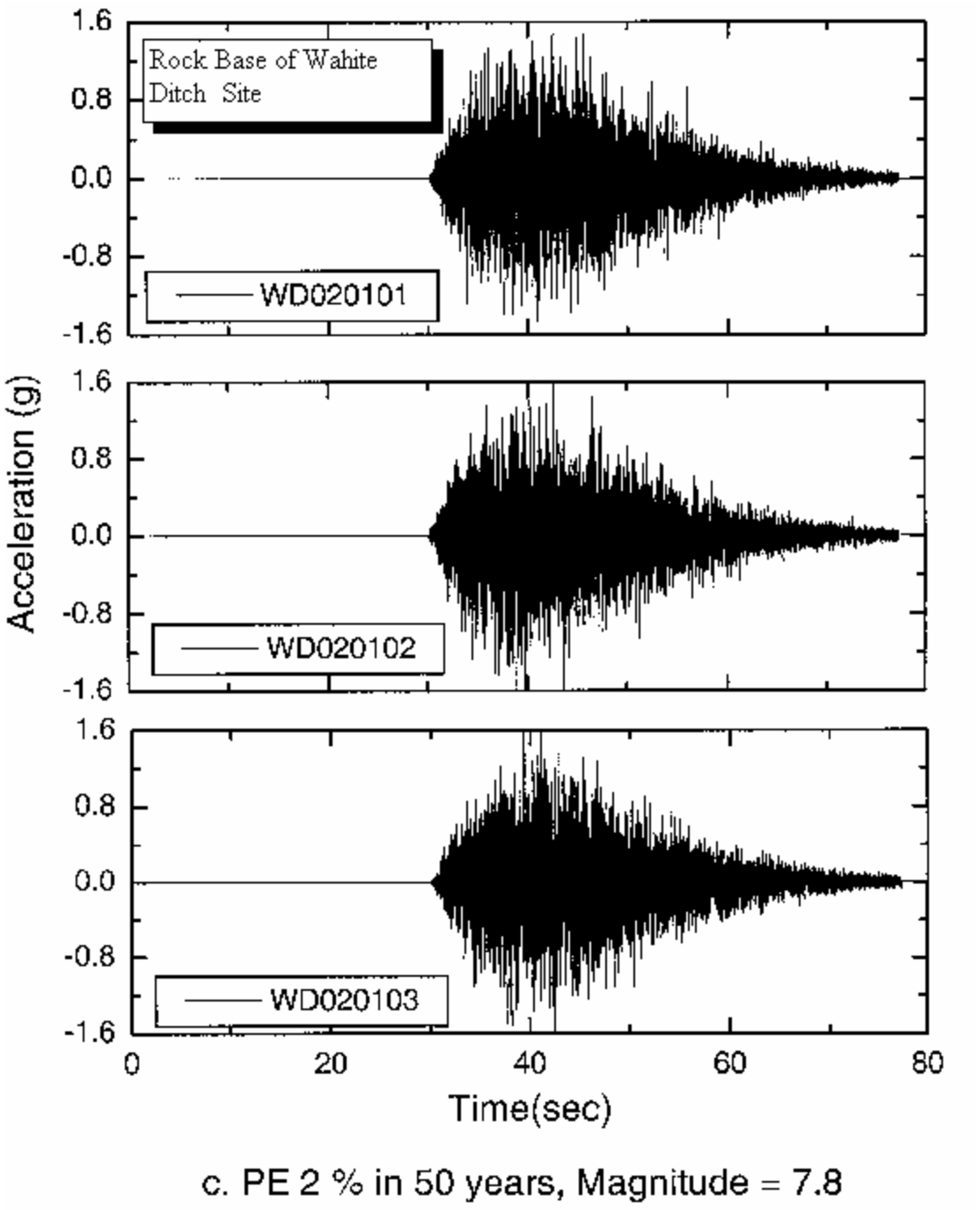

Figure 39c Acceleration Time Histories for the Wahite Ditch Site, PE 2% in 50 Years, Magnitude = 7.8

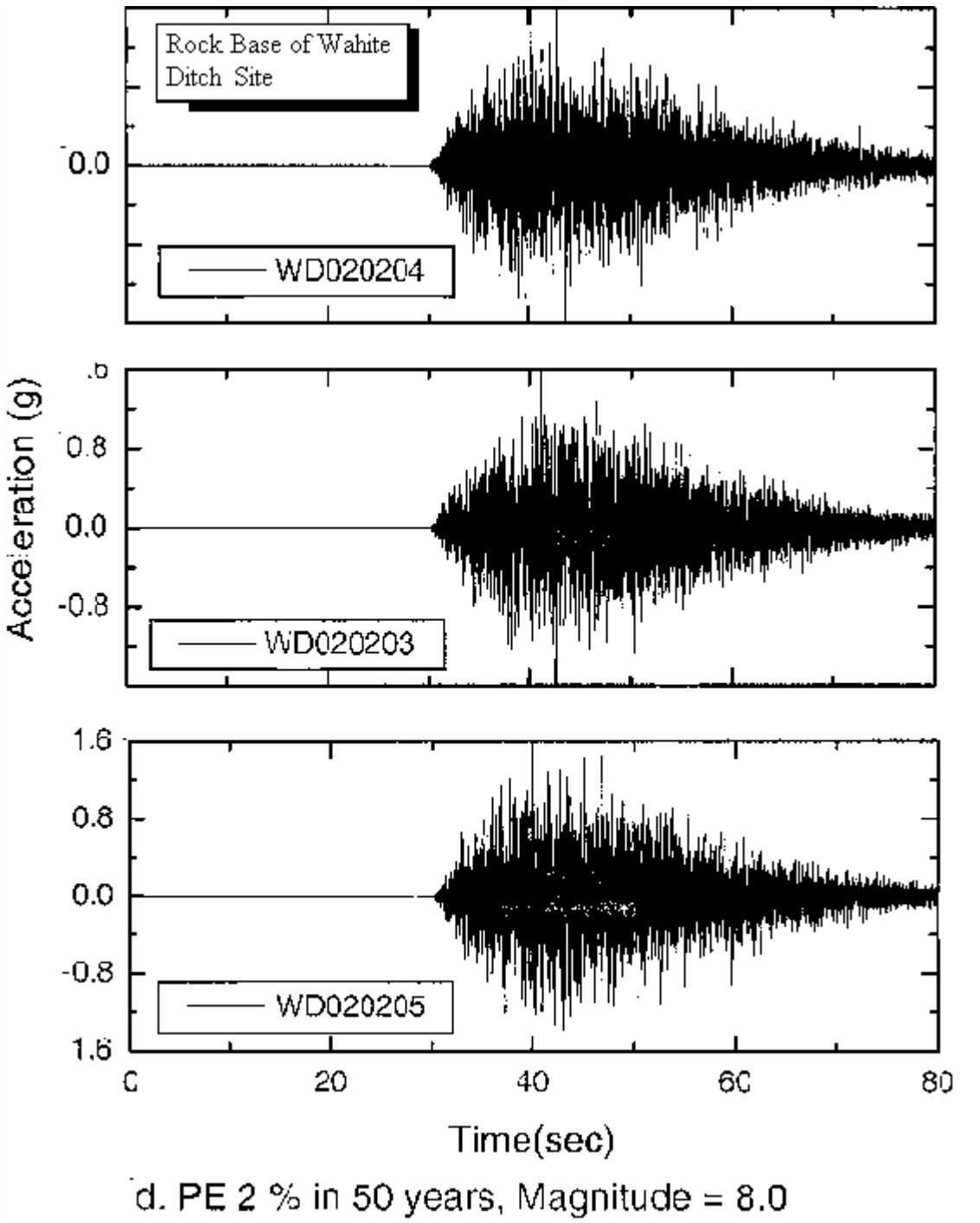

Figure 8.39d Acceleration Time Histories for the Wahite Ditch Site, PE 2% in 50 Years, Magnitude = 8.0

Table 8.25a shows the peak horizontal acceleration for the design earthquake at the soil surface, bridge abutment and pier respectively for PE 10% in 50 years, Table 8.25b shows similar information for PE 2 % in 50 years.

8.2.3.2 Resulting Ground Motion Time Histories

Figures 8.44a and b contain six-plots of surface ground acceleration at EL. 307.2 for PE 10 % in 50 years and earthquake magnitude M6.4 and M7.0. Similarly Figures 8.44c and d contain plots for PE 2% in 50 years and M7.8 and M8.0 respectively.

Figures 8.45a, b, c and d contain plots of design acceleration time history at the abutment for (a) PE 10 % in 50 years M6.4, (b) PE 10 % in 50 years M7.0, (c) PE 2% in 50 years M7.8 and (d) PE 2% in 50 years M8.0.

Similarly, Figure 8.46a, b, c and d contain plots for the pier.

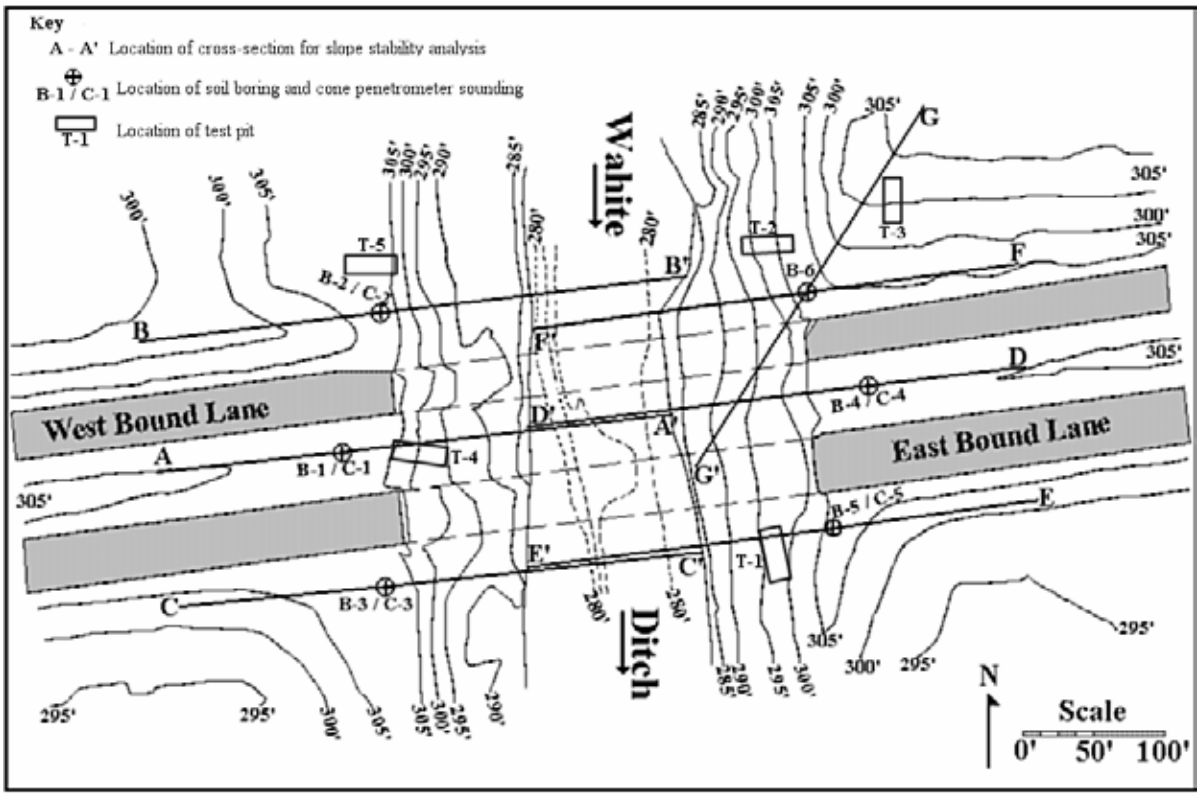

Figure 8.40 Wahite Ditch Site Topography, Cross-Section and Boring Locations

Table 8.25 Detail of Peak Ground Motion Used at the Wahite Ditch Site Rock Base, Ground Surface, Bridge Abutment and Pier

a. PE 10% in 50 years

File Name	Max. acc. at rock-base EL. 106.0 (g)	Max acc. at soil-surface EL 307.2 (g)	Max acc. at bridge abutment EL 301.2 (g)	Max acc. at bridge pier EL 269.9 (g)
WD100101*	0.126	0.153	0.153	0.139
WD100102*	0.119	0.152	0.151	0.127
WD100105*	0.13	0.151	0.151	0.120
WD100201*	0.124	0.185	0.185	0.169
WD100202*	0.142	0.171	0.170	0.146
WD100205*	0.166	0.18	0.180	0.157

b PE 2% in 50 years

File Name	Max. acc. At rock-base EL. 106.0(g)	Max acc. at soil-surface EL 307.2 (g)	Max acc. at bridge abutment EL 301.2 (g)	Max acc. at bridge pier EL 269.9 (g)
WD020101*	1.549	0.437	0.440	0.430
WD020102*	1.769	0.478	0.482	0.512
WD020103*	2.129	0.512	0.514	0.522
WD020202*	1.589	0.44	0.446	0.466
WD020203*	1.855	0.525	0.527	0.538
WD020205*	1.559	0.447	0.449	0.444

8.2.3.3 Vertical Seismic Response of Soil

Herrmann (2000) stated that vertical rock motion is of the same order of magnitude as the horizontal rock motion. *SHAKE91* was used to transmit the horizontal rock motion from the rock base to the ground surface. No such solution is available for transmission of vertical motion. Therefore the following procedure was adopted for vertical ground motion determination:.

1. Use *SHAKE91* to transfer the P-wave.
2. Adjust peak vertical ground motion as 2/3 of peak horizontal ground motion.
3. Adjust the time history to reflect adjustment in (2) above.

The calculated vertical time histories of acceleration at soil surface, base of bridge abutment and at bridge pier were also modified as above.

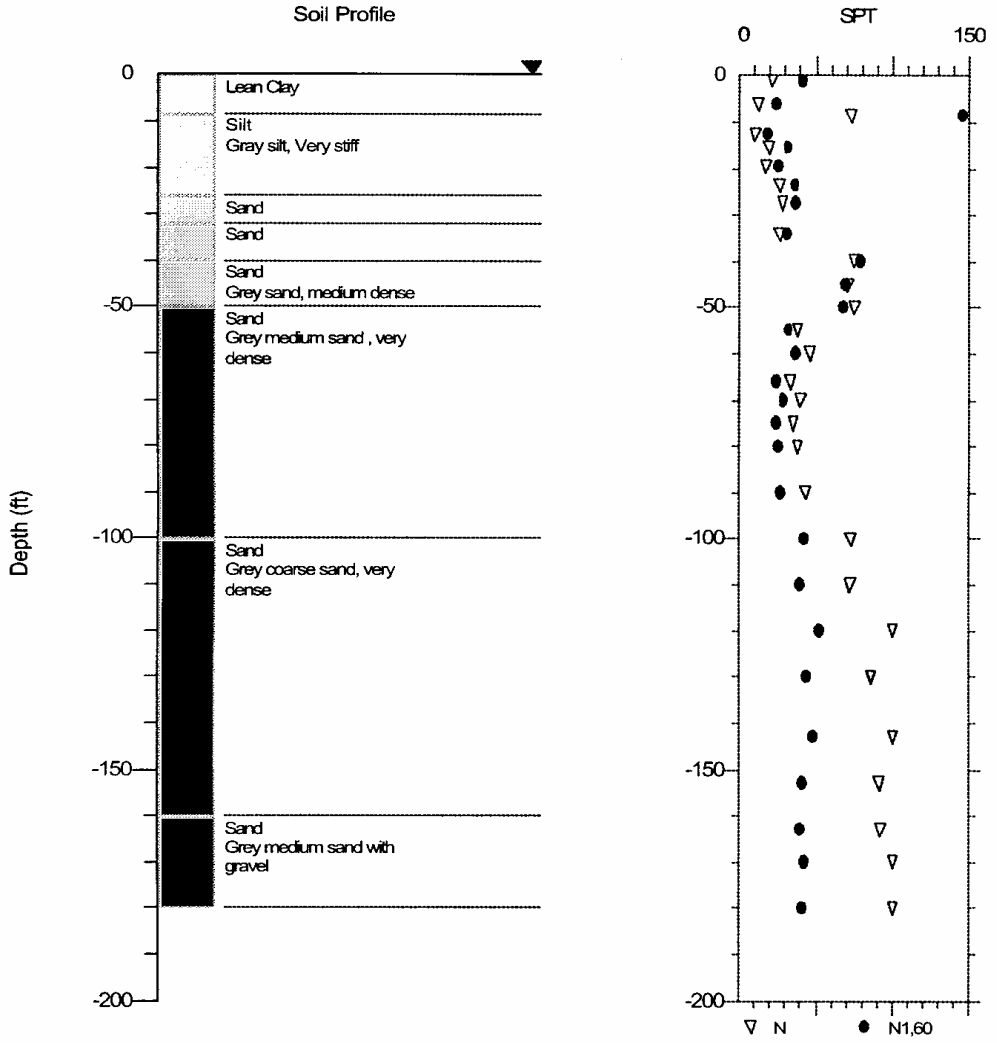


```
Notes:
      CSR analysis using SHAKE results.
      CSR File: D:\I-O SF Pe10%\SF100103\Sf100103.grf
      CRR using SPT Data and Seed et. al. Method in 1997 NCEER Workshop.
      Earthquake File for SHAKE Analysis: D:\SF\SF100103.ACC
      Earthquake Magnitude for CRR Analysis:  6.2
      Magnitude Scaling Factor (MSF):  1.62
      Depth to Water Table for CRR Analysis (ft):  0
      Depth to Water Table for Cn Calculation (ft):  0
      Depth to Base Layer for CSR Analysis (ft):  219.6
      MSF Option: I.M. Idriss (1997)
      Cn Option: Liao & Whitman (1986)
      Ksigma Option: L.F. Harder & R. Boulanger (1997)
      SPT Energy Ratio: USA/Safety/Rope: 0
```

Figure 8.41 Soil Profile Wahite Ditch Site Boring B-1

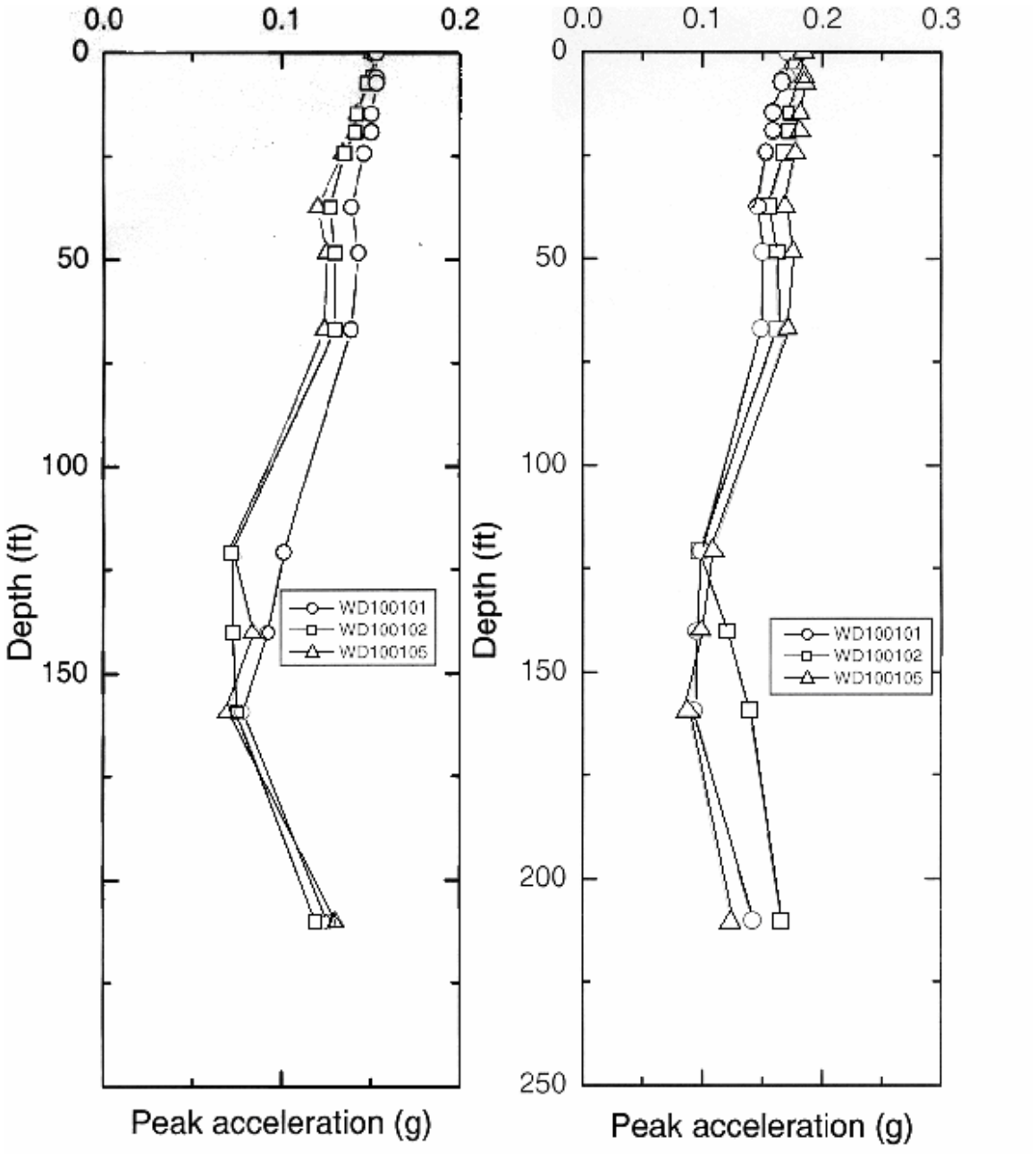

Figure 8.42 Peak Ground Acceleration vs. Depth for PE 10% in 50 Years Magnitudes 6.4 and 7.0 Wahite Ditch Site

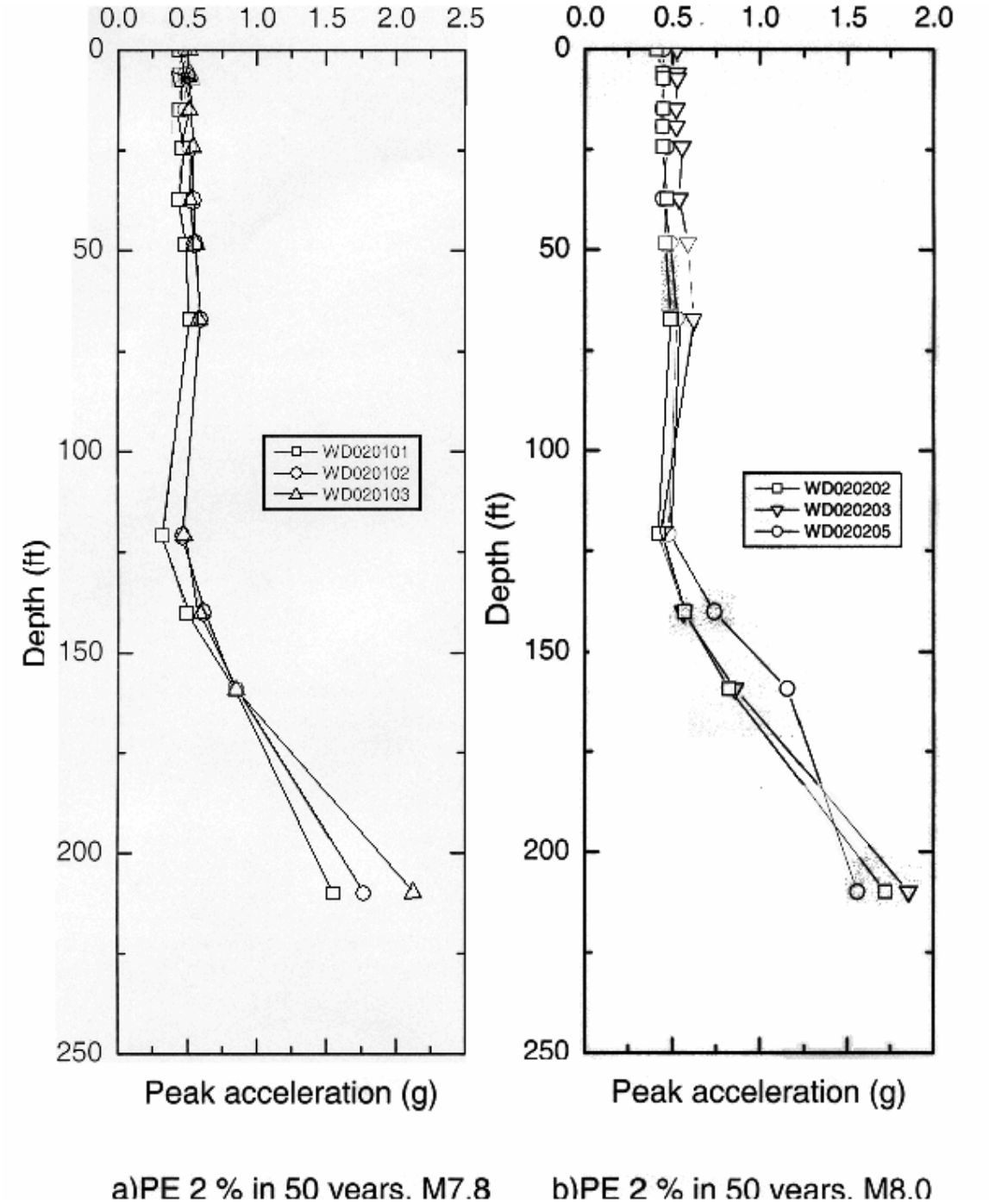

Figure 8.43 Peak Ground Acceleration vs. Depth for PE 2% in 50 Years Magnitudes 7.8 and 8.0 Wahite Ditch Site

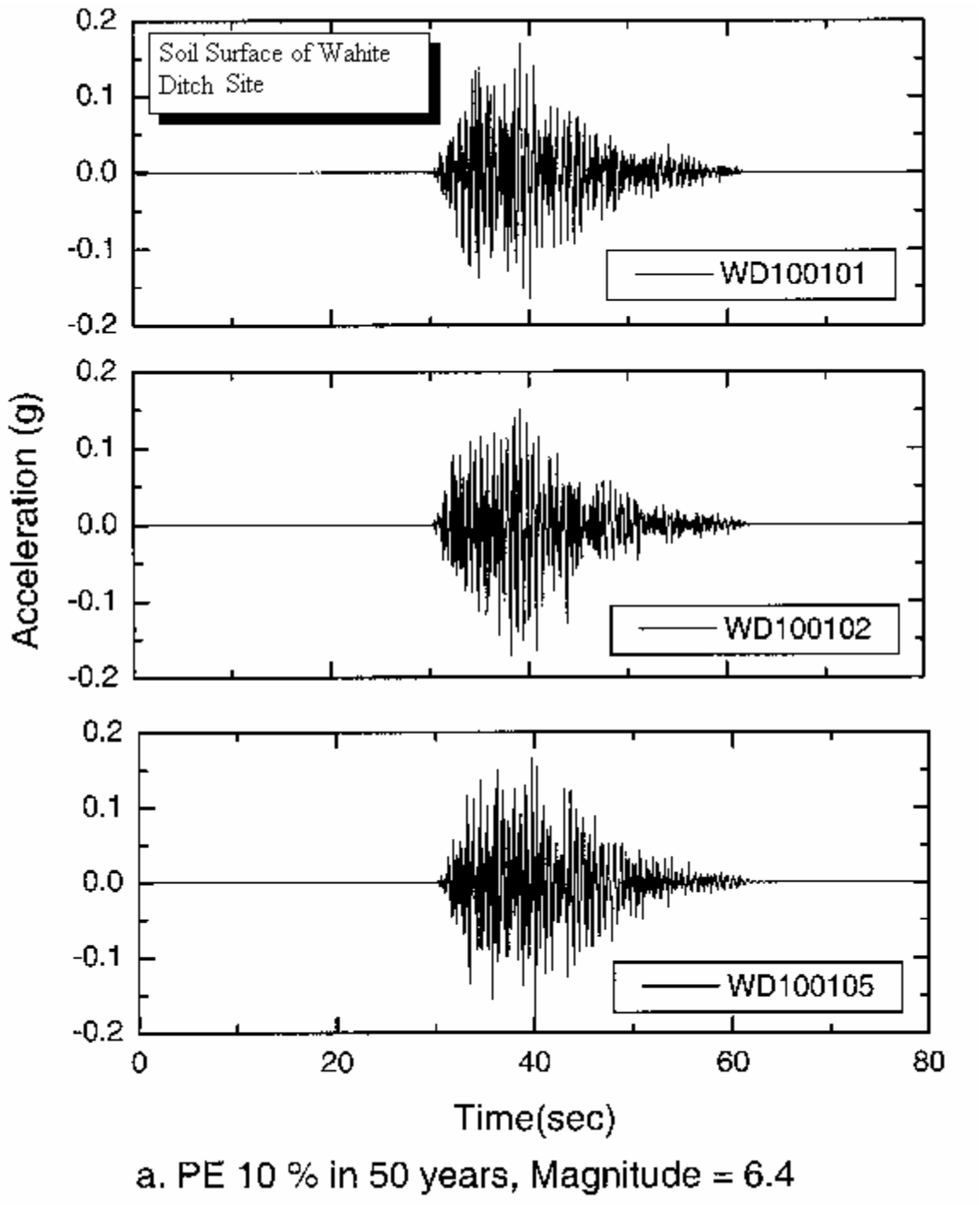

Figure 8.44a Ground Acceleration at the surface of the Wahite Ditch Site, PE 10% in 50 years, Magnitude = 6.4

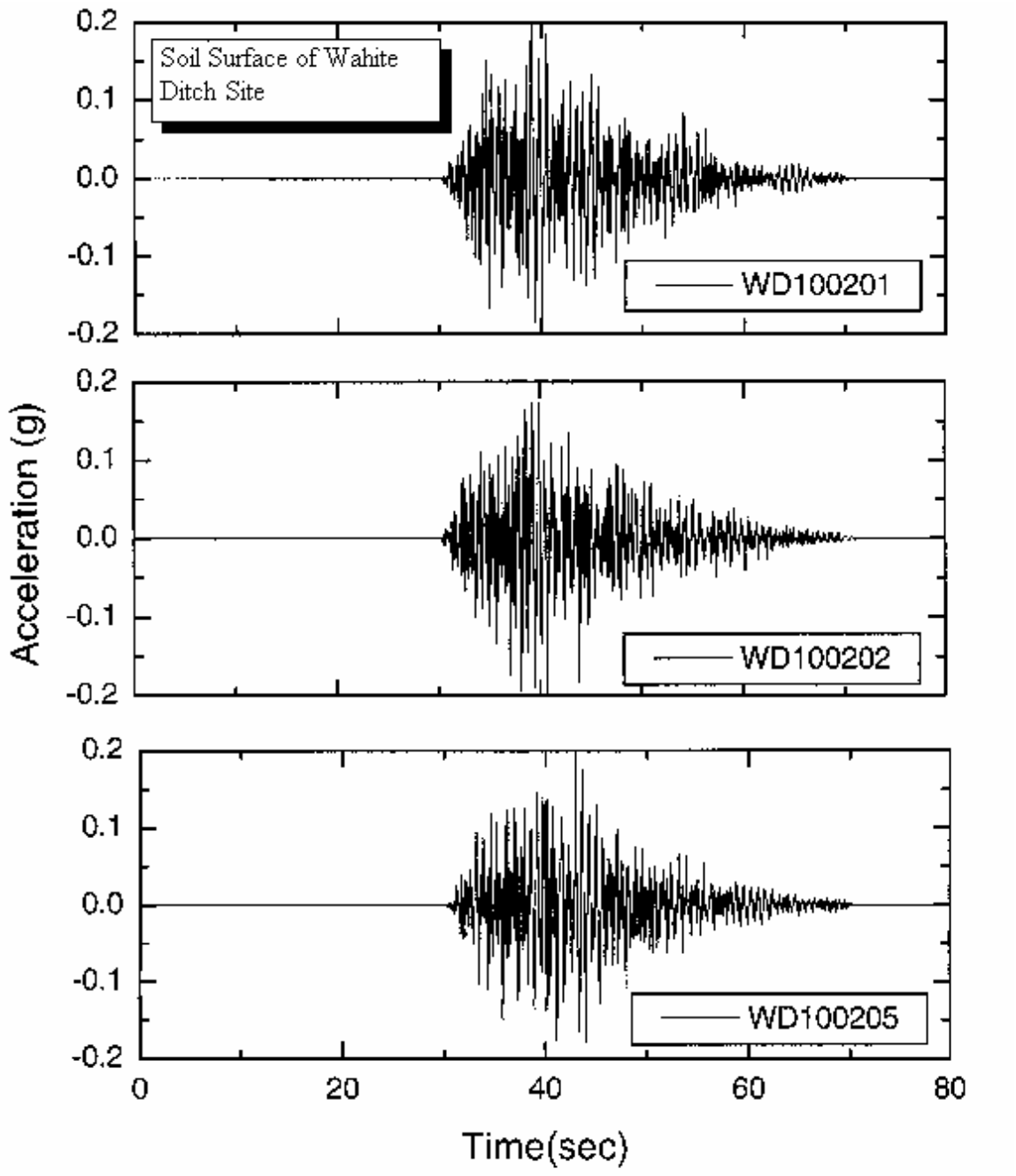

b. PE 10 % in 50 years, Magnitude = 7.0

Figure 8.44b Ground Acceleration at the surface of the Wahite Ditch Site, PE 10% in 50 years, Magnitude = 7.0

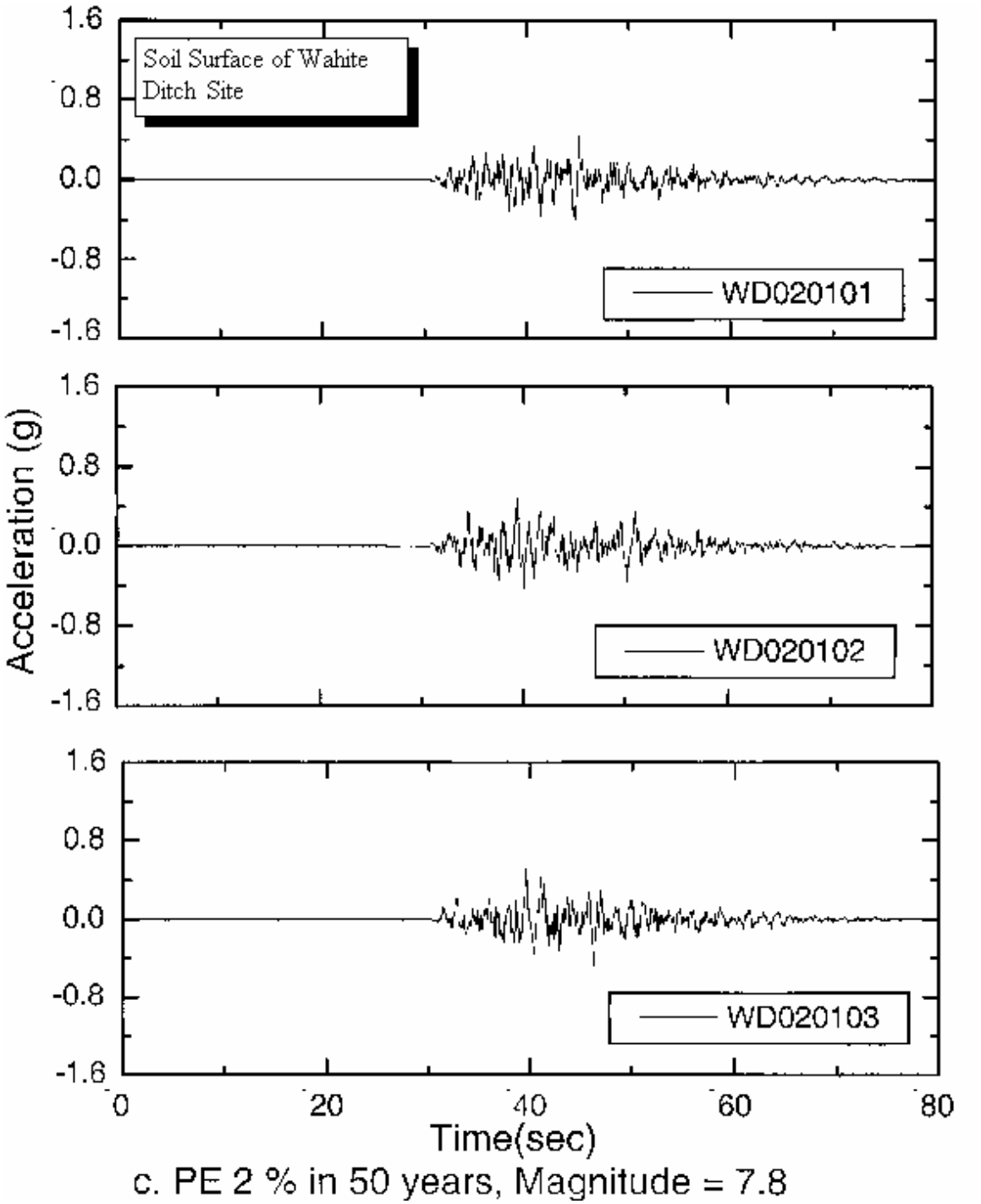

c. PE 2 % in 50 years, Magnitude = 7.8

Figure 8.44c Ground Acceleration at the surface of the Wahite Ditch Site, PE 2% in 50 years, Magnitude = 7.8

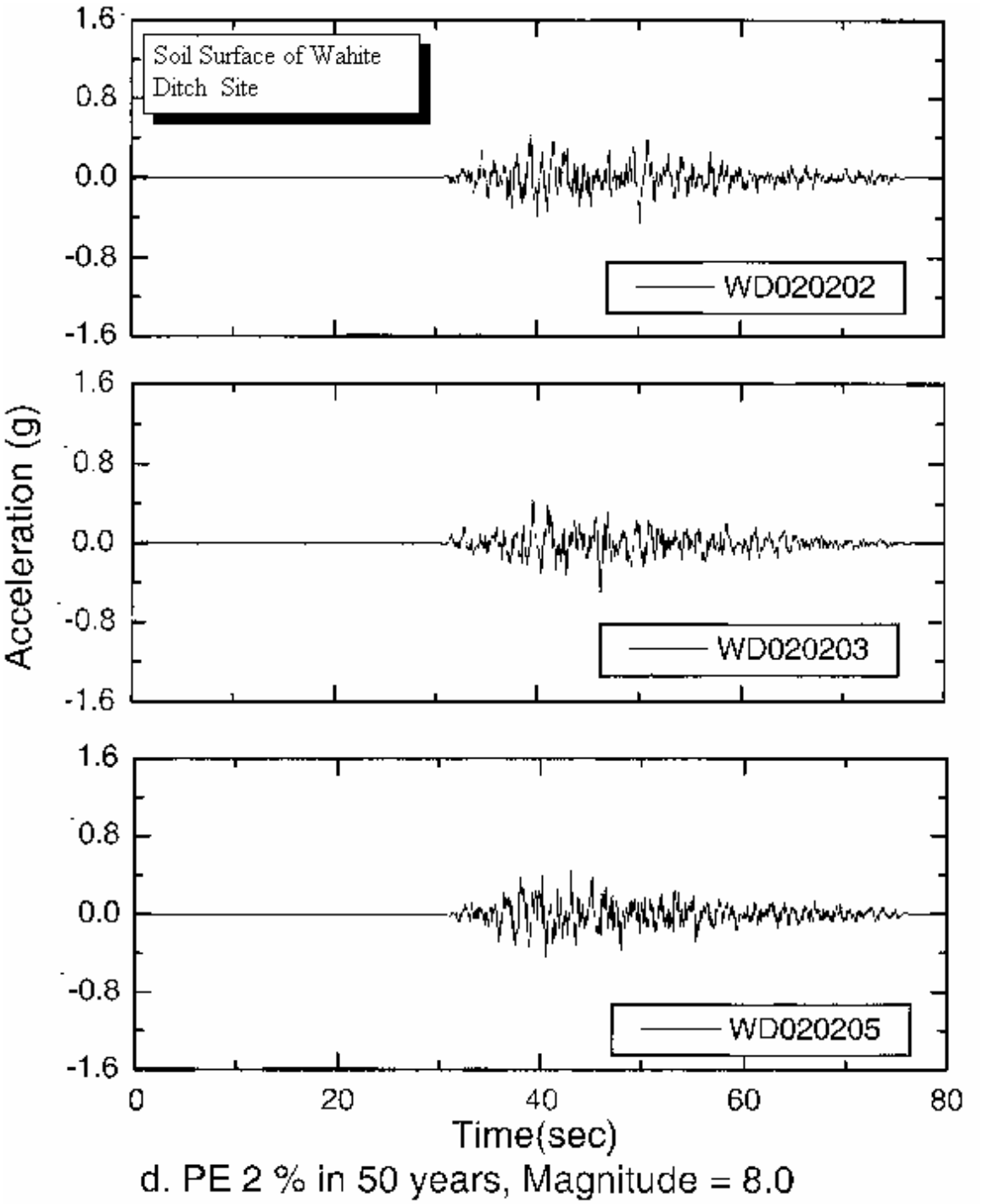

Figure 8.44d Ground Acceleration at the surface of the Wahite Ditch Site, PE 2% in 50 years, Magnitude = 8.0

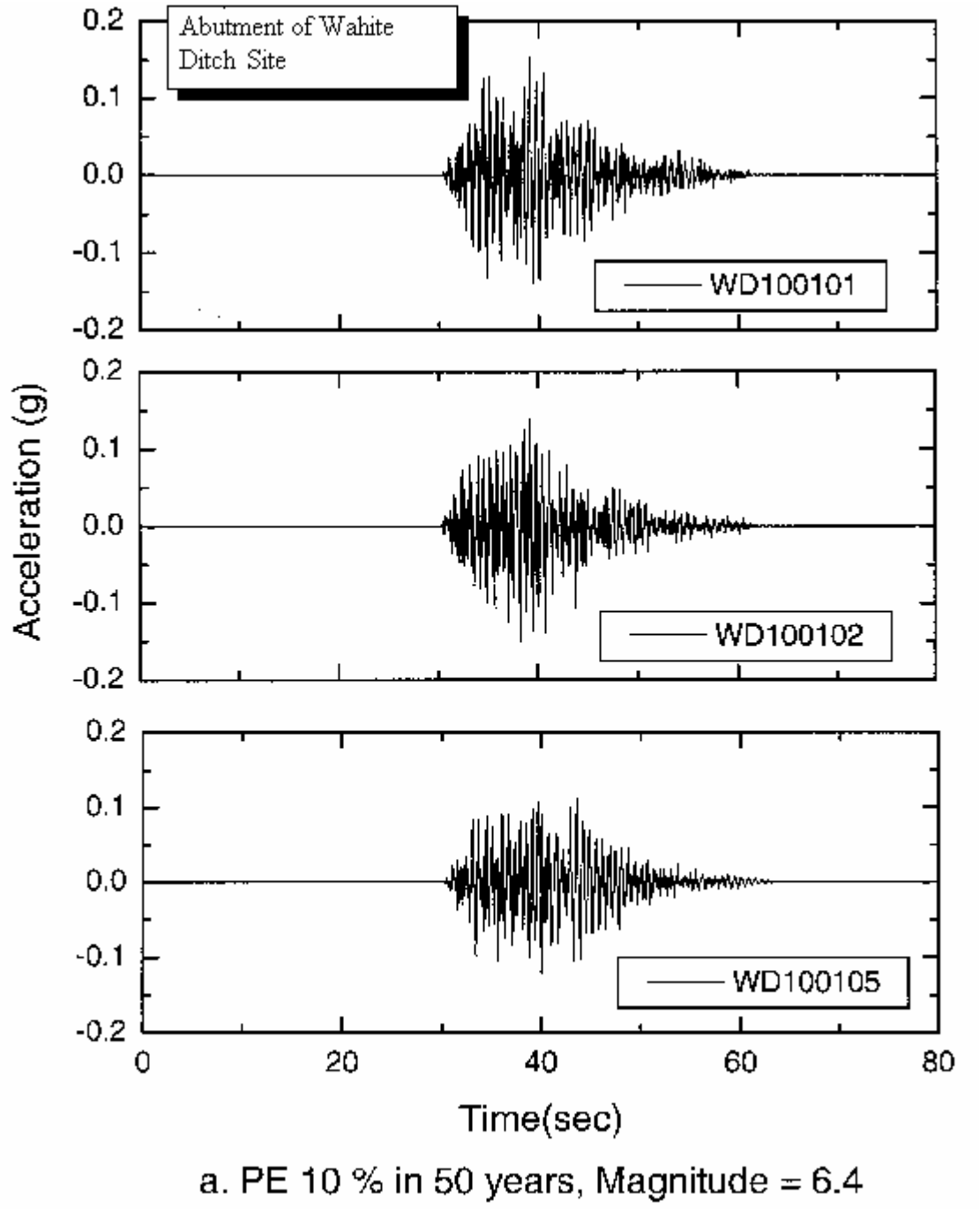

Figure 8.45a Ground Acceleration at the Abutment of the Wahite Ditch Site, PE 10% in 50 years, Magnitude = 6.4

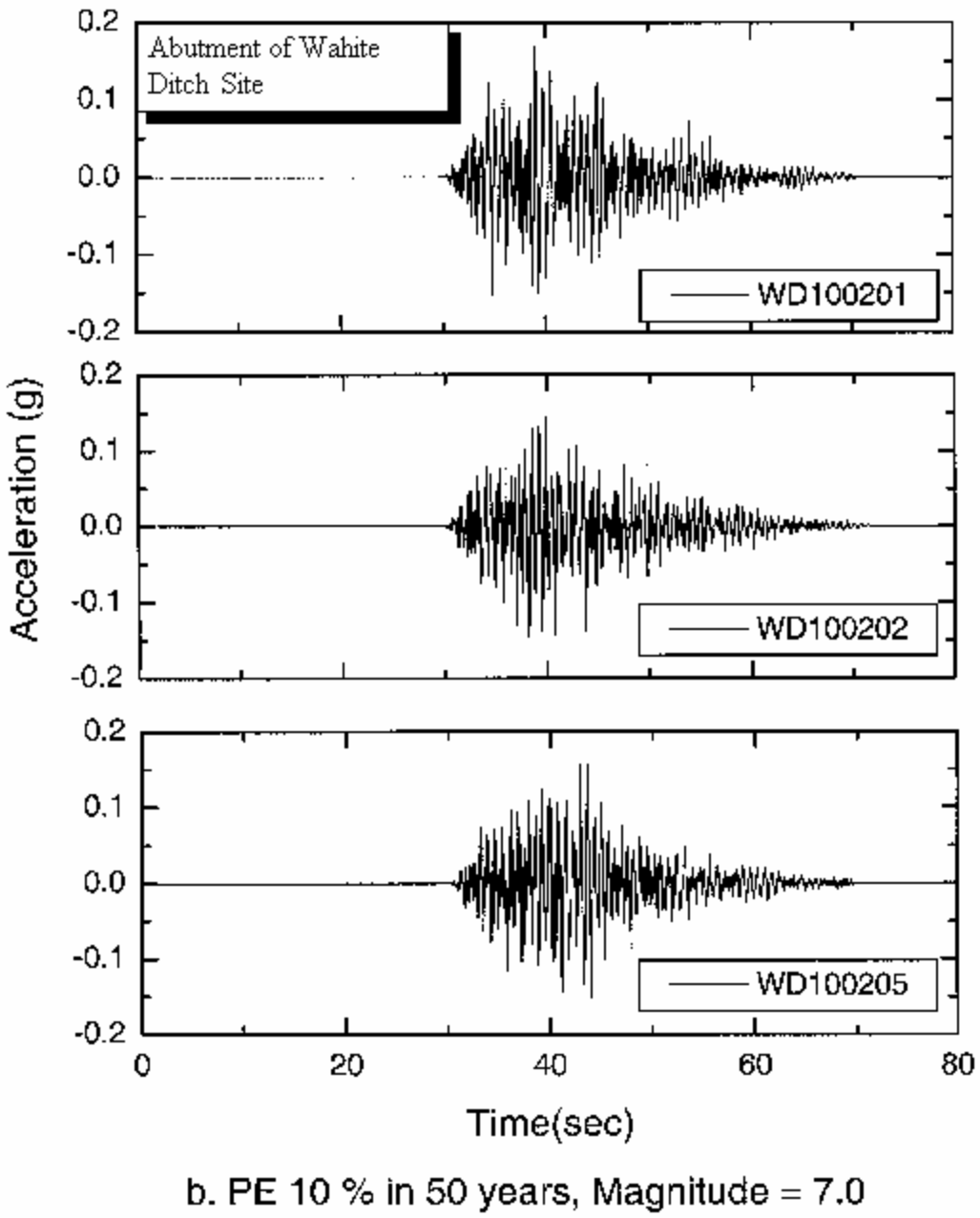

Figure 8.45b Ground Acceleration at the Abutment of the Wahite Ditch Site, PE 10% in 50 years, Magnitude = 7.0

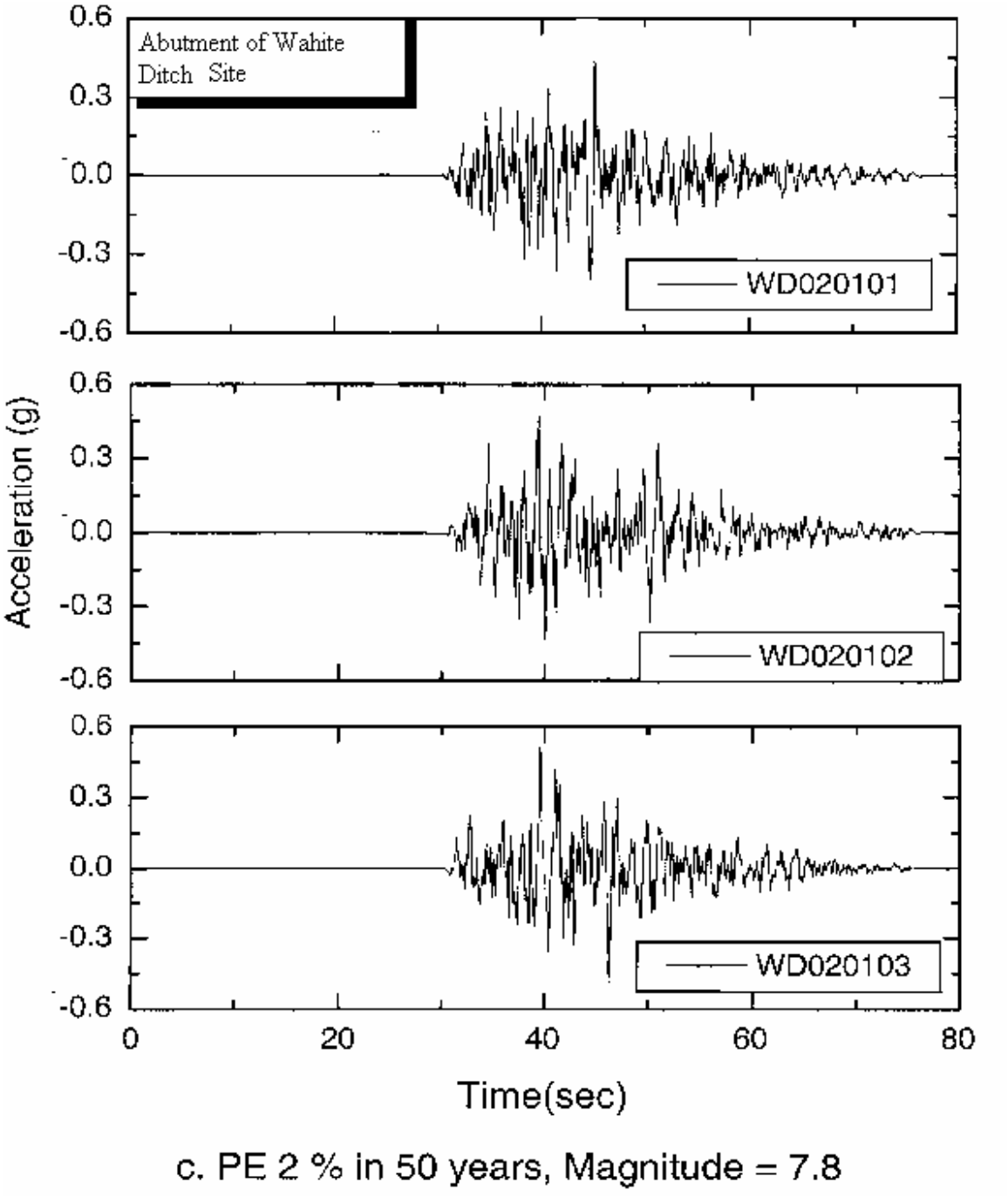

Figure 8.45c Ground Acceleration at the Abutment of the Wahite Ditch Site, PE 2% in 50 years, Magnitude = 7.8

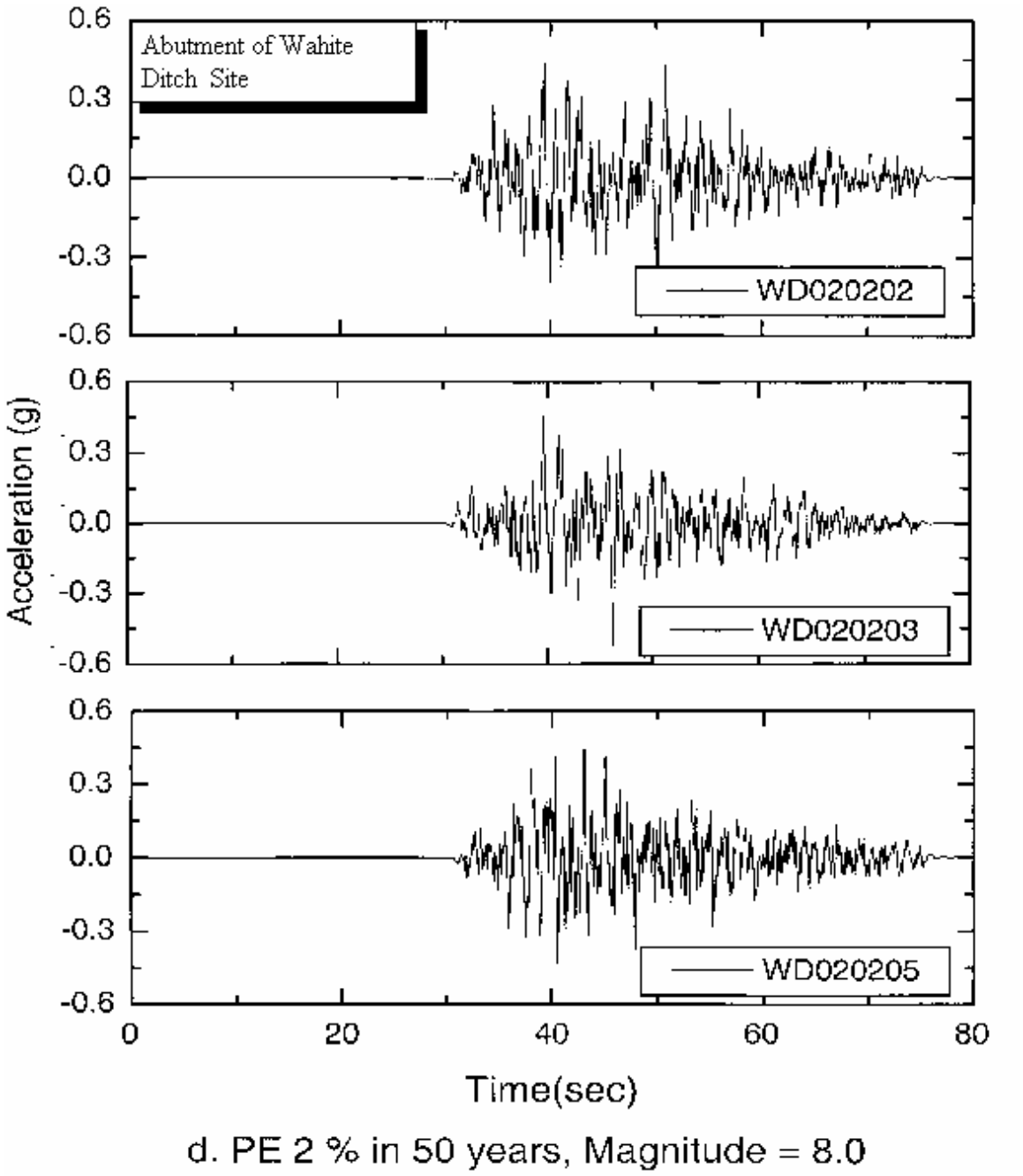

Figure 8.45d Ground Acceleration at the Abutment of the Wahite Ditch Site, PE 2% in 50 years, Magnitude = 8.0

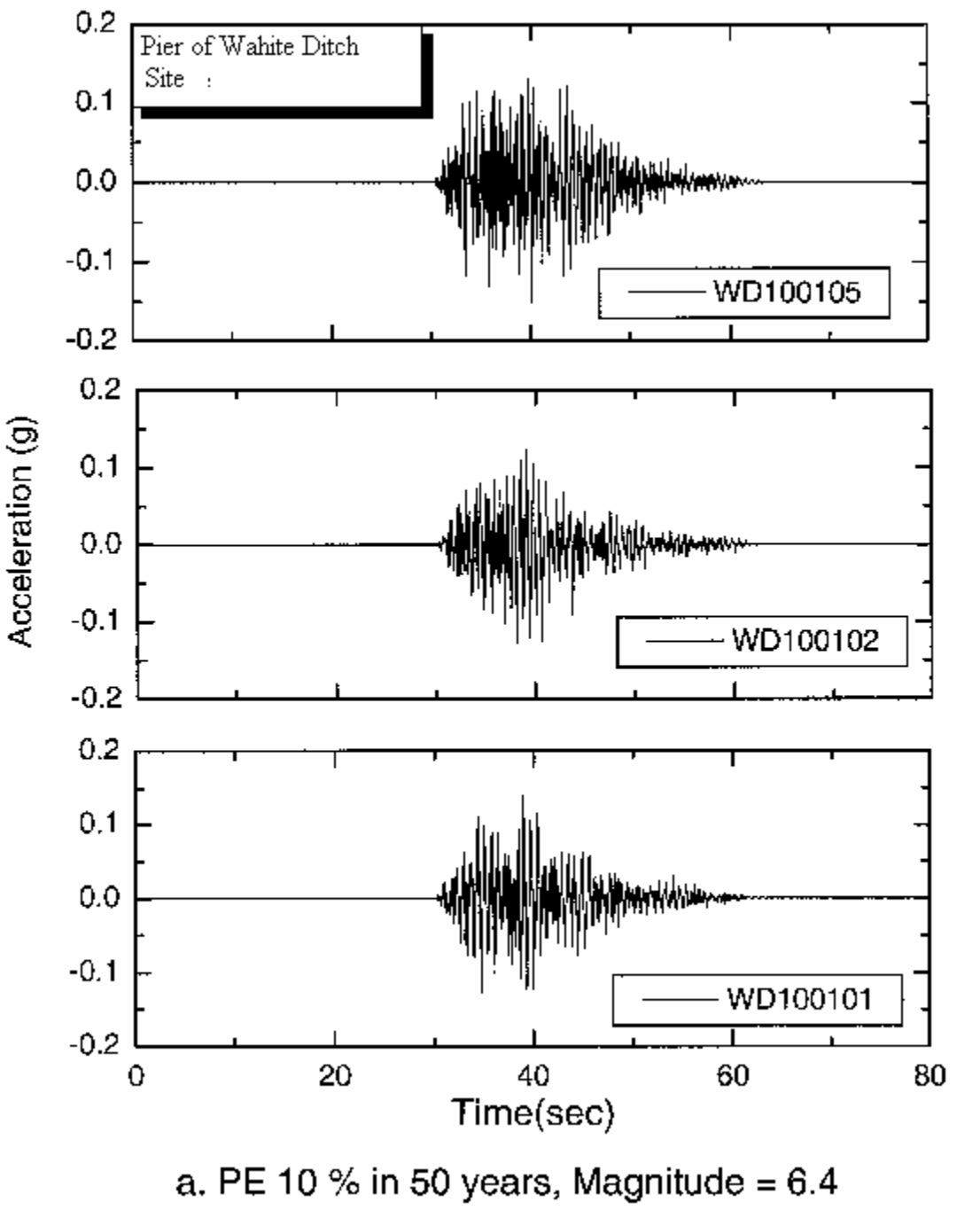

Figure 8.46a Ground Acceleration at the Pier of the Wahite Ditch Site, PE 10% in 50 years, Magnitude = 6.4

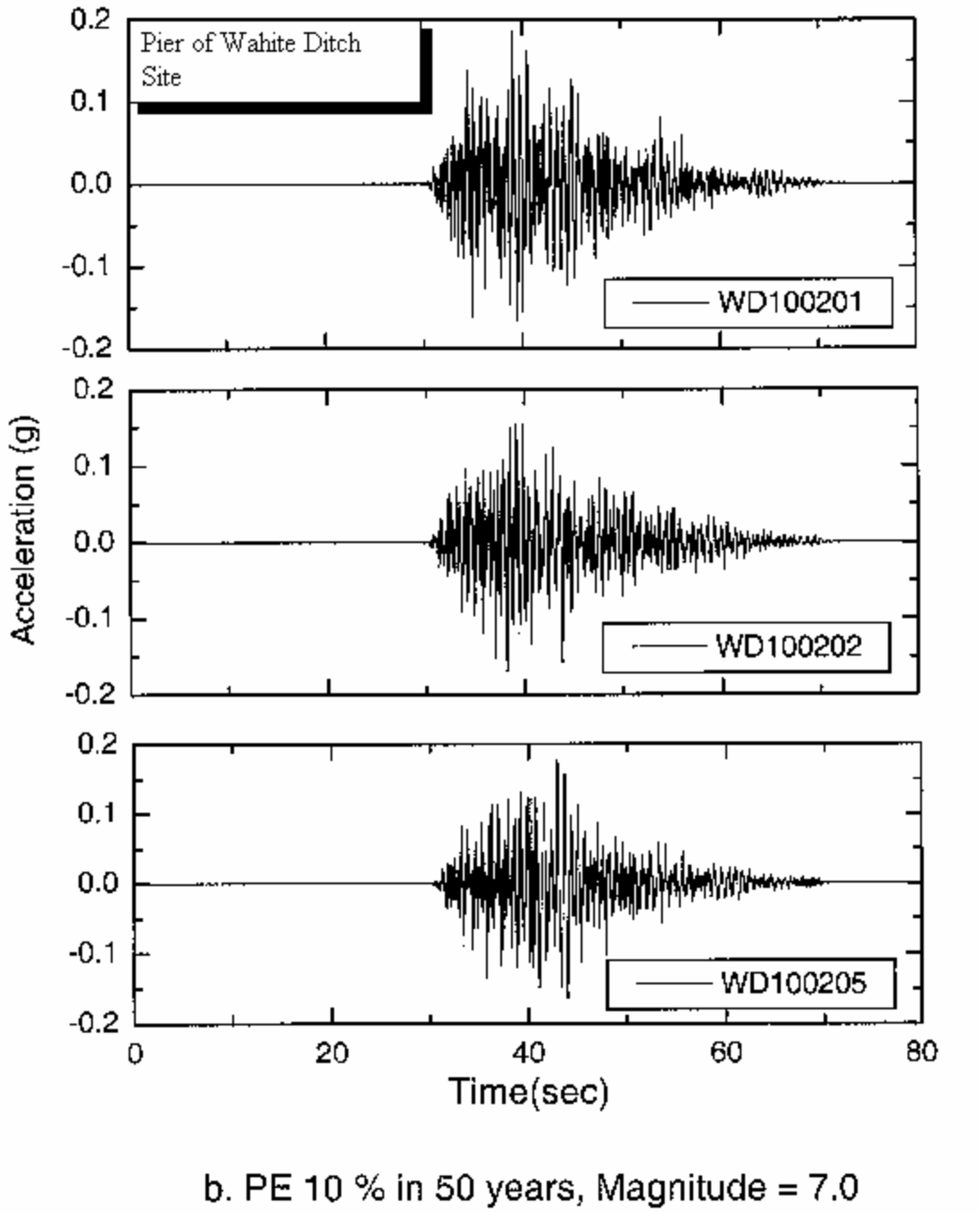

Figure 8.46b Ground Acceleration at the Pier of the Wahite Ditch Site, PE 10% in 50 years, Magnitude = 7.0

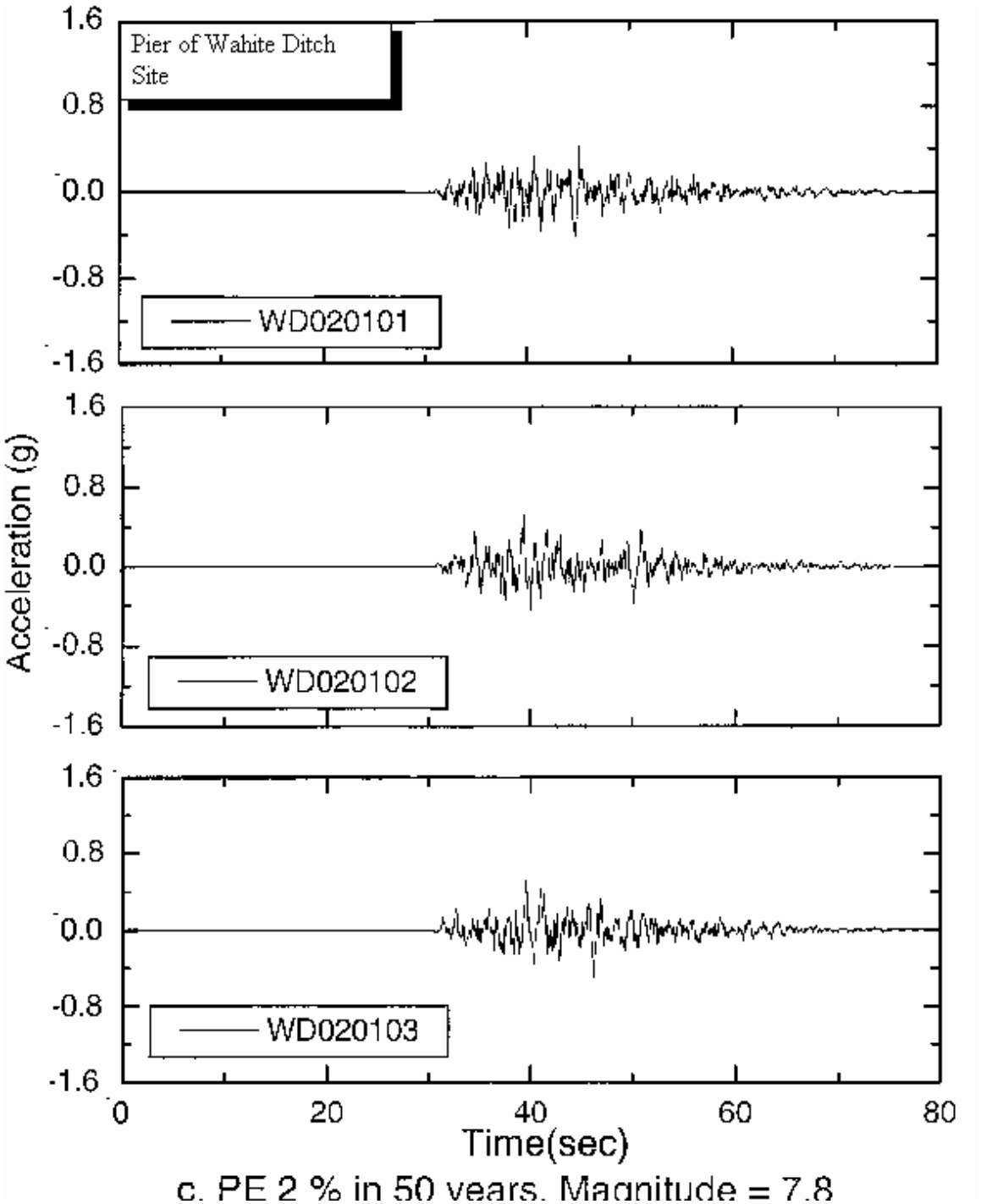

c. PE 2 % in 50 years, Magnitude = 7.8

Figure 8.46c Ground Acceleration at the Pier of the Wahite Ditch Site, PE 2% in 50 years, Magnitude = 7.8

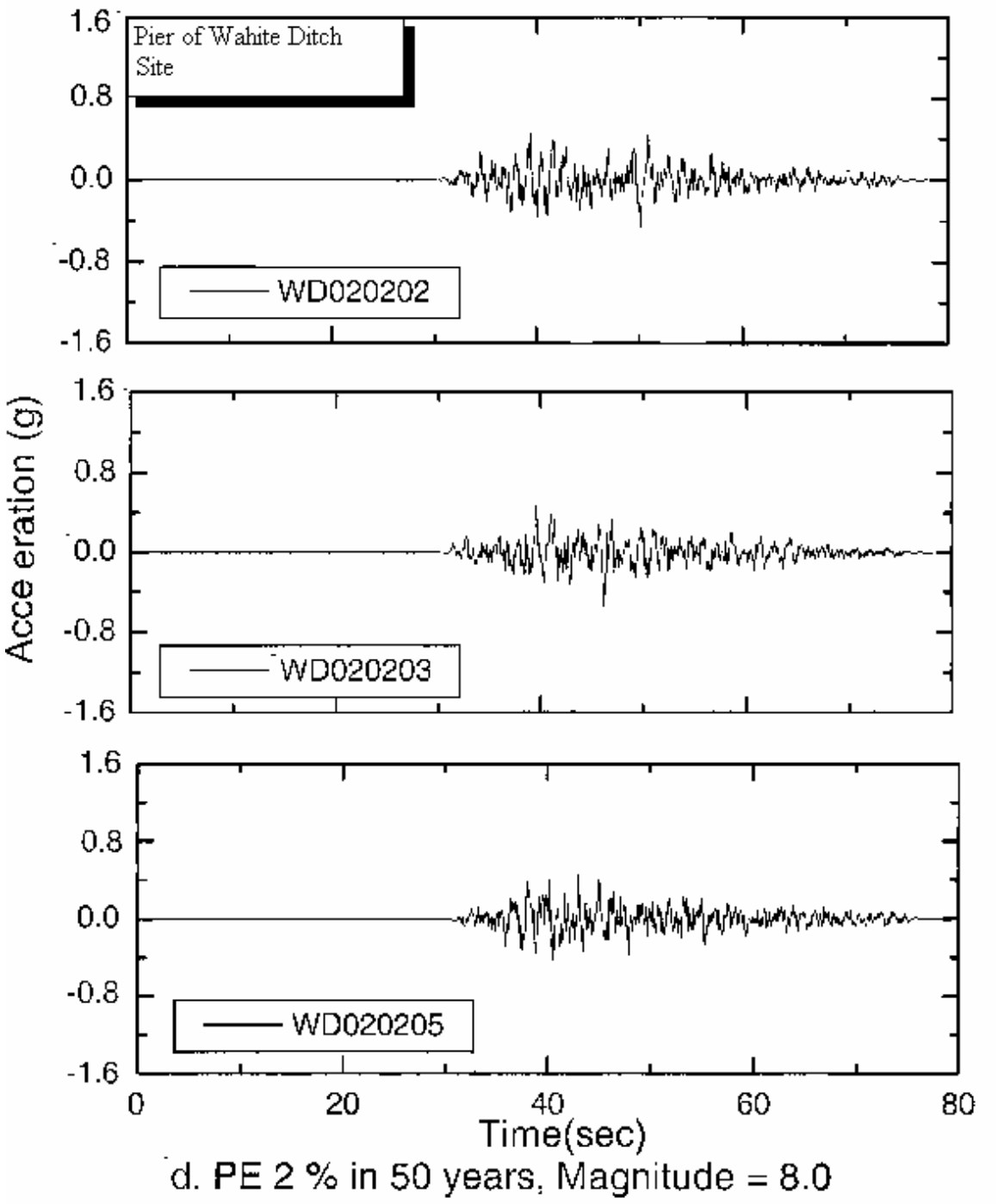

Figure 8.46d Ground Acceleration at the Pier of the Wahite Ditch Site, PE 2% in 50 years, Magnitude = 8.0

The time histories of the modified vertical acceleration at soil surface, base of bridge abutment and pier of each site are presented in Appendix F. It appears by examination of the horizontal and vertical time histories of any one event that:

- (k_h)max and (k_v)max do not occur at the same instant of time.
- The frequency content of these two ground motions are quite different.

8.2.4 Liquefaction Potential Analysis

The liquefaction potential of Wahite Ditch site is evaluated by the Seed and Idriss (1971) simplified method as modified by Youd and Idriss (1997). The procedure to obtain liquefaction potential is explained in Section 5.

8.2.4.1 Cyclic Stress Ratio (CSR) and Cyclic Resistant Ratio (CRR) and Factor of Safety (FOS)

Figure 8.47 shows soil profile and N-values with depth, which have been used for liquefaction analysis. A plot of CSR, CRR and factor of safety FOS, CRR/CSR with depth for PE 10% in 50 years and Magnitude 6.4 is plotted. For details see Appendix G.

It appears that the soil does not liquefy for an earthquake with a M6.4 PE 10% in 50 years. However, for a PE 10 % in 50 years and M7.0, the soil liquefies between depths of 120 to 130 ft.

In this manner, the soil profile was analyzed for 4-ground motion for each magnitude that gives the greatest depths of liquefaction. A listing of FOS and the depth at which soil liquefy is given in Table 8.26.

8.2.5 Slope Stability of Abutment Fills

Slope stability analyses were performed for the Wahite Ditch site. Cross-section locations are shown on Figure 8.40. Soil properties used for the analysis are given in Table 8.27. An example analysis output for Cross-Section C-C' is shown on Figure 8.48. A summary of all analyses is included in Table 8.28.

The anticipated behavior is similar to that described for the St. Francis River Site. The site slopes are expected to be stable under static conditions (F.S. range from 3.48 to 7.76) and 10% PE loads (F.S. range from 2.05 to 7.40) for both low and high ground-water conditions. Under 2% PE loads, factors of safety are greater than one for all analyzed sections for low ground-water conditions. Under high water conditions factors of safety are greater than one but less than 1.10 for sections A-A', C-C', E-E', and F-F', indicating marginal stability.

This site is expected to be stable under small earthquake conditions. The site is less sensitive to ambient ground-water levels (which are affected by water levels in the river) than at the St. Francis River Site. Stability analysis under large earthquake conditions indicates marginal stability at the Wahite Ditch Site when ground-water levels are high.

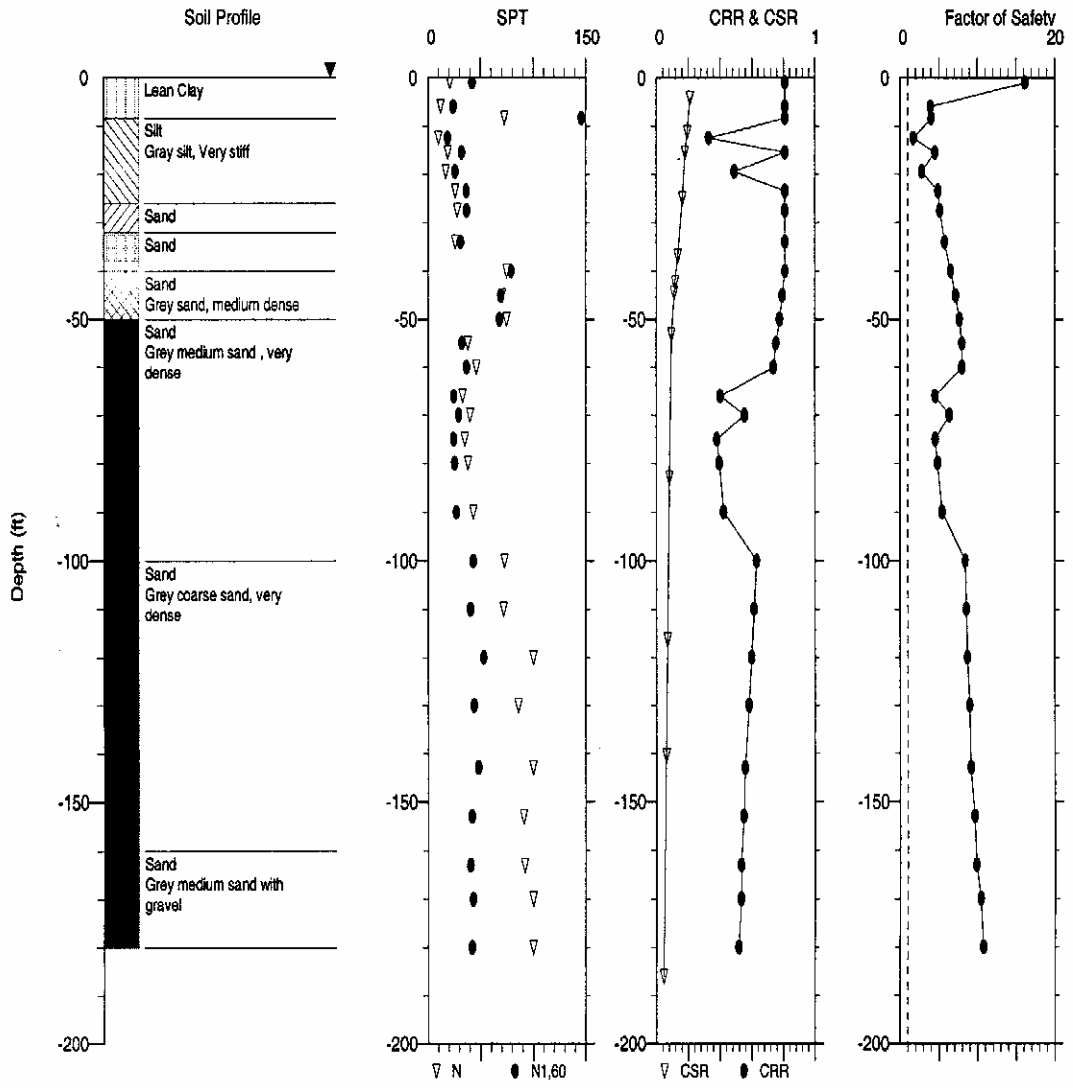

Notes:
CSR analysis using SHAKE results.
CSR File: D:\I-O SF Pe10%\SF100103\Sf100103.grf
CRR using SPT Data and Seed et. al. Method in 1997 NCEER Workshop.
Earthquake File for SHAKE Analysis: D:\SF\SF100103.ACC
Earthquake Magnitude for CRR Analysis: 6.2
Magnitude Scaling Factor (MSF): 1.62
Depth to Water Table for CRR Analysis (ft): 0
Depth to Water Table for Cn Calculation (ft): 0
Depth to Base Layer for CSR Analysis (ft): 219.6
MSF Option: I.M. Idriss (1997)
Cn Option: Liao & Whitman (1986)
Ksigma Option: L.F. Harder & R. Boulanger (1997)
SPT Energy Ratio: USA/Safety/Rope: 0

Figure 8.47 Soil Profile, CSR, CRR and Factor of Safety Against Liquefaction at the White Ditch Bridge Site for PE 10% in 50 Years and Magnitude = 6.4

Table 8.26 The Different Zones of Soil Liquefaction for Different Factors of Safety, Wahite Ditch Site

Factor of Safety	Depth of soil Liquefy(ft)			
	PE10% in 50 years		PE 2% in 50 years	
	M6.4	M7.0	M7.8	M8.0
1.0	No	120 to 130	20 to 201	20 to 201
1.1	No	120 to 130	20 to 201	20 to 201
1.2	No	120 to 130	20 to 201	20 to 201
1.3	No	120 to 130	20 to 201	20 to 201
1.4	No	120 to 130	20 to 201	20 to 201

Table 8.27 Soil Properties Used For Slope Stability Analysis, Wahite Ditch Site

Soil Characteristics*				
	γ_{moist} (pcf)	$\gamma_{saturated}$ (pcf)	c (psf)	ϕ (deg.)
Levee Fill	121.3	133.5	858	30
SP	134.9	141.9	0.0	40
Sand Lens	134.9	141.9	0.0	40
Gravel Lens	140.0	145.0	0.0	45

* Soil characteristics obtained from slope stability procedures, Section (5.5.1)

8.2.6 Flood Hazard Analysis Results

Water levels appear to be too low during normal conditions to pose a significant risk of exiting the channel, even in the event of levee failure. Furthermore, the roadway is elevated above the surrounding land. One section of roadway located 0.1 to 0.5 miles west of the ditch is at low elevation and could potentially flood.

The remaining section of the roadway east of the Wahite Ditch appears to be elevated and is not anticipated to experience flooding due to levee failure**.**

8.2.7. Structure Response of Wahite Ditch Bridges and Abutments

8.2.7.1 New Wahite Ditch Bridge

8.2.7.1.1 Bridge Description

The bridge under consideration in this section is denoted as Bridge A-5648, located in Stoddard County on US 60 where it crosses the Wahite drainage ditch. The bridge was designed in 1992 with seismic considerations. This 279 foot 9 inch bridge consists of three spans of prestressed concrete girders. The interior diaphragms each consist of a horizontally placed C15x33.9 channel section. The general elevation of the bridge is shown in Figure 8.49.

Table 8.28 Slope Stability Results, Wahite Ditch Site

Factor of Safety for Most Sensitive Potential Failure Plane							
Cross-Section	A - A'	**B - B'**	**C – C'**	**D - D'**	**E – E'**	**F – F'**	**G – G'**
Static							
Low GW	3.97	4.11	3.85	4.05	3.92	3.94	7.76
High GW	3.83	4.02	3.74	3.98	3.51	3.48	5.30
Pseudo-Static Set 1* 10% PE in 50 years							
Low GW (0.123)	2.41	2.53	2.32	2.40	2.40	2.41	4.23
High GW (0.123)	2.14	2.39	2.06	2.20	2.07	2.10	2.79
2% PE in 50 years							
Low GW (0.350)	1.32	1.38	1.27	1.29	1.29	1.28	2.14
High GW (0.350)	1.10	1.25	1.06	1.11	1.10	1.10	1.39
Pseudo-Static Set 2 10% PE (HGA, VGA)							
Low GW (0.123,+0.006)	2.40	2.52	2.31	2.38	2.38	2.39	4.22
Low GW (0.123,-0.006)	2.43	2.54	2.34	2.41	2.41	2.42	4.25
High GW (0.123,+0.006)	2.12	2.38	2.05	2.18	2.06	2.08	2.77
High GW (0.123,-0.006)	2.15	2.40	2.08	2.21	2.09	2.12	2.80
2% PE (HGA, VGA)							
Low GW (0.350,+0.007)	1.30	1.37	1.25	1.28	1.27	1.27	2.12
Low GW (0.350,-0.007)	1.33	1.39	1.28	1.30	1.30	1.30	2.15
High GW (0.350,+0.007)	1.09	1.24	1.05	1.10	1.09	1.09	1.38
High GW (0.350,-0.007)	1.12	1.26	1.07	1.12	1.11	1.11	1.41
Pseudo-Static Set 3 10% PE (HGA, VGA)							
Low GW (0.008,+0.082)	3.69	3.90	3.57	3.74	3.70	3.68	7.40
Low GW (0.008,-0.082)	3.83	3.91	3.71	3.91	3.86	3.80	7.15
High GW (0.008,+0.082)	3.51	3.94	3.43	3.66	3.25	3.25	4.82
High GW (0.008,-0.082)	3.66	3.78	3.57	3.81	3.39	3.37	5.06
2% PE (HGA, VGA)							
Low GW (0.060,+0.233)	2.58	2.80	2.49	2.57	2.56	2.57	5.22
Low GW (0.060,-0.233)	3.26	3.27	3.15	3.30	3.26	3.24	5.54
High GW (0.060,+0.233)	2.27	2.86	2.20	2.35	2.18	2.22	3.00
High GW (0.060,-0.233)	3.03	3.13	2.94	3.13	2.88	2.91	4.10

* Peak ground acceleration values calculated with the computer program *SHAKE*, Section 5.4
HGA – Horizontal Ground Acceleration
VGA – Vertical Ground Acceleration
PE – Probability of Exceedance in 50 years

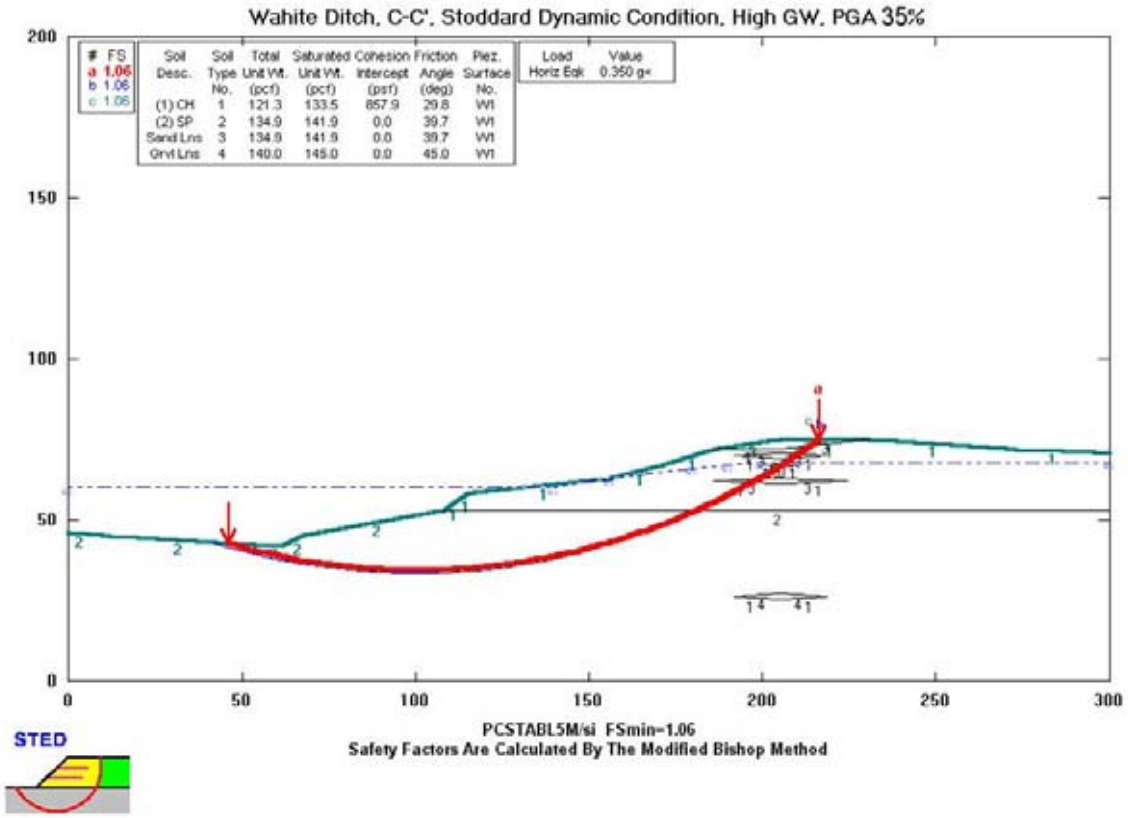

Figure 8.48 Example Slope Stability Results for the Wahite Ditch Site

.

The bridge superstructure is supported by two intermediate bents through fixed bearings and two integral abutments at its ends. Each bent consists of a reinforced concrete cap beam and two reinforced concrete columns. Deep pile foundations support both bents and abutments. There are 20 piles for each column footing and 14 piles for each abutment footing.

8.2.7.1.2 Bridge Model and Analysis

All of the components of the structure were included in the bridge model. These components include the girders, diaphragms, cross-frames, interior bents and columns, and the bridge deck. The deck was represented by 24 shell elements with a thickness of 8.5 inches. All girders, cross-frames, and diaphragms were modeled as 167 frame members. Each frame section was then assigned member properties, such as material type and cross-section dimensions. The model also included 120 nodes.

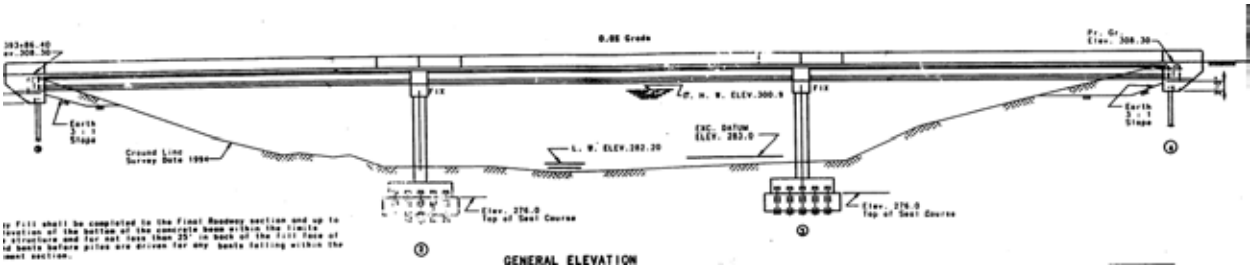

Figure 8.49 Bridge General Elevation (New Wahite Ditch Bridge)

To further assist in modeling ground soil conditions in *SAP2000*, springs were used at the base of each column (six columns total, three on each interior bent). Springs were also placed at the ends of the bridge on each abutment footing. The stiffness constants of the springs were taken from Appendix F.

Rigid elements were used to model the integral abutments in *SAP2000*. Because of their presence, the bridge is relatively stiff and is expected to experience small displacements during earthquakes. Therefore, a response spectrum analysis was used for the bridge model. For each analysis with one directional earthquake excitation, 30 Ritz-vectors were considered associated with the earthquake direction. In Table 8.29, a sampling of five of the significant vibration modes are listed with its period in seconds and a brief description of the motion represented within the given mode. Their corresponding mode shapes are illustrated in Figures 8.50-8.54.

The bridge was analyzed under a total of twelve response spectra described in Section 8.1.3. Six of the spectra correspond to a 10% PE level while the others to a 2% PE level. At each PE level of earthquakes, three were considered as near-field and the other three as far-field. The internal loads such as shear and moments and the abutment displacements were obtained at various critical locations.

Table 8.29 Natural Periods and their Corresponding Vibration Modes (New Wahite Ditch Bridge)

Mode Number	Period (seconds)	Motion Description
1	0.2686	Vertical
2	0.2558	Transverse twisting
3	0.0915	Longitudinal
4	0.0854	Vertical with twisting
5	0.0729	Transverse

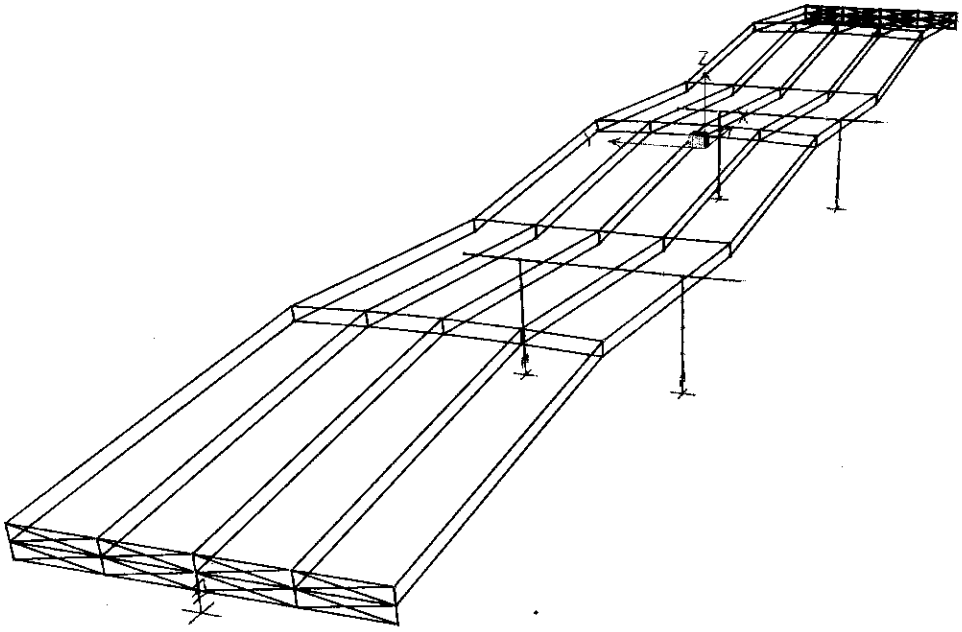

Figure 8.50 Mode 1, Period 0.2686 Seconds (New Wahite Ditch Bridge)

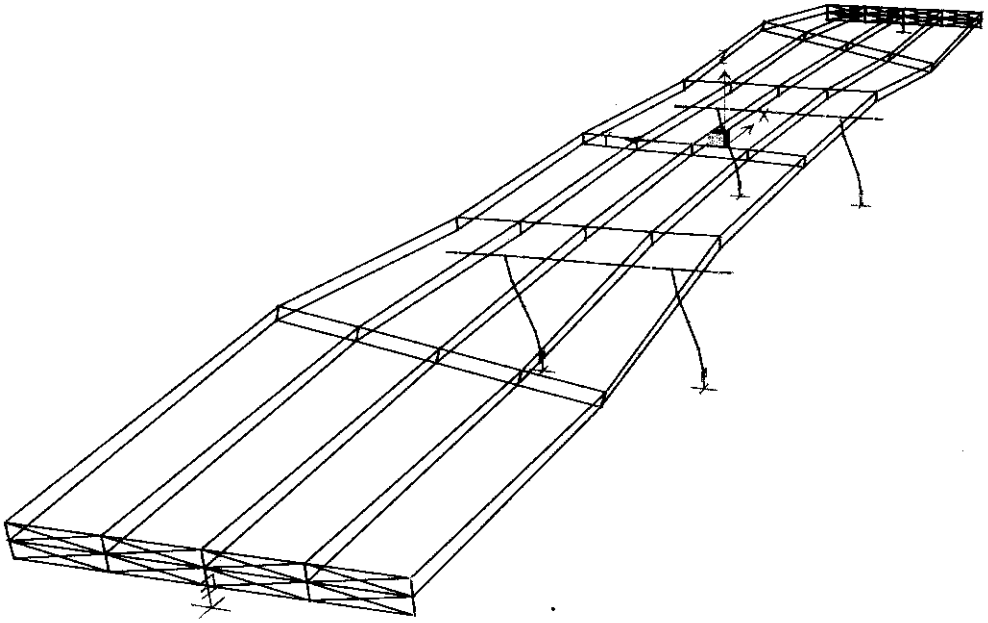

Figure 8.51 Mode 2, Period 0.2558 Seconds (New Wahite Ditch Bridge)

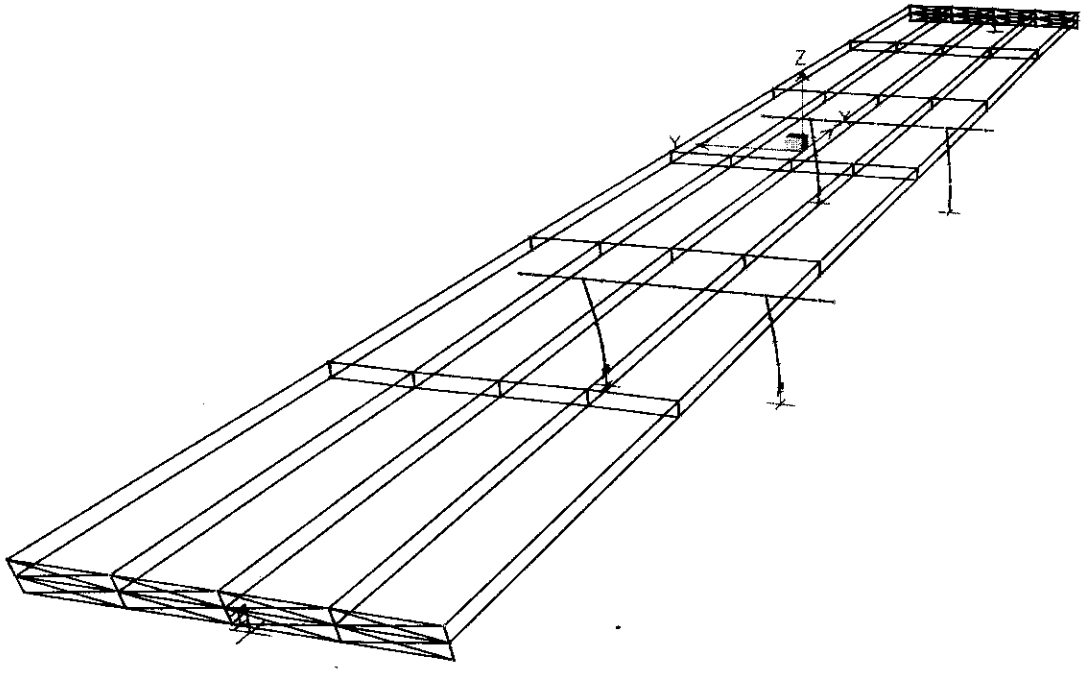

Figure 8.52 Mode 3, Period 0.0915 Seconds (New Wahite Ditch Bridge)

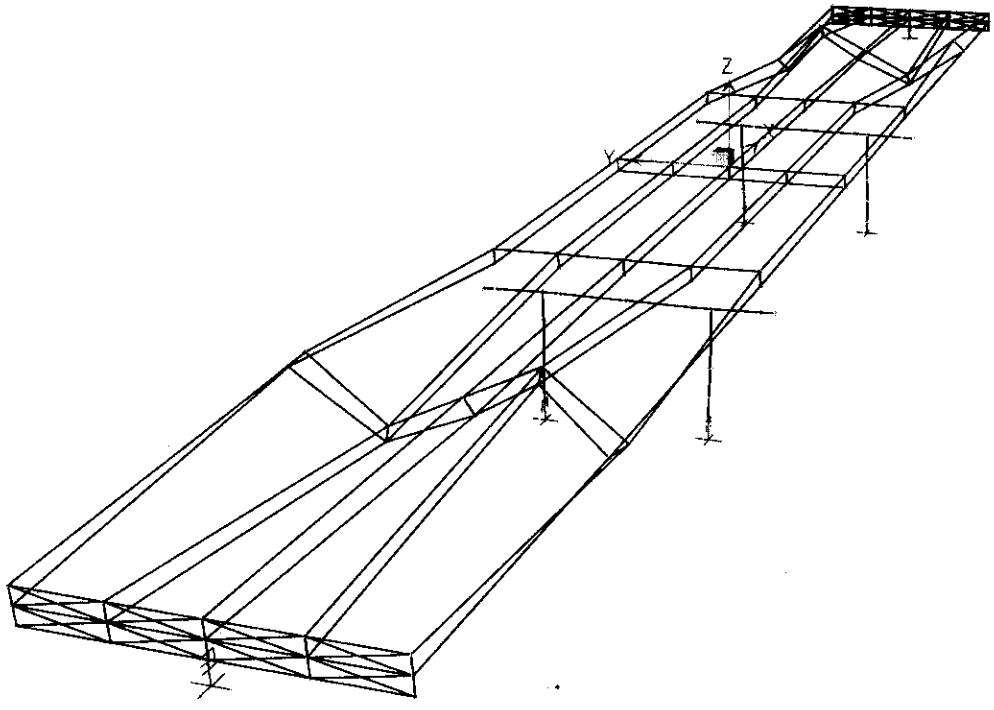

Figure 8.53 Mode 4, Period 0.0854 Seconds (New Wahite Ditch Bridge)

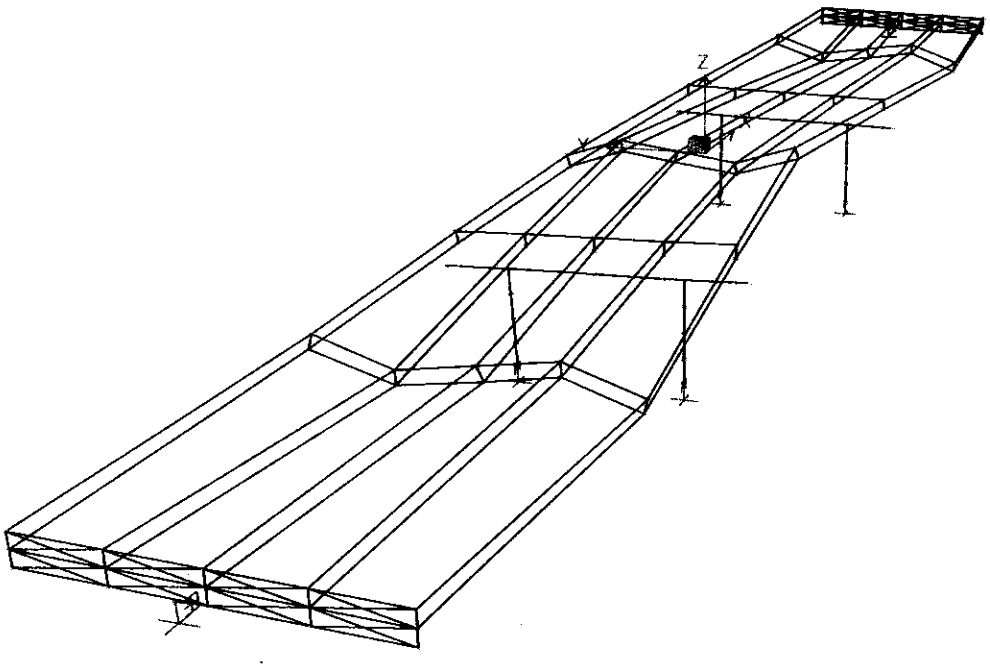

Figure 8.54 Mode 5, Period 0.0729 Seconds (New Wahite Ditch Bridge)

8.2.7.1.3 Description of Bridge Evaluation

The evaluation procedure is the same as used for the bridges at the St. Francis River Site. Whether or not the C/D ratios were greater than one indicated if their associated components would experience problems in an earthquake.

8.2.7.1.3.1 Load Combination Rule

The same load combination rule was used for the evaluations at the Wahite Ditch Bridge site as at the St. Francis River Site. This rule was used throughout these calculations for various types of demands on the structure (shear, moment, and axial forces, as well as transverse and longitudinal displacements).

8.2.7.1.3.2 Minimum Support Length and C/D Ratio for Bearing

This bridge has integral abutments without expansion joints. It is not susceptible to the dropping of exterior spans during earthquake excitations.

8.2.7.1.3.3 C/D Ratios for Shear Force at Bearings

The first C/D ratios calculated in this section define the behavior of the shear keys located at the bearing pads on the cap beams at the interior bents. There are four shear keys on each of the two interior bents, with 10 reinforcing bars in each key. From the bridge analysis the shear demand at each of these points was determined and the maximum demand among these points was used

to compute the C/D ratio for the "worst case". Before these shear values were used in determining the C/D ratios, the values were compared to 20% of the axial dead load at that location (FHWA, 1995). The greater of these two values were used in the subsequent calculations.

In all cases except for two of the 2% earthquakes, the shear capacities of the keys were adequate. For these two earthquakes, the capacity was only approximately 85% of the demand. However, in several other cases, the C/D ratio for the shear was very close to one, indicating that the capacity just barely exceeds the demand. In these cases, it is advisable to pay careful attention to the shear keys, as they could pose problems under the stronger earthquakes.

8.2.7.1.3.4 C/D Ratios for Columns/Piers

In this section, the C/D ratios were calculated for all columns on the interior bents. The elastic moment demands for the top and bottom of each column in the transverse and longitudinal directions due to transverse, longitudinal, and vertical earthquake motions were determined from the response spectrum analysis.

The maximum demand from the possible combinations was then used in conjunction with the determined capacity for the column to determine a C/D ratio for the columns. In most cases, the initial C/D ratios were below one, indicating insufficient column strength for elastic seismic demand. However, when the columns experience inelastic deformation, the seismic demand reduces due to energy dissipation. To account for the above effect, the ductility indicator was used with these ratios. Since the two interior bents each had multiple columns, a multiplier of 5 was applied to each ratio (AASHTO, 1996). In all cases, this multiplier increased the ratios to values above one.

As for the bridges at the St. Francis River Site, the footings of these columns were determined to have moment capacity considerably higher than the capacities of the columns even when the axial force is zero. Therefore, the footings are expected to perform satisfactorily. The plot for the moment versus rotation is presented in Appendix H for the case of axial load equal to zero.

8.2.7.1.3.5 C/D Ratios for Reinforcement Anchorage in Columns

For both the top and bottom of the columns, the adequacy of the anchorage of longitudinal reinforcement must be checked. The tops of the columns used straight anchorage, whereas the bottoms of the columns had hooked anchorage. Because in both cases (top and bottom) the capacity was greater than the demand, the C/D ratio was one for both cases, indicating that the anchorage should be adequate. As explained in Section 8.1.7.1.3.5, the values of the C/D ratios here are not actual ratios of the capacity length and the demand length. Rather, they are values dictated by the FHWA Manual based on the location of the anchorage and the relationship of the capacity length and the demand length.

8.2.7.1.3.6 C/D Ratios for Splices in Longitudinal Reinforcement

This section is not applicable to this structure, as the columns have no splices.

8.2.7.1.3.7 C/D Ratio for Transverse Confinement

The C/D ratios for all cases were above one. This indicates that there should be minimal problems with the transverse confinement on the columns of this bridge.

8.2.7.1.3.8 C/D Ratio for Column Shear

In all cases of 2% motions and for four of the 10% motions, "Case B" was chosen, based on definitions from the FHWA Manual (1995). This case was needed because at least one of the moment C/D ratios was less than one for each earthquake (before applying the ductility indicator) and $V_i(c) > V_u(d) > V_f(c)$. When "Case B" was used, the relationship for the column shear C/D ratio was the column moment C/D ratio multiplied by an FHWA-defined multiplier. This multiplier was based on column geometry (L_c = length of column and b_c = width of column) as well as the various shear parameters defined in Section 8.1.7.1.3.8.

For the remaining two 10% earthquakes, "Case B" did not apply because the initial C/D ratios for the columns under these earthquakes were above one. Therefore, the C/D ratios for these earthquakes were determined simply as a ratio of the initial capacity of the column to the maximum shear force in the column.

8.2.7.1.3.9 C/D Ratio for Diaphragm Members

The axial capacity of the diaphragm members (C15x33.9) was calculated based on critical buckling stress (Table 3-36 in AISC LRFD, 1998). This table gave values of the stress based on the effective length to radius of gyration ratio (KL/r). In this case, K was taken to be one to simulate a pin-pin connection at the ends of the member.

In all cases, the axial capacity of these members appeared to be sufficient, as all C/D ratios were above one. This indicates that there should be minimal problems with these members.

8.2.7.1.3.10 C/D Ratio for Abutment Displacements

In all cases, the longitudinal and transverse displacements of the abutments under the combined effect of three earthquake effects were found to be less than their respective allowable values specified in the FHWA Manual (1995). This indicates that the abutments should remain damage-free in the event of an earthquake.

8.2.7.1.4 Summary of Problem Areas

A summary of all C/D ratios for all earthquakes for this bridge is shown in Table 8.30. Based on the above study, the bridge generally experienced minor problems.

The only components that warrant attention are the shear keys located on the bent cap beams of the structure. In several cases, the resulting C/D ratio was less than one, indicating the possibility of failure for these shear keys.

8.2.7.1.5 Comparison of AASHTO Response Spectrum vs. Site-Specific Response Spectrum

The same response spectrum shown for the New St. Francis Bridge was used for the New Wahite Bridge as well. The New Wahite Bridge Site is not far from the New St. Francis Bridge Site. Therefore, the maximum ground accelerations for these sites are nearly the same. For this reason, an A value of 0.18 was again used for this response spectrum.

The results from the AASHTO response spectrum analysis were compared to several of the site specific 10% earthquake response spectrum analyses that were run on the New Wahite Bridge. It was expected that these results would be reasonably close to one another. These results are summarized in Table 8.31.

Table 8.30 Summary of all Earthquakes for New Wahite Ditch Bridge

C/D Ratio Name	020101	020102	020103	020202	020203	020205	100101	100102	100105	100201	100202	100205
r_{bd}	---	---	---	---	---	---	---	---	---	---	---	---
$r_{bf\text{-}trans}$	1.23	1.07	**0.83**	1.17	**0.84**	1.00	1.84	2.38	2.51	1.81	1.78	2.00
$r_{bf\text{-}long}$	5.58	5.51	4.28	5.36	4.38	4.90	6.92	7.89	8.13	6.86	6.83	7.33
$r_{ec\text{-}final}$	2.95	2.55	1.95	2.80	1.98	2.40	4.47	5.98	6.39	4.38	4.32	4.91
$r_{ec\text{-}final}$	3.58	3.09	2.37	3.39	2.40	2.91	5.42	7.24	7.75	5.31	5.24	5.94
$r_{ec\text{-}final}$	2.75	2.38	1.83	2.60	1.85	2.24	4.16	5.55	5.93	4.07	4.02	4.56
$r_{ec\text{-}final}$	3.30	2.85	2.19	3.12	2.22	2.69	4.99	6.66	7.12	4.89	4.83	5.48
$r_{ec\text{-}final}$	2.95	2.55	1.95	2.80	1.98	2.40	4.47	5.98	6.39	4.38	4.32	4.91
$r_{ec\text{-}final}$	3.58	3.09	2.37	3.39	2.40	2.91	5.42	7.24	7.75	5.31	5.24	5.94
$r_{ec\text{-}final}$	2.75	2.38	1.83	2.60	1.85	2.24	4.16	5.55	5.93	4.07	4.02	4.56
$r_{ec\text{-}final}$	3.30	2.85	2.19	3.12	2.22	2.69	4.99	6.66	7.12	4.89	4.83	5.48
$r_{ca\text{-}bottom}$	1.00	1.00	1.00	1.00	1.00	1.00	1.00	1.00	1.00	1.00	1.00	1.00
$r_{ca\text{-}top}$	1.00	1.00	1.00	1.00	1.00	1.00	1.00	1.00	1.00	1.00	1.00	1.00
r_{cs}	---	---	---	---	---	---	---	---	---	---	---	---
$r_{cs\text{-}adj}$	---	---	---	---	---	---	---	---	---	---	---	---
r_{cc}	3.30	2.85	2.19	3.12	2.22	2.69	4.99	6.66	7.12	4.89	4.83	5.48
r_{cv}	2.33	2.01	1.54	2.20	1.56	1.89	3.52	6.37	6.80	3.45	3.40	3.86
r_{dpgm}	5.92	5.13	3.79	5.87	3.97	5.08	11.10	12.49	12.72	10.31	10.77	10.76
$r_{ad\text{-}trans}$	127.64	111.51	94.63	122.43	94.03	108.29	202.68	218.95	215.80	199.98	181.80	211.24
$r_{ad\text{-}long}$	89.52	77.69	61.50	84.98	62.07	74.38	136.34	174.20	180.07	133.18	131.17	142.25

Table 8.31: Comparison of AASHTO Response Spectrum vs. Site Specific Response Spectrum (New Wahite)

Due to Transverse EQ	transverse		longitudinal	
	response spectra	AASHTO	response spectra	AASHTO
Column 2, top	9490		560	
	7093		419	
	9685		571	
	8645		507	
average	8728	8781	514	625

Due to Transverse EQ	transverse		longitudinal	
	response spectra	AASHTO	response spectra	AASHTO
Column 2, bottom	10336		734	
	7724		550	
	10546		749	
	9391		665	
average	9499	8085	675	475

Due to Longitudinal EQ	transverse		longitudinal	
	response spectra	AASHTO	response spectra	AASHTO
Column 2, top	24		1	
	25		1	
	25		1	
	30		1	
average	26	36	1	0

Due to Longitudinal EQ	transverse		longitudinal	
	response spectra	AASHTO	response spectra	AASHTO
Column 2, bottom	12		644	
	13		648	
	13		680	
	15		831	
average	13	19	701	903

8.2.7.2 Old Wahite Ditch Bridge

8.2.7.2.1 Bridge Description

The bridge under consideration in this section is denoted as Bridge L-927, located in Stoddard County on US 60 where it crosses the Wahite drainage ditch. The bridge was built in 1952 without seismic considerations in design. This 279 foot 9 inch bridge consists of five spans supported by steel girders. The interior diaphragms each consist of two diagonal L3x2½x5/16 members crossed over one another. The general elevation of the bridge is shown in Figure 8.55.

The bridge superstructure is supported by four intermediate bents through expansion and fixed bearings and two seat-type abutments at its ends. Each bent consists of a reinforced concrete cap beam and two reinforced concrete columns (tapered). There is a reinforced concrete diaphragm placed between each pair of columns on each bent for additional restraint in the transverse direction. Deep pile foundations support both bents and abutments. There are 6 piles for each column footing on bents 2 and 5, 8 piles for each column footing on bents 3 and 4, and 6 piles for each abutment footing.

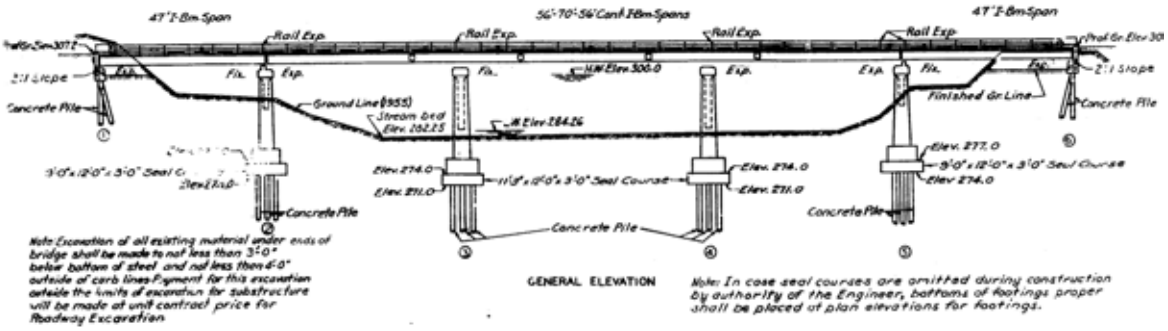

Figure 8.55: Bridge General Elevation (Old Wahite Ditch Bridge).

8.2.7.2.2 Bridge Model and Analysis

All of the components of the structure were included in the bridge model. These components include the girders, diaphragms, cross-frames, interior bents and columns, and the bridge deck. The deck was represented by 61 shell elements with a thickness of 6.5 inches. All girders, cross-frames, and diaphragms were modeled as 550 frame members. Each frame section was then assigned member properties, such as material type and cross-section dimensions. The model also included 356 nodes.

To take soil effect into account, springs and dashpots were used at the base of each column (eight columns total, two on each interior bent). Springs were also placed at the ends of the bridge on each abutment footing. The stiffness constants of the springs were taken from Appendix F.

Rigid elements were used to model the seat-type abutments in *SAP2000*. Because this bridge was to be analyzed using a response-spectrum analysis, no "gap" elements could be used (as they had been on the Old St. Francis Bridge). However, for comparison, several cases were run for this bridge using a non-linear time history analysis. This time history analysis did include the necessary "gap" elements to model the expansion joints.

In this way, the two models could then be compared to note how close the results were to one another. For each analysis with one directional earthquake excitation, 30 Ritz-vectors were considered associated with the earthquake direction. In Table 8.32, a sampling of five of the significant vibration modes are listed with its period in seconds and a brief description of the motion represented within the given mode. Their corresponding mode shapes are illustrated in Figures 8.56-8.60.

The bridge was analyzed under a total of twelve response spectra described in Section 8.1.3. Six of the spectra correspond to a 10% PE level while the others to a 2% PE level. At each PE level of earthquakes, three were considered as near-field and the other three as far-field. The internal loads such as shear and moments and the abutment displacements were obtained at various critical locations.

Table 8.32 Natural Periods and their Corresponding Vibration Modes (Old Wahite Ditch Bridge)

Mode Number	Period (seconds)	Motion Description
1	0.5641	Longitudinal
2	0.3518	Longitudinal
3	0.1809	Vertical
4	0.1229	Transverse
5	0.1025	Longitudinal

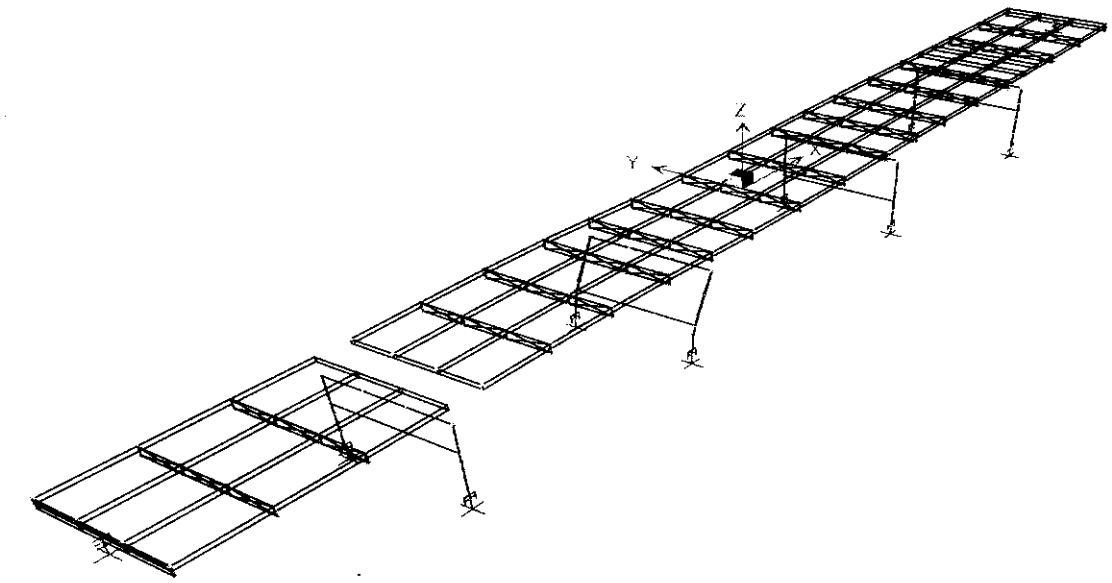

Figure 8.56: Mode 1, Period 0.5641 Seconds (Old Wahite Ditch Bridge)

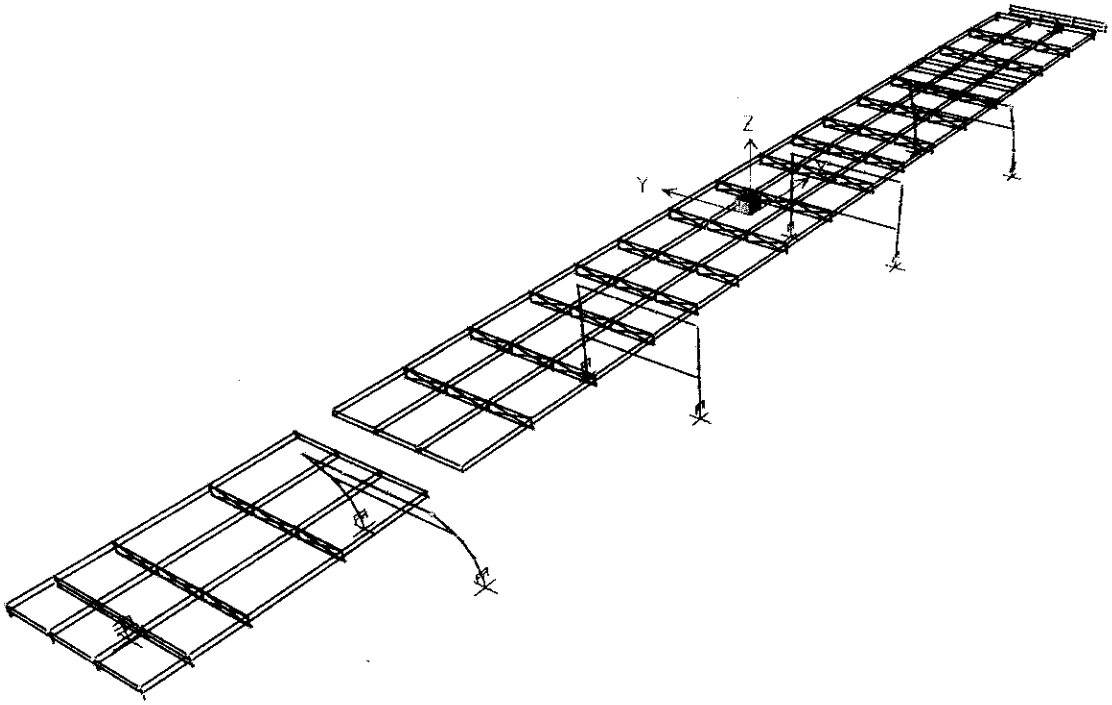

Figure 8.57: Mode 2, Period 0.3518 Seconds (Old Wahite Ditch Bridge)

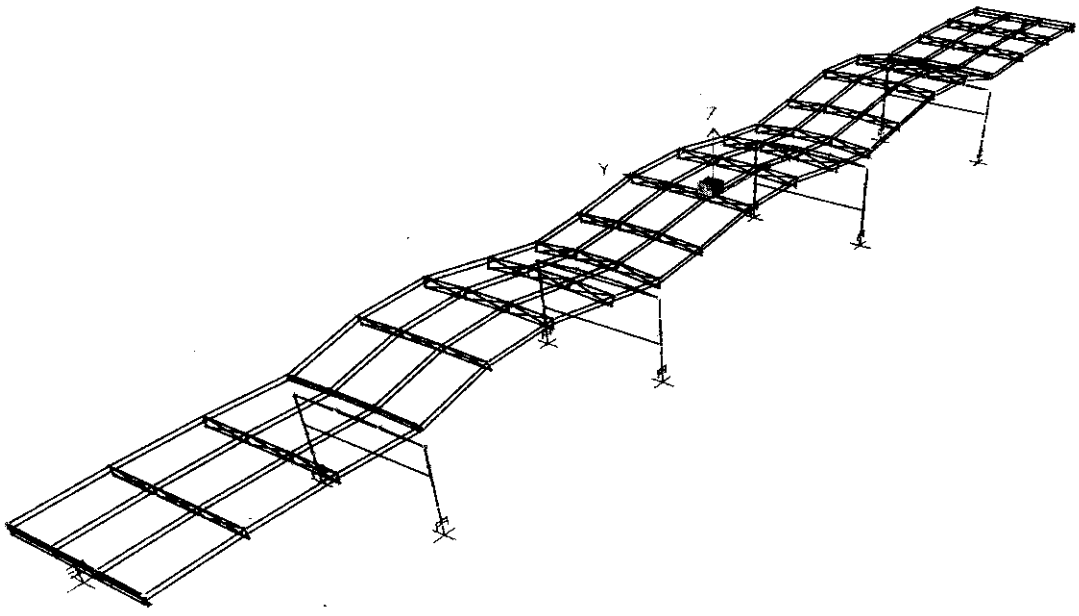

Figure 8.58: Mode 3, Period 0.1809 Seconds (Old Wahite Ditch Bridge)

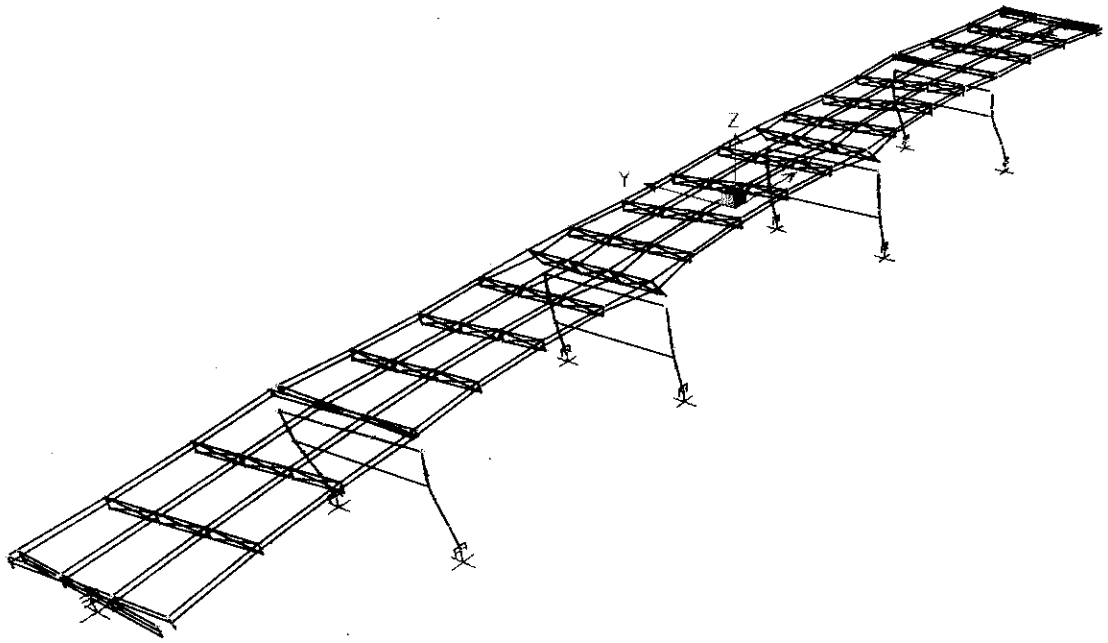

Figure 8.59: Mode 4, Period 0.1229 Seconds (Old Wahite Ditch Bridge)

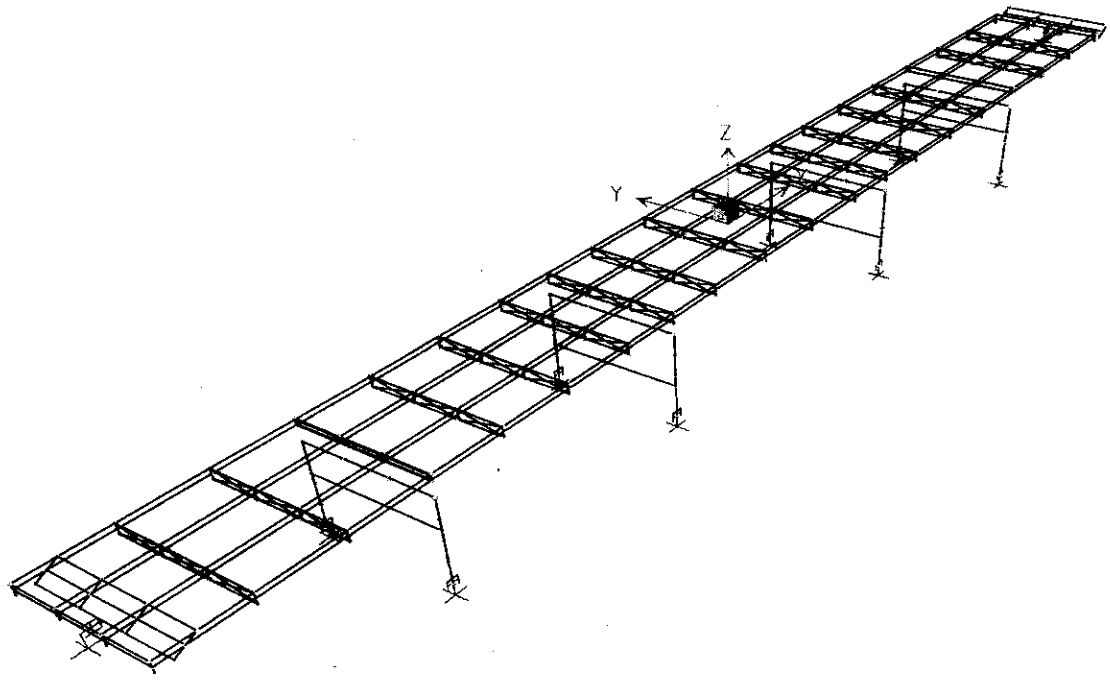

Figure 8.60 Mode 5, Period 0.1025 Seconds (Old Wahite Ditch Bridge)

8.2.7.2.3 Bridge Evaluation

This section briefly presents the results and explains the reasoning behind the calculations in the evaluation of this bridge. The evaluation procedure is the same as used for the bridges at the St. Francis River Site. Whether or not the C/D ratios were greater than one indicated if their associated components would experience problems in an earthquake.

8.2.7.2.3.1 Load Combination Rule

The same load combination rule was used for the evaluations at the Wahite Ditch Site as at the St. Francis River Site. This rule was used throughout these calculations for various types of demands on the structure (shear, moment, and axial forces, as well as transverse and longitudinal displacements).

8.2.7.2.3.2 Minimum Support Length and C/D Ratio for Bearing

Because this bridge uses seat-type abutments, bearing and support length are essential components that must be examined. The capacity, or actual support length for this bridge, was estimated at 18 inches. However, based on the definition of required support by FHWA, approximately 20 inches of length was needed. This indicates that the bearing and support length for this bridge could lead to the dropping of spans during an earthquake.

8.2.7.2.3.3 C/D Ratios for Shear Force at Bearings

The shear forces from each of the transverse, longitudinal, and vertical earthquake motions were combined to determine their total effect. The force demands at the bearing pads on the cap beams at the interior bents exceeded the capacities of the two bolts available for all of the 2% and 10% earthquakes. This indicates possible shear failures in the areas around the connecting bolts at the bearing pads.

The C/D ratios for embedment length and edge distance requirements of the bolts are evaluated with the same procedures as used for the bridges at the St. Francis River site. The embedment length of the 1" diameter bolts appears to be inadequate, as the length taken from the bridge plans is 10 inches, and 17 inches are required for proper embedment. This indicates that there may be problems with the embedment caused by axial forces acting on these bolts.
The edge distance required for these bolts is 7 inches, and from the bridge plans, it appears that only approximately 6 inches are available. This would imply possible problems with the edge distances for these bolts.

8.2.7.2.3.4 C/D Ratios for Columns/Piers

In this section, the C/D ratios were calculated for all columns on the interior bents. The elastic moment demands for the top and bottom of each column in the transverse and longitudinal directions due to transverse, longitudinal, and vertical earthquake motions were determined from the response spectrum analysis.

The maximum demand from the possible combinations was then used in conjunction with the determined capacity for the column to determine a C/D ratio for the columns. In most cases, the initial C/D ratios were below one, indicating insufficient column strength for elastic seismic demand. However, when the columns experience inelastic deformation, the seismic demand reduces due to energy dissipation. To account for the above effect, the ductility indicator was used with these ratios. Since the four interior bents each had multiple columns, a multiplier of 5 was applied to each ratio (AASHTO, 1996). In most cases, this multiplier increased the ratios to values above one. However, on all of the 2% earthquakes, 2 of the columns had C/D ratios less than one even after the implementation of the ductility indicator. This was due to very high moments at the bottoms of the columns on the fixed bent.

As for the bridges at the St. Francis River site, the footings of these columns were determined to have moment capacity considerably higher than the capacities of the columns even when the axial force is zero. Therefore, the footings are expected to perform satisfactorily. The plot for the moment versus rotation is presented in Appendix H for the case of axial load equal to zero.

8.2.7.2.3.5 C/D Ratios for Reinforcement Anchorage in Columns

For both the top and bottom of the columns, the adequacy of the anchorage of longitudinal reinforcement must be checked. The tops and bottoms of the columns used straight anchorage. The anchorage at the tops of the columns caused somewhat of a problem, since the available length of anchorage was less than the required length of anchorage. All C/D ratios for top-of-column anchorage were less than one, indicating the possibility of failure within this region.

As for the bottom of the columns, further explanation is required. Because the capacity anchorage length was greater than the demand length, the FHWA Manual dictated that the C/D ratio was to be 1.5 multiplied by the C/D ratio of the footing. However, since the capacity of the footings was estimated to be much larger than that of the columns, it was deemed unnecessary to determine numerical values for the footing C/D ratios. Therefore, each C/D ratio for the bottoms of the columns was assigned a value of 1.0 to convey the fact that this anchorage should be adequate based on the capacities of the footings.

8.2.7.2.3.6 C/D Ratios for Splices in Longitudinal Reinforcement

This section is not applicable to this structure, as the columns have no splices.

8.2.7.2.3.7 C/D Ratio for Transverse Confinement

This section is not applicable, as the columns have no transverse reinforcement. This would indicate that the columns will perform inadequately. However, the C/D ratios for these columns were still computed for informational purposes.

8.2.7.2.3.8 C/D Ratio for Column Shear

In all cases of 2% motions and for 10% motions, "Case B" was chosen, based on definitions from the FHWA Manual (1995). This case was needed because at least one of the moment C/D ratios was less than one for each earthquake (before applying the ductility indicator) and $V_i(c) > V_u(d) > V_f(c)$. When "Case B" was used, the relationship for the column shear C/D ratio was the minimum column moment C/D ratio multiplied by an FHWA-defined multiplier, which is the same as was done for the previous bridges.

The shear forces seen by these columns were very large, especially at the bottoms of the columns. Because the maximum shear forces were always found at the column base, the dimensions of the column base were used in the calculations. These large shear forces and lack of transverse confinement of the columns led to very low C/D ratios for almost all cases. Only for one of the 10% earthquakes was the ratio above one. This indicates a problem with column shear capacity that must be retrofitted.

8.2.7.2.3.9 C/D Ratio for Diaphragm Members

The axial capacity of the diaphragm members (L3x2½x5/16) was obtained from AISC LRFD, 1998. This method is the same as was used for the bridges at the St. Francis River Site.

As done for the St. Francis River Bridges, two calculations for the same C/D ratio were exercised. The first uses the full length of the member spanning diagonally from top to bottom of the diaphragm/cross-frame. The second calculation uses half of the total length of the member. This was done because of the possibility of failure within the connection where the diagonal members meet, thus removing the intermediate brace. The axial capacity was found to be less than the demand in most cases, which indicates that these members may have problems under the influences of strong earthquake motions.

8.2.7.2.3.10 C/D Ratio for Abutment Displacements

In all cases, the longitudinal and transverse displacements of the abutments under the combined effect of three earthquake effects were found to be less than their respective allowable values specified in the FHWA Manual (1995). This indicates that the abutments should remain damage-free in the event of an earthquake.

8.2.7.2.4 Summary of Problem Areas

A summary of all C/D ratios for all earthquakes for this bridge is shown in Table 8.33. This bridge experienced problems with a variety of components.

First, the available support length is slightly less than the minimum requirement, indicating possible problem dropping of the exterior spans off their supports earthquake motion. Next, the shear capacity of bolts at the bearing pads on the interior bents appears to be inadequate, as the demand outweighed the capacity in all cases. Also, the bolt embedment length and edge distance appear to be inadequate, indicating possible problems with these components as well.

The next components of concern are the columns of the structure. Because the ductility indicator, which increases the column C/D ratios by five times, was used, all columns appeared to perform sufficiently, except for the bottoms of the columns on the fixed pier under five of the 2% ground motions. Associated with the column moment C/D ratios, the shear capacity of columns is also inadequate. For all of the 2% and five of the six 10% earthquakes, the column shear C/D ratio was less than one, which indicates some cause for concern. This is also in part due to the lack of transverse reinforcement in the columns.

The final components of concern are the diagonal members in the cross-frames and diaphragms of the bridge. As indicated by the C/D ratios, these members performed rather poorly. The C/D ratios for these members were raised above one in all cases by using the half-length of the member. However, there still exists the possibility of a problem that may warrant further investigation.

8.2.7.2.5 Time History vs. Response Spectrum Analysis

This bridge was analyzed using a response spectrum analysis, much like its new counterpart at the Wahite Ditch Site. However, this structure was more similar to the Old St. Francis River Bridge, which had been analyzed using a non-linear time history analysis. Therefore, several cases using a non-linear time history analysis needed to be run on this bridge to form a basis for comparison. The results from two analyses are compared in Table 8.34.

Four earthquake cases were run, choosing two each of 2% and 10% earthquakes, with one being near-field and one being far-field for each likelihood level. Only the longitudinal and transverse earthquake effects were analyzed, as they are the major contributors to the earthquake response of the structure. Also, the vertical responses seemed to change very little, as noted from the comparison of time history results to the response spectrum results for the St. Francis River bridges.

In all cases that were compared, the results of the two analyses were reasonably close. The differences between the values were typically low. These results indicate that the response spectrum analysis is an adequate alternative to the time history analysis for this bridge.

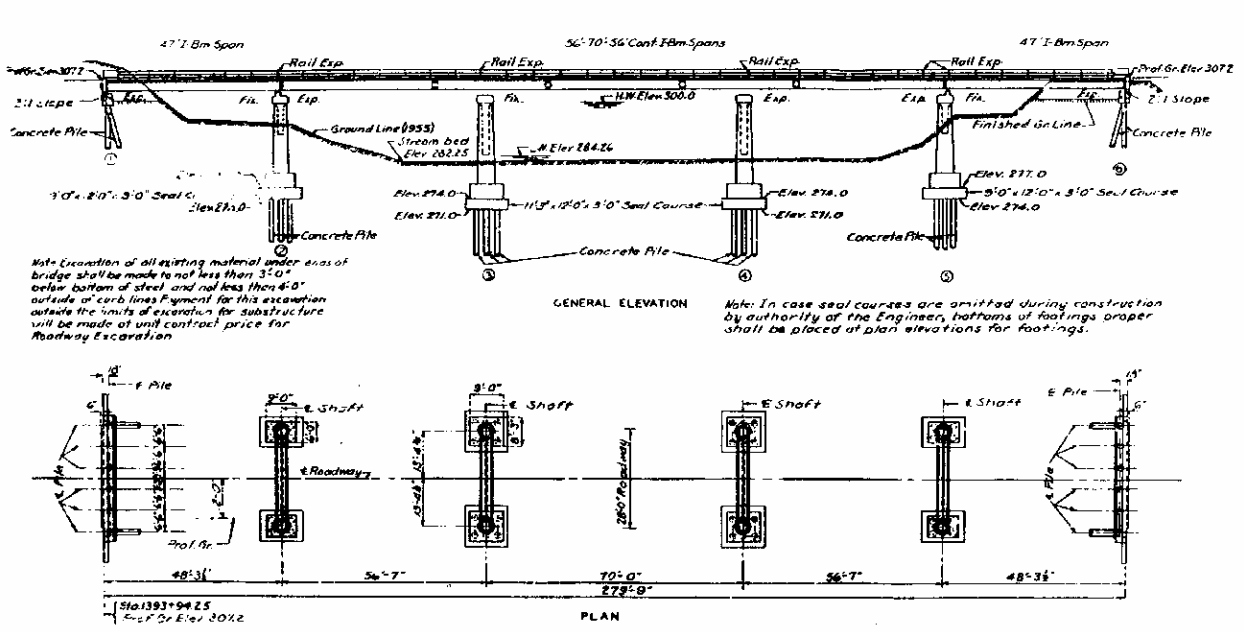

Figure 8.61 Bridge General Elevation (Old Wahite Ditch Bridge)

Table 8.33 Summary of all Earthquakes for the Old Wahite Ditch Bridge

C/D Ratio Name	020101	020102	020103	020202	020203	020205	100101	100102	100105	100201	100202	100205
r_{bd}	**0.90**	**0.90**	**0.90**	**0.90**	**0.90**	**0.90**	**0.90**	**0.90**	**0.90**	**0.90**	**0.90**	**0.90**
$r_{bf\text{-}trans}$	**0.07**	**0.06**	**0.07**	**0.08**	**0.06**	**0.06**	**0.16**	**0.14**	**0.13**	**0.13**	**0.13**	**0.10**
$r_{bf\text{-}long}$	**0.54**	**0.46**	**0.46**	**0.48**	**0.45**	**0.42**	**0.74**	**0.68**	**0.65**	**0.68**	**0.66**	**0.64**
$r_{bf\text{-}embed}$	**0.59**	**0.59**	**0.59**	**0.59**	**0.59**	**0.59**	**0.59**	**0.59**	**0.59**	**0.59**	**0.59**	**0.59**
$r_{bf\text{-}edge\ dist.}$	**0.86**	**0.86**	**0.86**	**0.86**	**0.86**	**0.86**	**0.86**	**0.86**	**0.86**	**0.86**	**0.86**	**0.86**
$r_{ec\text{-}final}$	5.30	4.80	4.94	4.99	4.88	4.77	6.51	6.31	6.23	6.26	6.21	6.10
$r_{ec\text{-}final}$	9.42	8.54	8.78	8.86	8.67	8.47	11.57	11.22	11.07	11.12	11.04	10.83
$r_{ec\text{-}final}$	**0.80**	**0.75**	**0.65**	**0.74**	**0.66**	**0.61**	2.97	2.76	2.98	2.43	2.52	2.29
$r_{ec\text{-}final}$	1.18	1.11	**0.97**	1.11	**0.98**	**0.90**	4.42	4.11	4.42	3.60	3.75	3.41
$r_{ec\text{-}final}$	6.44	5.78	6.14	6.01	6.13	6.08	8.15	8.04	8.11	7.94	7.97	7.81
$r_{ec\text{-}final}$	11.44	10.27	10.92	10.67	10.90	10.81	14.48	14.28	14.41	14.10	14.16	13.87
$r_{ec\text{-}final}$	**0.34**	**0.30**	**0.31**	**0.37**	**0.29**	**0.27**	**0.80**	**0.65**	**0.63**	**0.62**	**0.62**	**0.49**
$r_{ec\text{-}final}$	**0.50**	**0.45**	**0.45**	**0.55**	**0.43**	**0.39**	1.17	**0.96**	**0.92**	**0.91**	**0.92**	**0.72**
$r_{ec\text{-}final}$	6.51	5.85	6.22	6.05	6.22	6.19	8.16	8.05	8.12	7.96	7.99	7.84
$r_{ec\text{-}final}$	11.57	10.39	11.06	10.76	11.05	10.99	14.49	14.30	14.43	14.14	14.19	13.94
$r_{ec\text{-}final}$	3.16	2.48	2.51	2.67	2.59	2.09	5.24	4.83	4.36	4.65	4.24	3.88
$r_{ec\text{-}final}$	4.65	3.64	3.70	3.92	3.81	3.08	7.70	7.11	6.41	6.83	6.23	5.71
$r_{ec\text{-}final}$	5.33	4.83	4.96	5.00	4.90	4.79	6.54	6.34	6.27	6.29	6.24	6.14
$r_{ec\text{-}final}$	9.46	8.58	8.82	8.89	8.71	8.52	11.62	11.27	11.14	11.17	11.10	10.91
$r_{ec\text{-}final}$	**0.80**	**0.75**	**0.65**	**0.74**	**0.66**	**0.61**	2.98	2.77	2.98	2.43	2.52	2.29
$r_{ec\text{-}final}$	1.18	1.11	**0.97**	1.11	**0.98**	**0.90**	4.42	4.11	4.42	3.61	3.75	3.41
$r_{ca\text{-}bottom}$	1.00	1.00	1.00	1.00	1.00	1.00	1.00	1.00	1.00	1.00	1.00	1.00
$r_{ca\text{-}top}$	**0.64**	**0.58**	**0.59**	**0.60**	**0.59**	**0.57**	**0.78**	**0.76**	**0.75**	**0.75**	**0.75**	**0.73**
r_{cs}	---	---	---	---	---	---	---	---	---	---	---	---
$r_{cs\text{-}adj}$	---	---	---	---	---	---	---	---	---	---	---	---
r_{cc}	---	---	---	---	---	---	---	---	---	---	---	---
r_{cv}	**0.28**	**0.25**	**0.25**	**0.31**	**0.24**	**0.22**	**0.65**	**0.54**	**0.51**	**0.51**	**0.51**	**0.40**
r_{cross}	**0.45**	**0.36**	**0.37**	**0.39**	**0.35**	**0.33**	**0.80**	**0.68**	**0.63**	**0.67**	**0.64**	**0.60**
$r_{cross\text{-}0.5L}$	1.48	1.19	1.23	1.29	1.17	1.09	2.65	2.28	2.10	2.24	2.14	1.99
$r_{ad\text{-}trans}$	504	445	426	487	410	479	1286	1170	1179	1214	1060	1129
$r_{ad\text{-}long}$	91	78	81	81	76	80	143	126	128	122	119	123

Table 8.34 Comparison of Column Moments for Old Wahite Ditch Bridge

Due to 2% motions

Due to Transverse EQ	transverse		longitudinal	
	time history	response spectra	time history	response spectra
Column 1, bottom	11270	10721	908	1256
	10911	10152	917	1174
average	11091	10437	913	1215

Due to Longitudinal EQ	transverse		longitudinal	
	time history	response spectra	time history	response spectra
Column 1, bottom	28	27	45291	51199
	22	24	39931	44807
average	25	26	42611	48003

Due to Transverse EQ	transverse		longitudinal	
	time history	response spectra	time history	response spectra
Column 3, bottom	10943	10106	85	213
	10497	9572	70	190
average	10720	9839	78	202

Due to Longitudinal EQ	transverse		longitudinal	
	time history	response spectra	time history	response spectra
Column 3, bottom	17	20	125649	128584
	11	16	100706	105750
average	14	18	113178	117167

Due to 10% motions

Due to Transverse EQ	transverse		longitudinal	
	time history	response spectra	time history	response spectra
Column 1, bottom	4080	5175	372	578
	4611	6055	424	675
average	4346	5615	398	627

Due to Longitudinal EQ	transverse		longitudinal	
	time history	response spectra	time history	response spectra
Column 1, bottom	8	8	9130	10111
	10	10	11287	12569
average	9	9	10209	11340

Due to Transverse EQ	transverse		longitudinal	
	time history	response spectra	time history	response spectra
Column 3, bottom	3890	4855	50	90
	4390	5676	54	106
average	4140	5266	52	98

Due to Longitudinal EQ	transverse		longitudinal	
	time history	response spectra	time history	response spectra
Column 3, bottom	5	7	45961	49631
	6	8	57793	64090
average	6	8	51877	56861

8.2.7.2.6 Structural Response of Abutments

The Old Wahite Ditch Bridge abutment (11.65 m x 0.91 m) is supported on vertical and battered piles. All of piles are cylindrical concrete with a 0.406 m (16 inch) diameter and 10.67 m (35 ft) length. The plan and cross-section of the bridge abutment are shown in Figure 8.61.

The stiffness and damping factors are calculated using a pile length of 10.67 m (35 ft), a pile radius of 0.203 m (8 inch), an elastic modulus of concrete of 2.15×10^7 kN/m^2 (1.47×10^6 kips/ft)(Section F.6). Stiffness and damping factors of single batter piles are 0.8 times that of a vertical pile. (Prakash and Subramanayam, 1964)

The vertical load acting on the top of the bridge abutment is obtained from an analysis of the bridge structure. A vertical load of 51 kN (11365 lb) per meter of length was used in this analysis. The self-weight of the bridge abutment was calculated by multiplying its cross sectional area by the unit weight of the bridge abutment material (23.58 kN/m^3) (150.19 pcf). This calculation is done in the program itself. The lateral earth pressure behind the bridge abutment was calculated using a soil unit weight of 19.54 kN/m^3 (122 pcf), angle of internal friction of 33^o and friction angle between soil and abutment of 33^o. All of the loads were modified by a time dependent seismic coefficient.

8.2.7.2.6.1 Calculated Time Dependent Displacements of Abutment

Figure 8.63 a and b show the largest time histories of sliding, rocking and total permanent displacement of Old Wahite Ditch Bridge abutment for PE 10% in 50 years respectively. Fig. 8.64 a and b shows the time histories of sliding, rocking and total permanent displacement of Old Wahite Ditch Bridge abutment for PE 2% in 50 years respectively.

A plot of magnitude and significant number of cycles is given in Figure 8.63a. Table 8.35 shows displacement in one significant cycle. This is likely the displacement during a composite analysis.

Table 8.35 Displacement at Top of Old Wahite Ditch Bridge Abutment

Displacement at top of abutment	**PE 10% in 50 years**		**PE 2% in 50 years**	
	M6.4	**M7.0**	**M7.8**	**M8.0**
Sliding (m)	0.037	0.028	0.139	0.178
Rocking (m)	0.018	0.053	0.0513	0.064
Total (m)	0.056	0.080	0.190	0.242
Significant cycles	9	10	18	20
Disp. in 1-cycle	0.007	0.008	0.011	0.012

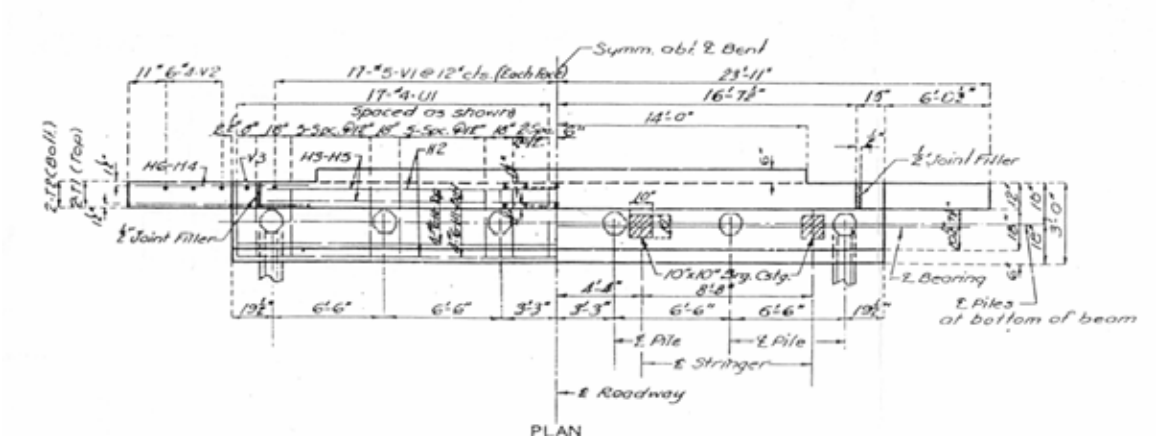

Figure 8.62a Plan of Old Wahite Ditch Bridge Abutment

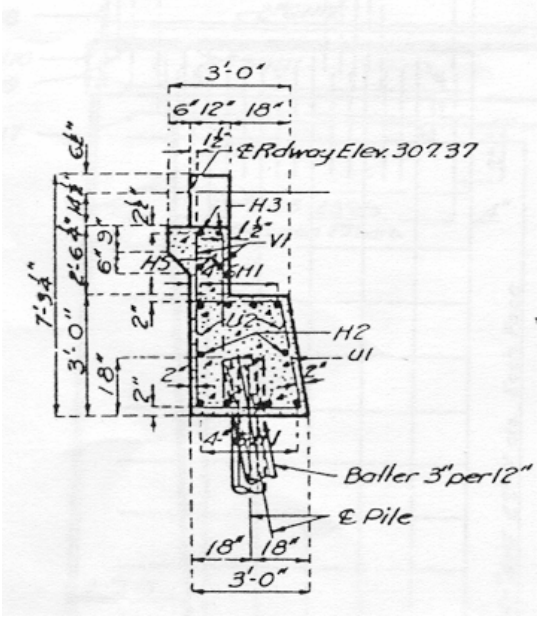

Figure 8.62b Cross Section of Old Wahite Ditch Bridge Abutment

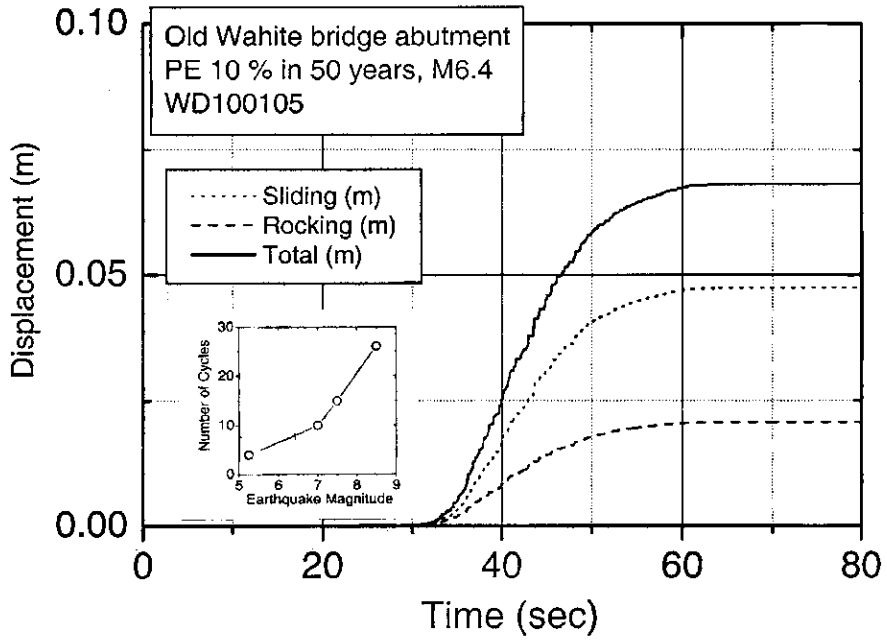

a. Magnitude 6.4

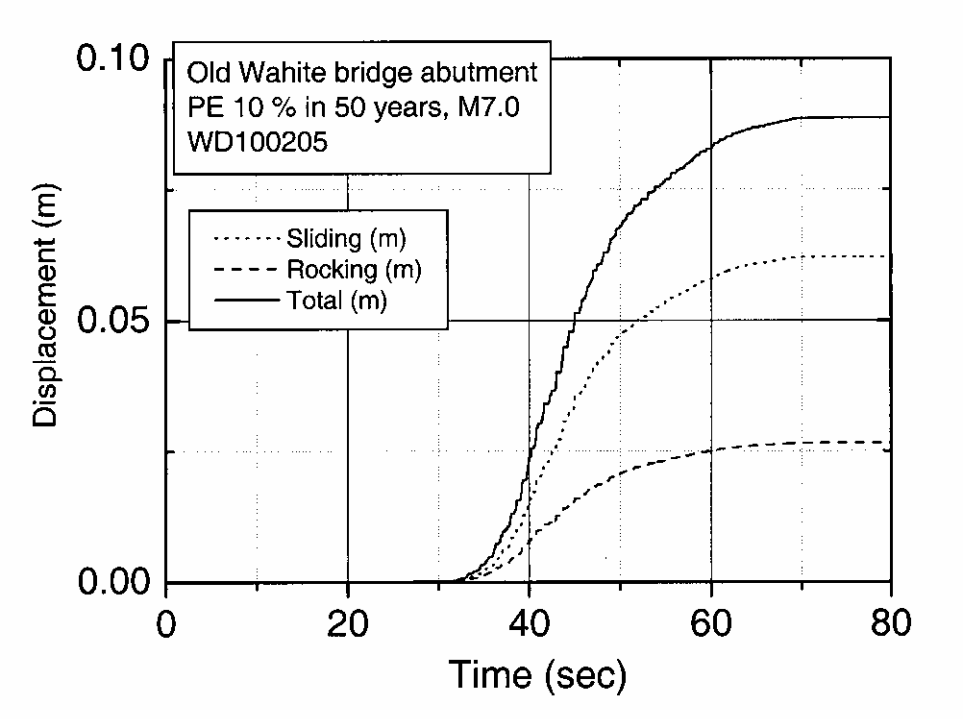

b. Magnitude 7.0

Figure 8.63 Time Histories of Sliding, Rocking and Total Permanent Displacement of the Old Wahite Ditch Bridge Abutment PE 10% in 50 Years, Magnitudes 6.4 and 7.0

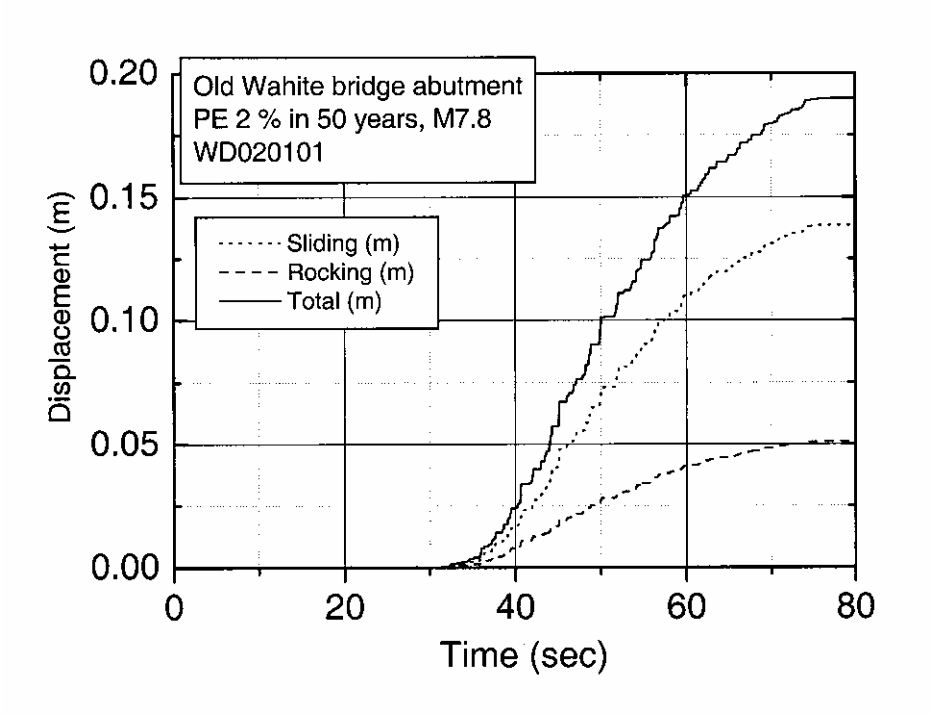

a. Magnitude 7.8

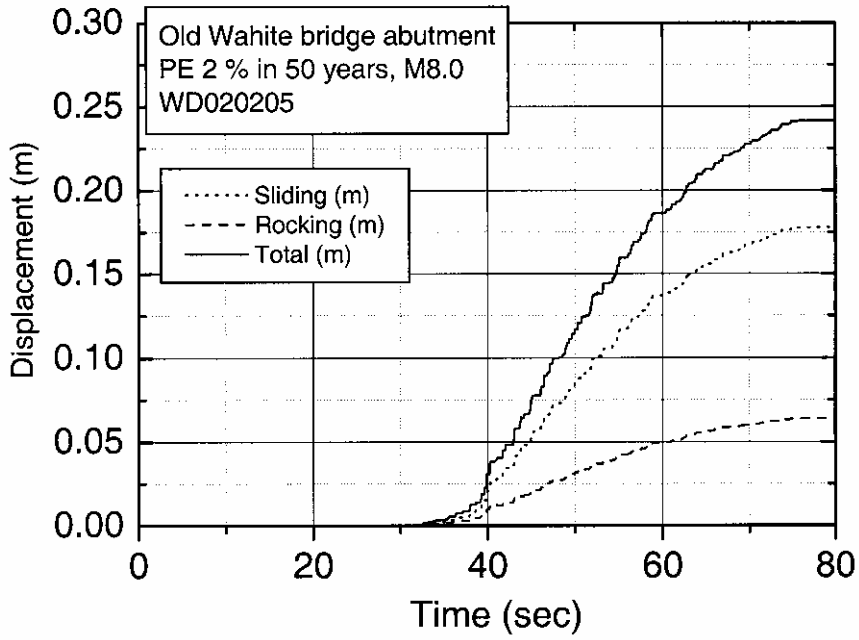

b. Magnitude 8.0

Figure 8.64 Time Histories of Sliding, Rocking and Total Permanent Displacement of the Old Wahite Ditch Bridge Abutment PE 2% in 50 Years, Magnitudes 7.8 and 8.0